AEROSOL COLLECTION IN GRANULAR BEDS

by

MALCOLM L. KENNARD

B.Sc., University of Nottingham, Nottingham, England, 1974

A THESIS SUBMITTED IN PARTIAL FULFILLMENT OF

THE REQUIREMENTS FOR THE DEGREE OF

MASTER OF APPLIED SCIENCE

in

THE FACULTY OF GRADUATE STUDIES

Department of Chemical Engineering

We accept this thesis as conforming

to the required standard

THE UNIVERSITY OF BRITISH COLUMBIA

August, 1978

In presenting this thesis in partial fulfilment of the requirements for an advanced degree at the University of British Columbia, I agree that the Library shall make it freely available for reference and study. I further agree that permission for extensive copying of this thesis for scholarly purposes may be granted by the Head of my Department or by his representatives. It is understood that copying or publication of this thesis for financial gain shall not be allowed without my written permission.

Department of Chemical Engineering

The University of British Columbia
2075 Wesbrook Place
Vancouver, Canada
V6T 1W5

Date 10th August 78

ABSTRACT

The filtration of aerosols using granular beds was studied to determine the feasibility of using such devices as high efficiency particle collectors. Based on the experimental data, it was attempted to derive expressions for predicting the aerosol removal efficiency of the granular bed.

Granular beds composed of fairly uniform, spherical nickel shot were employed in a 7.4 cm diameter copper column to collect solid, monodispersed, polystyrene latex aerosols. The collection efficiency of the granular bed was determined as a function of several variables, viz., aerosol diameter (0.109 to 2.02 μm); bed particle diameter (100 to 600 μm); bed depth (0.3 to 19 cm); superficial gas velocity (5 to 67 cm/sec); and flow direction (upflow and downflow).

The monodispersed, latex aerosols were generated by atomizing dilute hydrosols of aerosol particles. The aerosol number concentrations were measured at the inlet and outlet of the granular bed (using light scattering techniques), from which the bed collection efficiency was determined.

Using the concept of an isolated bed particle it was possible to quantitatively predict the collection efficiency of the bed. The collection of an aerosol by an isolated bed particle can be attributed to the following mechanisms:- inertial impaction, direct interception, diffusional deposition, gravitational deposition and electrostatic effects. In the present study electrostatic effects were eliminated by grounding the equipment and neutralizing the aerosol.

Equations based on individual collection mechanisms and combinations were fitted to the experimental data by multiple regression analysis. An empirical model was developed, which gave good predictions of the experimental bed collection efficiency. The single collector efficiency (EB) was calculated using the following empirical equation:

$$EB = 1.0\ St + 150{,}000\ NR^{4/3}\ Pe^{-2/3} + 1.5\ NG$$

and the overall bed collection efficiency (EBT) was calculated using the following theoretical equation:

$$EBT = 1 - \exp\left(-1.5\ \left(\frac{1-\varepsilon}{\varepsilon}\right)\frac{H}{d_c}\ EB\right)$$

The difference between the experimental and calculated bed efficiencies were generally less than ten percentage points.

Experimental results indicate that high collection efficiencies can be achieved with relatively shallow fixed beds of granular material. Inertial impaction was considered to be the dominant collection mechanism at high gas velocities, whilst diffusion and, to a lesser extent, gravity were considered dominant at low gas velocities. For all the experimental conditions studied, interception was shown to be insignificant.

TABLE OF CONTENTS

LIST OF TABLES

LIST OF FIGURES

ACKNOWLEDGEMENTS

I would like to thank my supervisor, Dr. Axel Meisen, for his considerate supervision and guidance throughout the course of this work.

Thanks are also due to the personnel in the Department of Chemical Engineering workshop for their cooperation and assistance.

The manuscript was typed by Mrs. Nina Thurston, whose work is much appreciated.

Finally, I would like to thank the British Columbia Ministry of the Environment and the University of British Columbia for financial assistance.

CHAPTER 1

INTRODUCTION

1.1 The Need for Particulate Control

In recent years the need to limit the emissions of pollutants has become a matter of increasing concern. Thus numerous new laws on emission standards have been introduced in an attempt to reduce the amount of these pollutants. Air pollution and especially air borne dusts and fumes, which are by-products of most process industries, constitute a difficult and expensive control problem. The need to control the emissions of these particulates is based on the following factors.

a) *Health hazard.* Inhalation of excessive dust, irrespective of its chemical composition can produce serious pulmonary diseases, with silicosis and asbestosis being the most common. Particles in the 0.1-1.0 μm range can readily reach the innermost portions of the lung and may be retained there. Many dusts act as irritants to the eyes and nose causing allergic responses, dermatitis and other skin disorders. Certain metal particles such as lead, beryllium and chromium may cause fever and nausea when inhaled.

b) *Effect on the environment.* Particulates may affect the atmospheric properties in the following ways:

i) visibility reduction, and discolouration

ii) fog formation and precipitation.

iii) solar radiation reduction

iv) temperature and wind distribution alteration.

Industrial dusts may settle on nearby fields and bodies of water with deleterious effects on the fauna and flora.

c) *Effect of materials.* Particulates can affect materials by soiling or chemical deterioration. For example, corrosion is enhanced by the deposition of acidic particles.

d) *Explosion risk.* Fine dusts of combustible materials dispersed in air at certain concentrations may burn rapidly or even explosively. Dusts such as grain, sugar, coal, plastics, sulphur, aluminium, and other dusts of light metals are the most explosive. The explosion risk increasing with decreasing particle size.

e) *Commercial value.* In some cases such as metal refining or smelting, the emitted dust may have a considerable economic value.

1.2 Conventional Dust Removal Equipment

There is increasing evidence that submicron particles are most hazardous and thus legislation should not only be based on the quantity but also the size of particulates. Most conventional control devices are, unfortunately, rather inefficient collectors of submicron particles. Hence there is a need to improve the existing methods and/or to develop new devices for the removal of fine particulates.

The conventional equipment available can be divided into the following groups.

a) *Electrostatic precipitators.* Here the particles are charged by passing them through a highly ionized region and subsequently removing them from the gas stream by electrostatic forces. Precipitators are able to collect fine particles but the power requirements are high and increase with mass loading. Furthermore, precipitators are generally large and therefore have high capital and maintenance costs.

b) *Fabric filters.* These are generally more effective than precipitators in the micron and submicron ranges. Unfortunately, most filter media have limited resistance to chemical attack, mechanical vibration and high temperatures. The media may be difficult or impossible to clean and filters therefore often have high operating costs.

c) *Wet scrubbers.* These devices operate on the principle of bringing the dusty gas stream into contact with a liquid phase. Numerous devices of different designs, sizes and performance characteristics are available and some of them are highly effective in the removal of submicron particles. However, scrubbers tend to have high pressure drops and power requirements. A further major disadvantage is that they cannot operate at high temperatures.

d) *Centrifugal collectors.* Here the particles are collected by inertial effects and cyclones are the most common devices of this type. They are cheap to operate and build since they have no moving parts. High collection efficiencies are achievable for particles greater than about 5 μm in diameter.

Thus the development of an efficient and low cost device for fine particulate removal is a pressing demand in industry.

1.3 The Granular Bed Filter

The granular bed, or packed bed filter, consists of fixed beds of solid granules through which the dusty gas flows. The dust particles are collected mainly by impaction on the granules and, to a lesser extent, by sieving.

Although beds of granular materials have been used for the removal of particulates from gas streams for some time, they have not achieved the same degree of acceptance as other devices. This could be due to the fact that past research efforts have provided little reliable data which could

be systematically analysed and related to industrial needs.

Until recently packed beds were operated batchwise. However, development of devices such as the panel bed filter (Raretsky[1]) and the fluidized bed filter (Black and Boubel[2]) have shown that relatively high removal efficiencies of submicron particles can be achieved with continuous operation. This demonstrates the feasibility of using beds to remove fine particulates from gases in industrial processes such as coal gasification.

1.3.1 Advantages of Granular Bed Filters

Apart from simplicity of design and ruggedness, granular bed filters have the ability to treat gases which:-

i) are at high temperatures

ii) undergo large changes in temperature and volume

iii) contain abrasive dusts

iv) have a wide range of particle sizes and concentrations

v) contain corrosive chemicals and moisture.

Packed bed filters may have low maintenance costs, depending on the efficiency of bed regeneration, and are more compact than some other types of conventional equipment. They can also remove particular matter simultaneously with gaseous pollutants provided a suitable absorbent material is used (Squires and Pfeffer[3]).

1.3.2 Disadvantages of Granular Bed Filters

In terms of particle removal efficiency granular filters are generally less effective than fibre filters. They also tend to have rather high pressure drops which are comparable with wet scrubbers of similar efficiency. A major drawback is the difficulty of separating the collected dust from the filter medium to prevent clogging. Several methods have been developed such as isolating a section of the bed and:-

i) dislodging the deposited particles by "puff back", i.e., flushing with

a pulse of air in the reverse direction to the dusty gas flow (Kalen[4]; Squires[3])

ii) using mechanical vibration of the bed (Englebrecht[5]), or

iii) continuous removal of the partially clogged section of bed and replacing it with fresh material (Egleson[6]). This method is relatively simple in case of fluidized beds (Meissner[7]) or spouted beds (Meisen and Mathur[8]). The removed granular material may be either washed for re-use or discarded depending on the particular circumstances.

Further problems may arise when very high concentrations of dusty gas are filtered. This causes rapid clogging and an increase in pressure drop. A simple remedy is to operate the bed in conjunction with a cyclone or bag filter to remove the majority of large particles.

A qualitative comparison of granular beds with conventional filters is given in Table I.

TABLE I. COMPARISON OF A GRANULAR BED WITH CONVENTIONAL PARTICLE COLLECTION EQUIPMENT

	Wet Scrubbers	Bag Filters	Electro-static Precip-itators	Cyclones	Granular Beds
High temp.	VP	VP	G	VP	VG
Gas capacity	G	VP	G	VG	G
Removal efficiency for fine particles	P	VG	G	VP	VG
Capital cost	VP	P	P	VG	VG
Operating cost	P	P	G	VG	VG
Reliability	P	P	P	VG	VG

Key: VP--very poor VG--very good
P --poor G --good

1.4 Background Information on Granular Bed Behaviour

The study of a granular bed as a particle collection device requires a knowledge of the mechanisms which contribute to the collection process. It is also necessary to predict the relative magnitude of these mechanisms in order to develop models of collection performance.

Most particle removal theories are based on the simple assumption that particles are captured upon touching the collector surface and that re-entrainment is absent (Dahneke[9]). Particles stick to surfaces mainly due to short range van der Waals and electrical forces[10,11]. It is therefore necessary to develop a mechanism whereby a particle travelling in a moving fluid is able to move across the fluid streamlines to a point close enough to the collector surface for these captive forces to come into effect.

1.4.1 Individual collection mechanisms pertinent to an isolated, spherical collector

In order to explain the different collection mechanisms, which may arise in granular beds, it is convenient to consider a single isolated collector particle. Calculation of the collection efficiency (or capture efficiency) of a single collector may then be reduced to the calculation of the efficiencies of the individual collection mechanism. The primary collection mechanisms are inertial impaction, direct interception, diffusional deposition, gravitational sedimentation, and electrostatic deposition. In order to determine which collection mechanisms are predominant in a filter medium, it is useful to introduce dimensionless parameters which characterize the interaction between the fluid, particles, and collectors. The separate collection mechanisms are discussed below.

a) *Inertial collection.* As shown in Fig. 1.1, the presence of a collector causes the gas streamlines to curve. Since the inertia of the

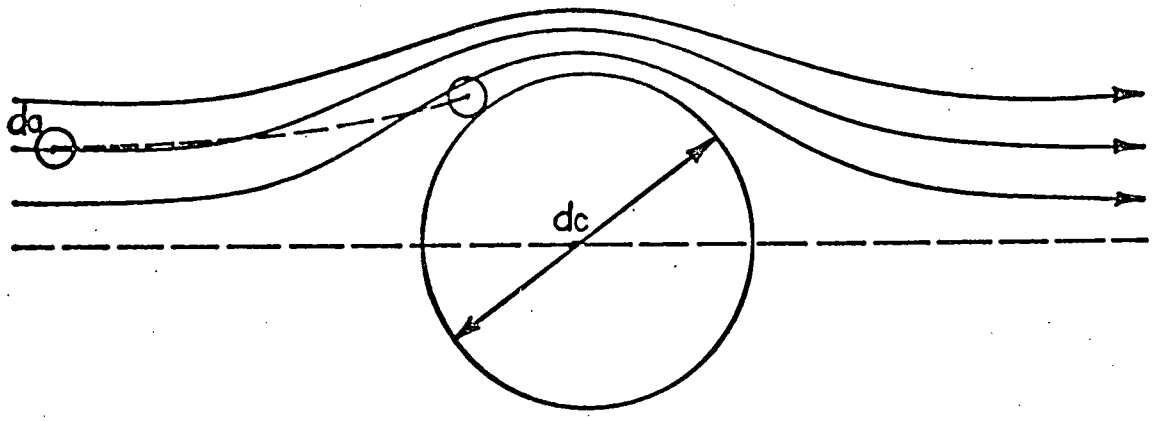

Fig. 1.1 Inertial Impaction

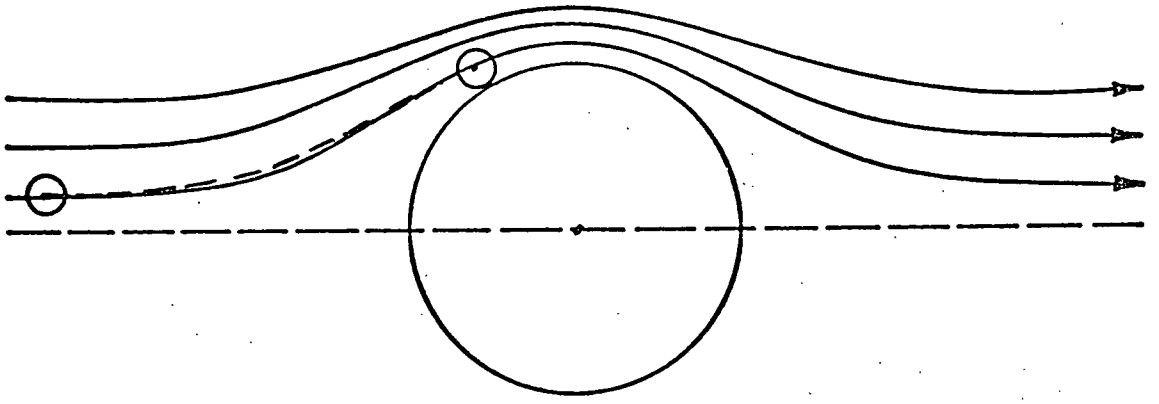

Fig. 1.2 Direct Interception

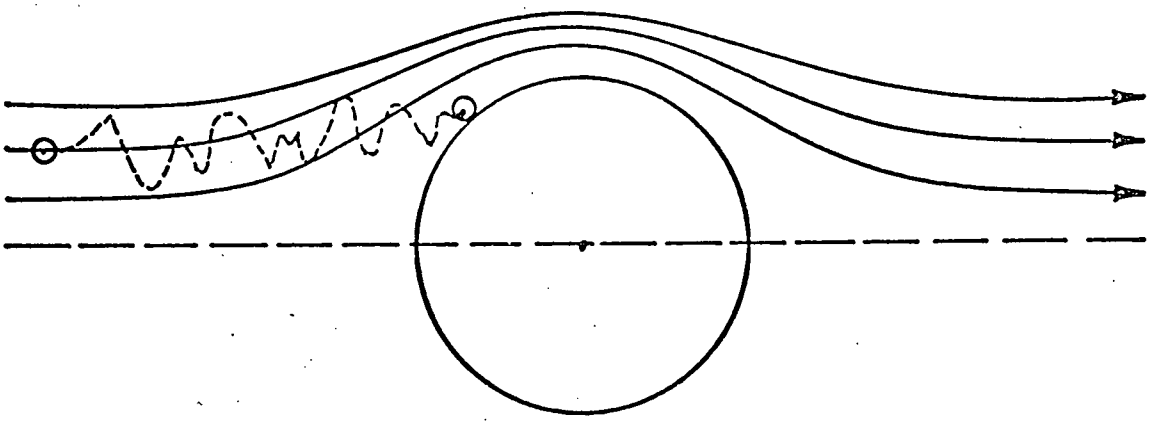

Fig. 1.3 Diffusional Interception

aerosol particles is greater than an equivalent volume of gas, their trajectories deviate from the streamlines and approach the collector surface. Two factors determine the collection efficiency:-

i) the velocity distribution of the gas around the collector, which is governed by the collector Reynolds number,

$$Re = \rho_F U d_c/\mu ,$$ and

ii) the trajectory of the particle, which is the result of the interaction between the fluid and particle. The interaction may be characterized by the Stokes number defined as

$$St = d_a^2 U \rho_F/9 \mu d_c$$

The inertial mechanism is usually dominant for particles greater than 1 to 2 μm in diameter. The mechanism increases with increasing fluid velocity, aerosol diameter and density, and decreasing collector size.

b) *Direct interception.* In this case it is assumed that the particles do not appreciably disturb the fluid flowfield and their trajectories coincide with the streamlines. A particle is captured when its centre approaches the collector surface within one particle radius (see Fig. 1.2). Capture is due solely to the size of the particle. This mechanism can be characterized by the parameter

$$NR = d_a/d_c$$

This effect is usually small in the case of submicron aerosol particles treated by beds of individual collector particles greater than 100 μm diameter.

c) *Diffusional deposition.* Because of Brownian movement the trajectories of submicron particles do not usually coincide with the gas streamlines. Thus a particle may migrate to the collector surface purely as a result of random diffusion (see Fig. 2.3). The Peclet number is used to describe this effect.

$$Pe = d_c U / D_a$$

where D_a is the effective diffusivity of the aerosol particle. Some workers prefer the dimensionless group

$$ND = Pe^{-2/3}$$

This group changes the magnitude of the diffusional parameter making it more comparable to the other dimensionless groups.

The diffusional effect increases with decreasing particle size and is usually the dominant collection mechanism for particles smaller than about 0.5 μm in diameter at low velocities.

d) *Gravitational deposition.* This represents sedimentation or settling of a particle due to gravity. In most cases the effect is only significant for particles greater than about 2 μm in diameter or at very low gas velocities. Gravitational deposition can be characterized by the parameter

$$NG = U_s/U$$

where U_s is the terminal velocity of the aerosol particle. If the particle obeys Stokes' law, U_s is given by

$$U_s = d_a^2 \, g \, \rho_a / 18 \, \mu$$

Depending on the direction of gas flow, the effect of gravity on collection may be either positive or negative (see Fig. 1.4). The collection efficiency increases with aerosol size and density and decreases with increasing gas flow.

e) *Electrical effects.* The aerosol particles and the collectors may carry electrostatic charges which can affect the motion of the aerosol around a collector and hence their collection. There are four types of electrical forces[12] resulting from these charges which may have to be considered. (i) The coulombic force between a charged collector and a charged aerosol particle, (ii) the electrical image force between a charged

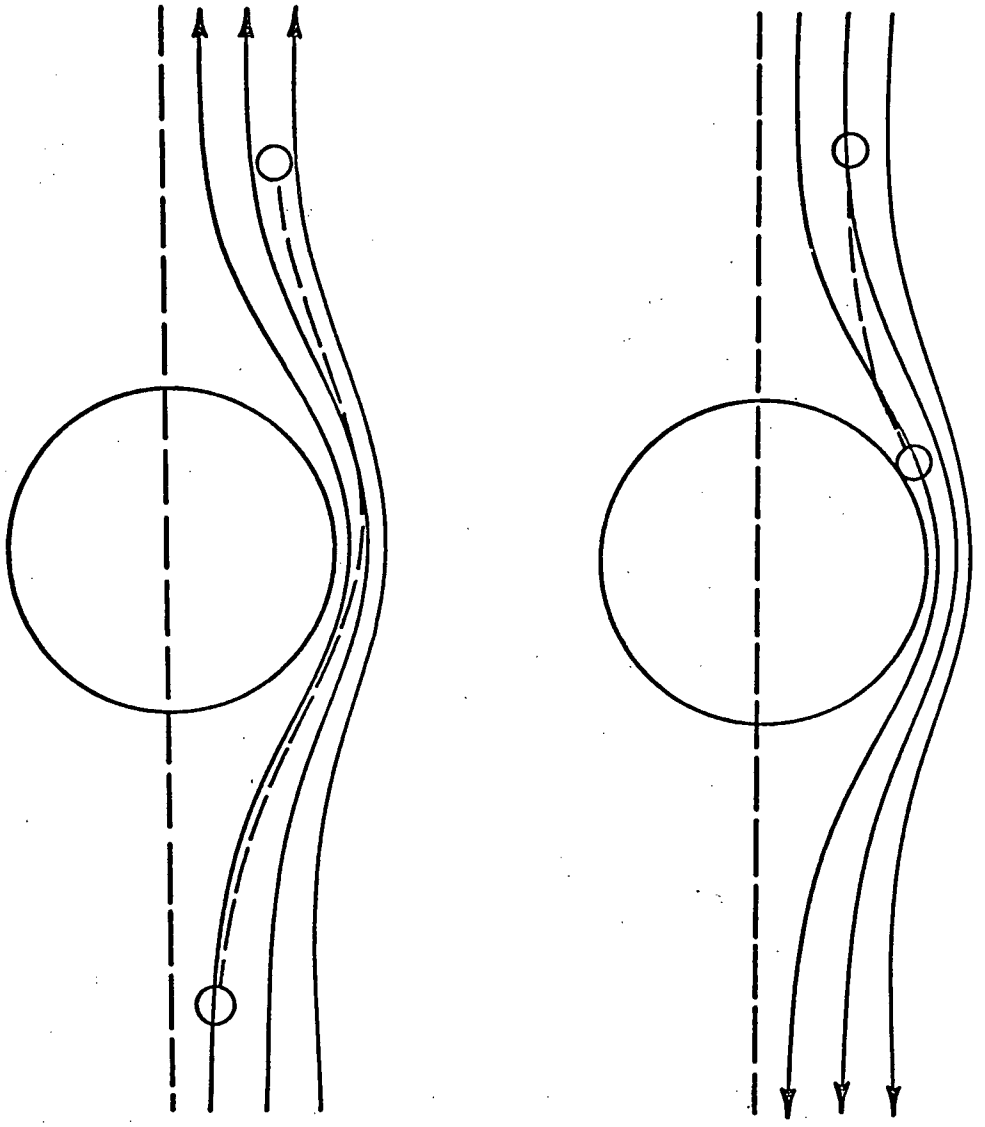

Fig. 1.4 Gravitational Settling

collector and a neutral particle, (iii) the image force between a charged particle and a neutral collector, and (iv) the space charge repulsion force effect.

1.4.2 The single particle collection efficiency

Each filtration mechanism described above is based on collection by an isolated collector particle. This approach was developed by Langmuir[13] who assumed that every filter element (e.g., bed particle) experiences similar filtration phenomena and therefore a single filter element efficiency may be defined. Consequently, the filtration efficiency of an actual filter can be calculated by summing the effects of all the elements of the filter.

In the case of a granular bed each element is assumed to be a sphere and the single collector efficiency may be defined as

$$E = \frac{\text{Number of particles impacting per unit time}}{\text{Number of particles that could impact per unit time if their trajectories were straight}}$$

Thus the theoretical calculation of filter efficiency of a granular bed is usually divided into two parts, i.e., prediction of the single collector efficiency and the summation of all the collector efficiencies by integration. (Further details are given in Chapter 3.)

It is also usually assumed that steady state filtration is taking place where any structural changes caused by the depositing particles are too small to be of any influence to the collection efficiency of the filter.

1.4.3 Limitations of the single collector efficiency approach

The various assumptions in this approach are rarely met in practice such as (i) the bed granules are completely spherical, (ii) that particles colliding with a collector are always retained[14], i.e., no bounce-off, (iii) that there is no re-entrainment, and (iv) that already deposited particles do not affect the collection efficiency of a collector. Therefore the method is oversimplified and is only useful when the individual

mechanisms are small or one is dominant. According to Fuchs[15] the total single collector efficiency is greater than any of the individual efficiencies but smaller than their sum. Thus the problem is how to combine the individual effects, especially when the aerosol diameter is in the range of 0.1-1.0 μm and the effects caused by the various mechanisms are comparable.

1.4.4 Interference effect

There is also the problem that the flow field round an isolated collector particle is obviously different from that of a collector particle inside a granular bed and therefore its collection efficiency is also changed. The flow differs because:-

i) The interstitial gas velocity in the bed is higher than a superficial gas velocity.

ii) The gas streamlines around the collector are different due to the close proximity of the neighbouring collectors.

Thus the 'interference effect' tends to increase the collection efficiency. However, there is disagreement as to how to account for this effect, especially because it may be different for the various collection mechanisms. The most plausible parameter to describe the interference effect is the bed porosity (ε). To determine the true collection efficiency of a collector, empirical or semi-empirical corrections must be introduced.

The single collector efficiency of a collector within a granular bed may therefore be written as

$$EB = f(\varepsilon, EI, ER, ED, EG \ldots)$$

where EI, ER, ED, and EG are the collection efficiences of the single collector due to inertia, interception, diffusion and gravity, respectively.

1.4.5 Total collection efficiency of the granular bed

Finally the single collector efficiency (EB) must be related to the

overall collection efficiency of the whole bed (EBT). By invoking a simplified model of the filter bed, i.e., assuming all the collectors are spherical and regularly packed, a simple equation can be developed to relate EB and EBT. This will be discussed in greater detail in Chapter 3.

1.5 Scope of the Present Work

The main objectives of this work were to investigate the removal of submicron aerosols by granular beds and to use the results for the development of an empirical equation for predicting the collection efficiency of the granular bed. To investigate the filtration process, the effect of the following variables on collection efficiency were considered: (i) aerosol size, (ii) collector size, (iii) gas velocity, (iv) direction of gas flow, and (v) granular bed depth. Other factors observed were:-

i) pressure drop across the bed as a function of gas flow rate, and

ii) the effect of humidity on collection efficiency.

Electrical effects were minimized by using metallic bed particles and grounding the equipment. Thus only inertia, interception, diffusion and gravity needed to be considered in developing an equation to predict the collection efficiency of the bed.

CHAPTER 2

PREVIOUS WORK

2.1 Introduction

Particulate separation from a gas stream by means of granular bed filters has been the subject of several theoretical and experimental studies. The experimental investigations deal mainly with the overall performance and methods of improvement. The theoretical work ranges from the analysis of the flow field and collection efficiencies of a single filter element to the overall calculation of the collection efficiency of the whole bed.

Although a substantial amount of work has been carried out, there is considerable disagreement and inadequate understanding of the filtration mechanisms. This is probably due to the fact that previous work is rather fragmentary and often presented in a way which precludes systematic analysis.

Several comprehensive reviews are available on particulate removal using granular beds (Fuchs[15], Davies[16], Dorman[17], Strauss[18], Silverman[19], Figueroa[20], Tardos[21], Pich[22]). Rather than repeating their reviews, the effect of various operating and design variables will be discussed in this chapter.

2.2 Effect of Fluid Velocity on Collection Efficiency

It has been noted by most workers that increasing the velocity through the filter causes the collection efficiency to decrease and then increase again. The minimum (see Figs. 2.1 and 2.2) is caused by diffusional effects becoming less important and inertial effects becoming dominant. The

velocity resulting in the minimum collection increases the smaller the aerosol. A typical plot of collection efficiency as a function of superficial gas velocity is shown in Fig. 2.1 and the following statements can be made about the resulting curve.

For diffusion: As the aerosol diameter increases the curve moves to the left. As the collector diameter increases the curve moves to the right.

For inertia: As the aerosol diameter increases the curve moves to the left and up. As the collector diameter increases the curve moves to the right and down.

For interception: As the aerosol diameter increases the curve moves up. As the collector diameter increases the curve moves down.

The ordinate of Fig. 2.2 is the penetration of the filter which is defined as (1 - collection efficiency).

Very little is known about the combined effects of inertia and diffusion, which are of particular importance for particles between 0.1-1.0 μm diameter. There is, also, considerable disagreement on which collection mechanism becomes dominant in a given size range. For instance, for the aerosol size range 1-2 μm diameter, Doganoglu[23] reported that gravity and inertia are dominant whereas Knettig[24], stated that only inertia is significant. For the same range and comparable gas velocities, McCarthy[25] concluded that interception and diffusion are dominant which is in direct disagreement with Doganoglu.

2.3 Effect of Aerosol Size on Collection Efficiency

It has been well established experimentally and theoretically that for fine particles the collection efficiency decreases with decreasing particle size. Further, it is generally accepted that this trend continues down to

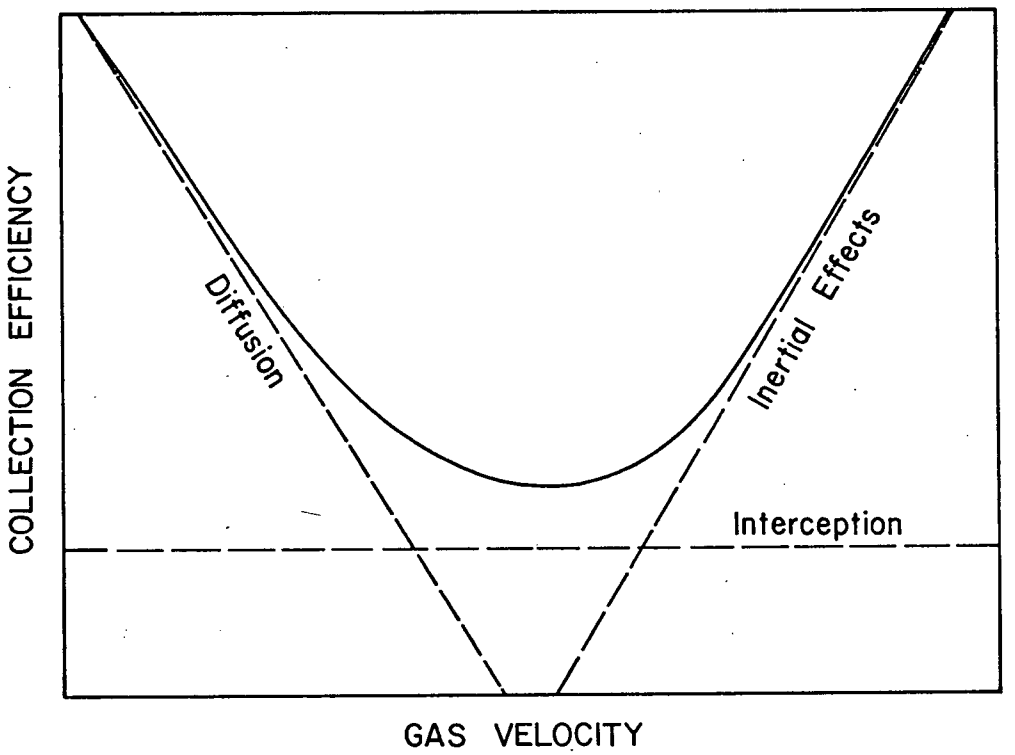

Fig. 2.1 The Effect of Gas Velocity on Collection Efficiency

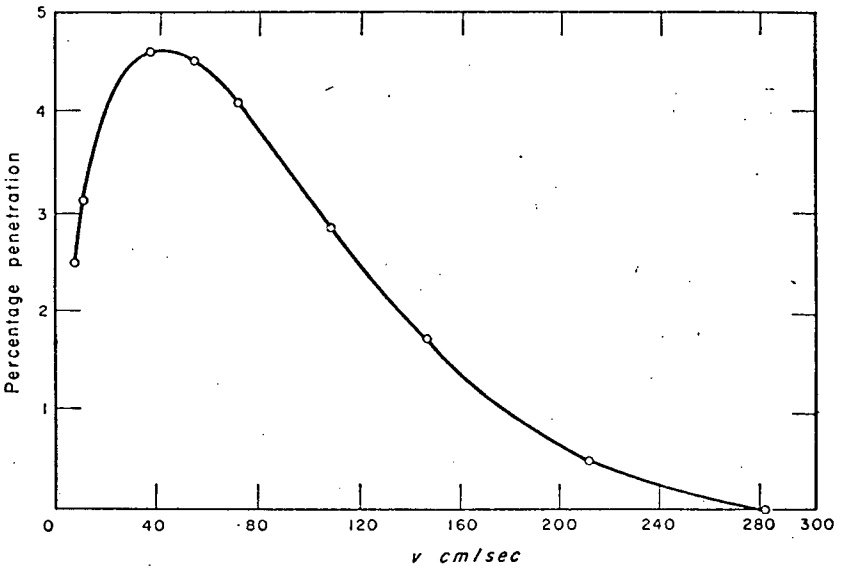

Fig. 2.2 Velocity Penetration Curve (Ramskill and Anderson[26])

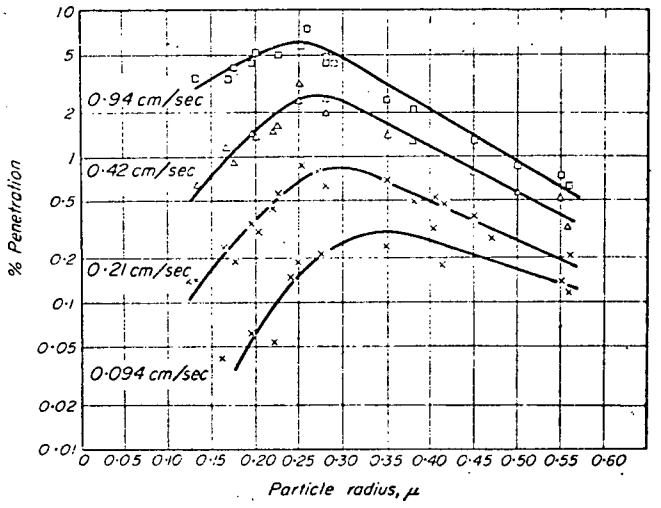

Fig. 2.3 Efficiency of a Glass Fibre Mat as a Function of Particle Size and Flow Rate (Thomas and Yoder[27])

Note: Penetration = (1 - collection efficiency)

about 0.3 μm after which the diffusional effect becomes dominant and increases the collection efficiency once again.

Fruendlich[28] showed that minimum collection occurred with aerosols between 0.2-0.4 μm in diameter. Chen[29], in experiments with 0.15 μm diameter aerosols, observed a minimum only for velocities below 4 cm/sec and La Mer[30] found no minimum collection efficiency even down to aerosols of 0.02 μm diameter. Thomas and Yoder[27] pointed out that the particle size producing the minimum collection efficiency increased with decreasing gas velocity (Fig. 2.3). Thus, once again, there is disagreement.

2.4 Effect of Collector Size and Bed Depth on Collection Efficiency

Most workers, who used collectors of various sizes, have shown that the collection efficiency increases with decreasing collector size. Also the efficiency increases exponentially with bed depth obeying Eq. 3.4 (see Chapter 3), i.e., EBT is proportional to $1 - \exp(-b.H)$ where 'b' is a constant.

2.5 Effect of the Direction of Gas Flow on Collection Efficiency

Work by Paretsky[31], Gebhart[32], Thomas[27], and Figueroa[20], demonstrated that gravity plays a small role in collection, by comparing bed efficiencies for upflow and downflow. However, Thomas showed that gravity can be important in collection of aerosols down to 0.3 μm in diameter for velocities between 1 and 4 cm/sec (see Figs. 2.4 and 2.5). At higher velocities the effect of the direction of flow on the collection of submicron particles reduces and can be assumed negligible at a velocity greater than 20 cm/sec.

2.6 Bounce-off and Re-entrainment

Bounce-off may occur with solid aerosols due to elastic collisions between the aerosol and collector surface and thus presents a problem in predicting the overall collection efficiency. Furthermore, there is the

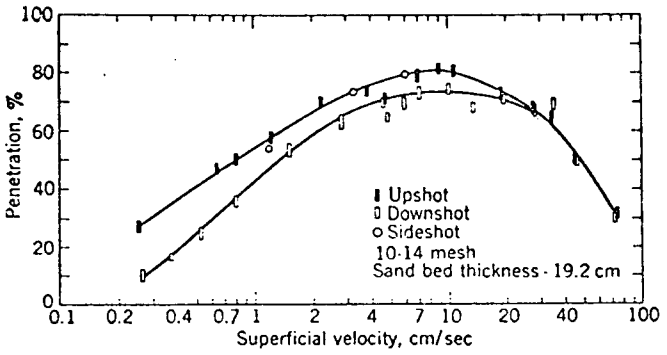

Fig. 2.4 Velocity Penetration Curve for 1.1 μm aerosol and 10-14 Mesh Sand (Paretsky[31])

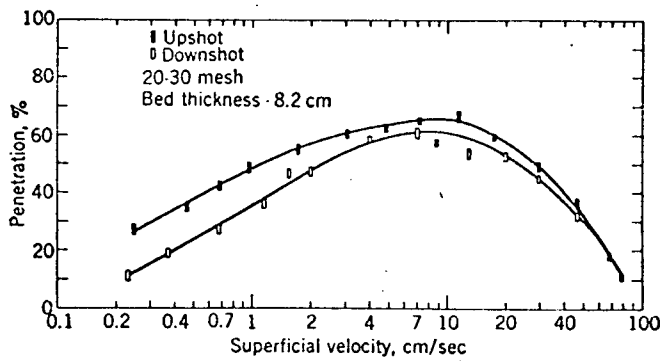

Fig. 2.5 Velocity Penetration Curve for 1.1 μm aerosol and 20-30 Mesh Sand (Paretsky[31])

possibility that re-entrainment[33] may occur if the gas velocity is high enough to detach deposited particles. Jordan[34] noted that velocities of 100 m/sec were needed to dislodge individual aerosols 2 μm in diameter from a glass slide and up to 4.5 m/sec to dislodge 10 μm diameter particles. Thus re-entrainment should be negligible in granular bed filtration where interstitial velocities are generally below 1-10 m/sec. There is, however, the phenomena observed by Leers[35] where particles deposit on one another to form "trees" and "chains". In this case much weaker forces are needed to break the adhesion of these chains.

Walkenhorst[36] concluded from his experiments on layers of wire gauze that

i) particles below 0.5 μm diameter adhere well after collision and are not removed even at gas velocities exceeding 6 m/sec

ii) for particles with diameters up to 1 μm, bounce-off may occur, as the velocity is increased the effect decreases due to enhanced inertial deposition

iii) for particles with diameters greater than 1 μm, increased inertial deposition outweighs any increased failure of adhesion.

The chances of bounce-off and re-entrainment can be reduced by coating the surface of the collectors with a non-volatile liquid such as dioctyl phthalate (DOP). Furthermore, retention may be improved by electrostatic charging of the aerosol (Balasubramanian[37], Mazumder[38]).

2.7 Review of Experimental and Industrial Studies Carried out on Granular Beds

Tables II and III provide a summary of work reported in the literature on the filtration of aerosols using granular beds. The information was obtained from the given references and converted into consistent units.

TABLE II. EXPERIMENTAL STUDIES

Researcher	Aerosol Type	Aerosol Diameter μm	Collector Type	Collector Diameter μm	Gas Velocity cm/sec	Column Diameter cm	Bed depth cm	Dominant Collection Mechanisms; Remarks
Katz and Macrae[39]	D.O.P. mist	0.3	Granular charcoal	470-910	16	10.6	2.8	Diffusion; work based on gas mask studies
Meissner and Mickley[7]	Sulphuric acid mist	2-14	Aluminum silicate	45-147	32-62	5	8-25	Inertial impaction; efficiency independent of mist concentration and bed age; study on fluidized beds
			Silica gell	57	35-78	5	8-25	
			Glass beads	254	37-85	5	8-25	
Ramskill and Anderson[26]	Sulphuric acid mist	0.3	Fibrous filter	--	5-280	--	81	Diffusion and inertia; determined an aerosol size with a minimum collection efficiency
	D.O.P.	0.2-0.8			5-280		81	
Thomas and Yoder[27]	D.O.P.	0.24-1.8	Lead shot	1500	0.75-1.5	3.8	90	Diffusion and gravity; studied upflow and downflow; electrical effects; determined an aerosol size with minimum collection efficiency
	Polystyrene latex	0.6-1.2	Sand	360-1600	0.1-2.2	3.8	3.6-7.6	
Anderson and Silverman[40]	Genetian violet	0.5	Polystyrene beads	323	25.4	3.5	2.54	Inertia; studied electrical effects; based on a fluidized bed
Yoder and Empson[41]	D.O.P.	0.2-2.0	Sand	360-1600	0.1-2.2	--	3.6	Diffusion; determined an aerosol size with a minimum collection efficiency, the size decreases with increasing velocity
	Polystyrene latex	0.5-1.2						
Scott and Guthrie[42]	D.O.P.	0.5-1.1	Silica gel	89	3-15	5.1	19.3-36	Diffusion; efficiency not affected by aerosol concentration
Silverman[43]	Uranine	0.25,0.97 7.03	Epoxy resin	102	2.5-6	--	1	Diffusion, inertia and interception; velocity for minimum collection found for each aerosol, where diffusion and inertia are weakest
Jackson and Calvert[44]	Fuel oil mist	6	Glass spheres	12700	183-762	35.6	15.2	Mainly inertial impaction; flow in the horizontal direction
			Berl saddles	12700	183-762	35.6	15.2	
			Raschig rings	12700	183-762	35.6	15.2	
			Intalex saddles	12700	183-762	35.6	15.2	
Mazumder and Thomas[38]	Uranine	0.16	Polystyrene spheres	1000	6-36	6	1.5-3	Mainly inertial impaction, studied improvement in collection efficiency due to electrical effects
			Copper spheres	3000	6-36	6		
			Epoxy resin	2000	6-36	6		

Table II (continued)

Researcher	Aerosol Type	Aerosol Diameter μm	Collector Type	Collector Diameter μm	Gas Velocity cm/sec	Column Diameter cm	Bed depth cm	Dominant Collection Mechanisms; Remarks
Calvert[45]	Fuel oil	1-1.8	Raschig rings Bed saddles	12700 12700	900 900	35.6 35.6	15	Inertial impaction
Black and Boubel[2]	Ammonium chloride	0.52	Glass shot	25	4-12	5.1	12.3	Interception and diffusion; studies on a fluidized bed; bed age and aerosol concentration play no effect on collection efficiency
Paretsky[31]	Polystyrene latex	1.1	Sand	841-1650	0.3-8.0	2.5-5	3-7-1.9	Mainly due to inertia and diffusion; upflow and downflow tests indicate gravity plays a role in collection
Yankel, Jackson and Patterson[46]	D.O.P.	0.67-1.4	Alumina	260	2.5-25	5.1	2.5-10	Interception, some diffusion; efficiencies decreased with increasing gas velocity; fixed and fluidized beds, upflow only
Gebhart, Roth and Stahlhofen[32]	Polystyrene	0.1-2.0	Glass beads	185-4000	0.7-14.2	8	10-40	Diffusion dominant for aerosols less than 0.7 μm diameter, gravity dominant for aerosols greater than 0.7 μm diameter; studies on upflow and downflow
Knettig and Beeckmans[24]	Methylene blue	0.8-2.9	Glass beads	425	8.8-24.6	12.7	1-12	Inertia; studies on fixed and fluidized beds
Doganoglu[23]	Methylene blue D.O.P.	1.1-1.75	Glass beads	110-600	2-45	15	8-12	Gravity dominant for gas velocity less than 8 cm/sec, inertia dominant for gas velocity greater than 8 cm/sec; studies on fixed and fluidized beds
Figueroa[20]	Polystyrene latex Methylene blue	0.5-2.0 1-2.0	Plastic beads Sand	305-495 680	3-18.5	10	3-9	Inertia and diffusion; studies on fixed and fluidized beds, upflow and downflow; high collection on plastic beds due to electrical effects
First and Hinds[47]	D.O.P. Polystyrene latex	0.8 0.36-1.1	Fibreglass mat	100-600	254-1524	7.6	1-95	Diffusion at low velocities, inertia at high velocities; bounce-off at high velocities
Doganoglu, Jog and Clift[48]	D.O.P.	0.6-3.0	Glass ballotini Glass spheres Copper shot	108-596 546 214	10-70 60-300 60-300	15	3-5	Inertia at high velocities, interceptions and gravity at low velocities
Azaniouch[49]	Na_2SO_4	5.2	Granular $CaCO_3$	3300	60-180	5	5-50	Mainly due to gravity and inertia; bounce-off occurs

TABLE III. INDUSTRIAL STUDIES

Researcher	Aerosol Type	Aerosol Diameter μm	Collector Type	Collector Diameter μm	Gas Velocity cm/sec	Remarks
Fairs and Godfrey[50]	Sulphur	80-10	Graphite	3000-13000	64	Panel bed filter used in removing fumes from an acid plant burning sulphur
Egleson[6]	Coal dust and ash	--	Coke particles	3175-10160	5-12	Filtration of dust residue from a coal gasification pilot plant, continuous operation of a packed bed filter; column diameter 30.5 cm and bed depth 259 cm
Englebrecht[5]	Dust	--	Steel turnings Sand	1000-6000 1000-6000	25-80	Study of a 'Lurgi' M.B. gravel bed filter; continuous operation with filtered dust removed by vibration of the bed, operation at 660°F
Black and Boubel[2]	NH_4Cl	0.52	Glass shot	250	4-12	Fluidized bed operating continuously; collection due to interception, diffusion and electrostatic forces; column diameter 5 cm, bed depth 10-30 cm
Squires and Pfeffer[3]	Power station fly ash	--	Sand	760	6	Study of a panel bed filter; continuous operation using a "puff-back" method to clean the filter

Table III (continued)

Researcher	Aerosol Type	Aerosol Diameter μm	Collector Type	Collector Diameter μm	Gas Velocity cm/sec	Remarks
Strauss and Thring[51]	Fumes	--	Crushed brick	2500-8000	25-100	Horizontal granular filter for fumes from oxygen-lanced open hearth steel furnace
Cook, Swany and Colpitts[52], Rush and Russel[54]	Fluoride particles	--	Alumina	--	--	Combination of granular bed (fluidized) and a filter bag for removal of fluorides in waste gases from aluminium smelting
Kalen and Zenz[4]	Catalyst	2-60	Sand	760	--	Filtering effluent from a cat cracker using a 'Ducon' granular bed filter; continuous operation using puff-back for cleaning
Dumont[55]	Radioactive Carbonaceous particles	--	Alumina Sand	--	--	Fluidized bed operation of a granula bed
Böhm and Jordan[56]	Na_2O_2	1.4	Sand	280-9700	2-5	Studies on a multilayer sandbed filter, for use with a liquid metal fast breeder reactor

Table III (continued)

Researcher	Aerosol Type	Aerosol Diameter μm	Collector Type	Collector Diameter μm	Gas Velocity cm/sec	Remarks
Reese[57]	Fly ash	--	Sand	3000-6000	--	A dry packed bed scrubber for removal of fly ash from flue gas from lumber mill operation; continuous recycling of the sand

2.8 Empirical Equations

Based on experimental and theoretical studies a large number of empirical equations have been suggested to predict the single collector efficiency. These equations, which account for one or more collection mechanisms, vary considerably in accuracy and range of application. Tables IV and V summarize these equations.

2.9 Theoretical Work on the Flow Field Within a Granular Bed

In the analysis of the filtration process,[70,71] the granular bed filter is usually assumed to be a homogeneous bed of spherical particles of uniform size through which the dusty gas flows. The first step in the calculation of the filter efficiency is to determine the flow field in the filter. The almost universally used model is to describe the gas flow round a single cylinder or sphere and then to extend this to calculate flow patterns and particle trajectories in a complex of spheres or fibres. However, to describe the geometrical structure of a granular bed is an extremely complex problem. Some idea of the complexity can be gained by considering the ordered packing of monosized spheres. There are six different ways in which the spheres may be packed, each with its own unique porosity. Although these packings have regular geometrical arrangements on which calculations may be based, one is really concerned with the void space through which the carrier gas will flow. These void spaces are so complex that any attempt at a geometrical description must introduce considerable simplification.

One model considers the spheres as obstacles to an otherwise straight flow of fluid without taking into account the effect of neighbouring spheres. This is called the 'loose' filter model[72]. However, this model gives a rather poor approximation for the flow field in an actual granular bed.

Another approach is the concept of a 'unit cell' developed by Happel[73]

TABLE IV. EMPIRICAL EQUATIONS FOR SINGLE COLLECTOR EFFICIENCY BASED ON ONE COLLECTION MECHANISM

Collection Mechanism	Researcher	Equation	Remarks	Equation No.
Inertia	Paretsky[31]	$EI = 2.0ST^{1.13}$	$St < 4.4 \times 10^{-2}$ $2000\ \mu m < d_c < 700$	2.1
	Langmuir and Blodgett[13]	$EI = 1 + \frac{0.75\ \ln(2St)^{-2}}{St - 1.214}$	For creeping flow	2.2
		$EI = \frac{St^2}{(St + 0.05)^2}$	For potential flow, $St > 0.02$	2.3
	Knettig and Beeckmans[24]	$EI = 3.76 \times 10^{-3} - 0.464St + 9.68St^2 - 16.2St^3$	$0.3 > St > 0.0416$, based on the experimental data of Herne[58]	2.4
	Landahl and Hermann[59]	$EI = \frac{St^3}{St^3 + 0.77St^2 + 0.22}$	$Re = 10$	2.5
	Behie and Beeckmans[60]	$EI = 0$	$St < 0.083$	
		$EI = 3.6 \times 10^{-3} - 0.232St + 2.42St^2 - 2.03St^3$	$0.6 < St < 0.083$	2.6
		$EI = \{St/(St + 0.5)^2\}$	$St > 0.06$	

Table IV (continued)

Collection Mechanism	Researcher	Equation	Remarks	Equation No.
Interception		$ER \simeq 2NR$	$St \to \infty$, inertia of the particles causes them to travel in a linear direction	2.7
		$ER \simeq \frac{3}{2} NR^2$	$St \to 0$, particles with no inertia follow the gas streamlines	2.8
	Friedlander[61]	$ER = 2Re^{\frac{1}{2}} NR^2$		2.9
	Natanson[62]	$ER = \frac{NR^2}{(2 - \ln Re)}$		2.10
Diffusive deposition	Langmuir[13]	$ED = \frac{1.71\ Pe^{-2/3}}{(2 - \ln Re)^{1/3}}$		2.11
	Johnstone and Roberts[63]	$ED = 8Pe^{-1} + 2.3\ Re^{1/8}\ Pe^{-5/8}$	Based on the analogy between heat and mass transfer	2.12
	Stairmand[64]	$ED = 2.83\ Pe^{-\frac{1}{2}}$	Potential flow	2.13
	Bousinesque[65]	$ED = 3.15\ Pe^{-\frac{1}{2}}$	Potential flow	2.14

Table IV (continued)

Collection Mechanism	Researcher	Equation	Remarks	Equation No.
	Tardos[66]	$ED = 3.96\ Pe^{-2/3}$	Creeping flow	2.15
	Natanson[62]	$ED = \frac{2.92\ Pe^{-2/3}}{(2 - \ln Re)^{1/3}}$	Pe >> 1, creeping flow	2.16
Gravitational deposition	Ranz and Wong[67]	$EG = \frac{Us}{U} = NG$		2.17

TABLE V. EMPIRICAL EQUATIONS FOR SINGLE COLLECTOR EFFICIENCY BASED ON COMBINATIONS OF COLLECTION MECHANISMS

Collection Mechanisms	Researcher	Equation	Remarks	Equation No.
Diffusion and Interception	Friedlander[61]	$EDR = \frac{6\ Re^{1/6}}{Pe^{2/3}} + 3\ NR^2\ Re^{\frac{1}{2}}$		2.17
Inertia and Interception	Davies[68]	$EIR = 0.16\ [NR + (0.5 + 0.8\ NR)\ St - 0.105\ NR\ St^2]$	$Re = 0.2$	2.18
Diffusion, Inertia and Interception	Davies[68]	$EDIR = 0.16\ [NR + (0.5 + 0.8\ NR)\ (\frac{1}{Pe} + St) - 0.105\ NR\ (\frac{1}{Pe} + St)^2]$		2.19
Gravity and Inertia	Doganoglu[23]	$EIG = 2.89\ St + 6.87\ NG$ $EIG = 5.83 \times 10^{-2}\ Re\ St + 1.42\ NG$	$d_c = 110$ m $d_c = 600$ m	2.20 2.21
Inertia, Diffusion, Interception and Gravity	Schmidt[69]	$E = 3.97\ St + (8\ Pe^{-1} + 2.3\ Re^{1/8}\ Pe^{-5/8}) + 1.45\ NR + NG$	Where $E = EI + ED + ER + EG$	2.22

and Kuwabara[74]. It assumes the spheres are homogeneously distributed and the fluid may be divided up into spherical regions or cells, each corresponding to one solid sphere. The volume of the cell is related to the porosity in such a way that the vol. of fluid/vol. of cell equals the porosity (ε). It is assumed the flow is purely viscous thus enabling the velocity of the streamlines and their direction at any point to be calculated.. The ideas of this concept have been used theoretically and experimentally by many workers[1,75,76,77] and the model has been extended to higher Reynolds numbers by le Clair and Hamielec[72].

Neale and Nader[78] approached the problem from a slightly different point of view. They assumed that the sphere is surrounded by a spherical fluid envelope whose dimension is computed in the same way as in the Happel-Kuwabara model with a modification that considers the entire sphere swarm as one large exterior porous mass. A different approach is to consider the bed of granules as a random cloud of identical particles and to use statistical methods of analysis. For example, Tam[79], interpreted the flow as the most probable one around one of the spheres. Creeping flow and no particle/particle interaction were assumed.

Statistical and unit cell models are still in their infancy and, although they describe reasonably well the flow through a packed bed, their complexity will probably preclude their use in engineering designs. Simpler and more easily applied models are still preferred.

CHAPTER 3

THEORY

3.1 Introduction

The predictive model of the collection of aerosols by a granular bed is based on a single granule within the bed. The overall bed collection efficiency (EBT) is first related to the single collector efficiency (EB). The latter is then expressed in terms of dimensionless groups, which characterize the design and operating conditions of the bed.

In defining the filtration process of aerosol removal by granular beds three sets of factors have to be considered, (i) the dispersed aerosol particles, (ii) the dispersion medium or fluid, and (iii) the collection medium. In this study only spherical aerosols and collectors are considered. The dispersion medium is air at atmospheric temperature and pressure, the effects of temperature and pressure variations being assumed negligible.

3.2 The Overall Bed Collection Efficiency (EBT) as a Function of the Single Collector Efficiency (EB)

In order to determine the relationship between EBT and EB a simplified model of the bed is used. The bed consists of a three dimensional array of uniform granules (diameter d_c) of a depth H. The voidage fraction of the bed is ε and each collector exhibits a collection efficiency of EB.

The analysis is based on an aerosol particle balance over a very small element of bed (see Fig. 3.1).

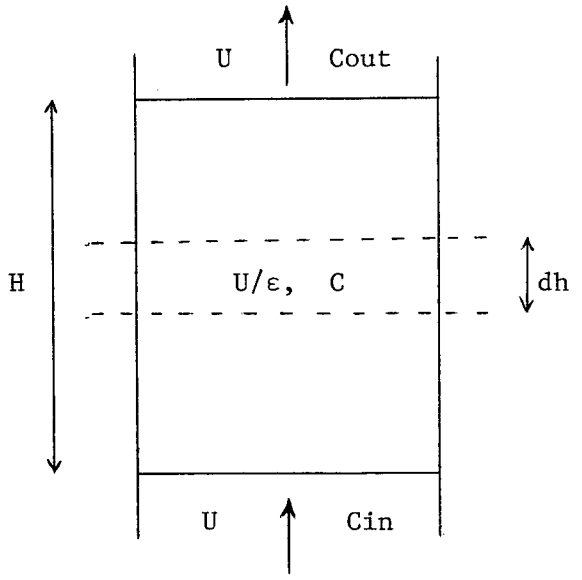

Figure 3.1. Schematic Diagram of the Granular Bed

The rate of aerosol removal is equal to the rate of change of the number of aerosol particles entering and leaving the element. Therefore for a unit cross section of bed it can be written

$$U\,dC = -\,C(U/\varepsilon)\;EB \times As\;dh \qquad [3.1]$$

where U = superficial gas velocity

U/ε = interstitial gas velocity

C = aerosol concentration in the element

As = projected area of a collector into the direction of flow

x = number of collectors per unit volume of bed = $6(1 - \varepsilon)/(\pi\, d_c^{\,3})$

The rate of removal of aerosol particles by the element for a unit cross-section of bed can be derived in the following manner.

The total area of collector available for filtration is EB x As dh and therefore the volume of gas swept clean by the collectors per unit time is (U/ε) EB x As dh.

Since the concentration of the aerosol is C, the rate of removal of aerosol is given by C(U/ε) EB x As dh.

Integrating equation 3.1 over the whole bed we have

$$Cout/Cin = \exp(-x\ As\ EB\ H/\varepsilon) \qquad [3.2]$$

where C = Cin at h = 0

C = Cout at h = H

Since $x = 6(1 - \varepsilon)/(\pi d_c^3)$

and $As = \pi d_c^2/4$ it follows that

$$Cout/Cin = \exp\{-1.5(1 - \varepsilon)H\ EB/\varepsilon\ d_c\} \qquad [3.3]$$

The overall bed efficiency is then given by

$$EBT = (Cin - Cout)/Cin = 1 - \exp\{-1.5(1 - \varepsilon)H\ EB/\varepsilon\ d_c\} \qquad [3.4]$$

Some workers prefer to use the bed penetration (P) to express the performance of a granular bed, which is defined as

$$P = 1 - EBT = Cout/Cin \qquad [3.5]$$

Equation 3.4 can be rearranged to give

$$EB = -\ln(1 - EBT)\ d_c\ \varepsilon/1.5(1 - \varepsilon)H \qquad [3.6]$$

Equation 3.6 allows the single collector efficiency to be calculated once EBT, ε, H and dC are either known or measured.

3.3 Calculation of Single Collector Efficiency from Basic Design and Operating Variables

In order to calculate the single collector efficiency (EB) an equation based on the design and operating variables of the filter must be developed. In this study two methods of producing this equation were considered. The first assumes that the individual collection mechanisms act independently of one another. Therefore the calculation of EB consists of calculating the contribution of the individual effects of each collection mechanism and summing them in some manner. The second method considers the individual collection mechanisms are interrelated and EB is calculated directly from the basic variables.

In the first method the individual collection efficiencies are based on the dimensionless groups describing the individual collection mechanisms.

Thus calculation of the individual efficiency for:

inertia (EI) is based on Re and St,

interception (ER) is based on Re and NR,

diffusion (ED) is based on Re and Pe, and

gravity (EG) is based on Re and NG.

If electrical effects are ignored, then single collector efficiency can be estimated by simple summation.

$$E = EI + ER + ED + EG \qquad [3.7]$$

However, this summation is an approximation and is only valid when one mechanism dominates. Furthermore, as mentioned in Chapter 1, the efficiency of an isolated collector differs when it is surrounded by other collectors. Therefore the value of E must be modified by some correction factor to obtain the true single collector efficiency within the bed (EB). For example, Eq. 3.7 may be rewritten as

$$EB = \alpha_1 ED + \alpha_2 ER + \alpha_3 ED + \alpha_4 EG \qquad [3.8]$$

or

$$EB = \alpha E \qquad [3.9]$$

Using these methods many equations (see Chapter 2) have been developed with varying degrees of accuracy and applicability. Several forms of these equations were fitted by multiple regression techniques to the experimental results of this study and will be discussed in Chapter 7.

The alternate method is to develop equations from basic variables such as gas velocity, aerosol and collector properties. The single collector efficiency (EB) was calculated directly from these variables and avoided the problem of having to combine the effects of the individual mechanisms. In this case the value of EB was determined using an equation of the form:

$$EB = f(d_a, d_c, U) \qquad [3.10]$$

Equations of this type were also fitted to the experimental results

using multiple regression.

3.4 Multiple Regression

All regressions were carried with the aid of computer programmes called MREG and CONREG developed by the Forestry Department at U.B.C. Multiple regression is a statistical technique for analysing a relation between a dependent variable Y and a set of independent variables X_1, X_2, X_3 ... X_n where n is the number of independent variables.

A relation of the form

$$Y = \alpha_0 + \alpha_1 X_1 + \alpha_2 X_2 + \alpha_3 X_3 \ldots \alpha_n X_n \qquad [3.11]$$

is chosen where the intercept of the regression equation is α_0 and the coefficients α_1, α_2 ... α_n are estimated by the least squares method. In the present work the dependent variable is the single collector efficiency EB and the independent variables are either the dimensionless groups St, ND, NR etc. or combinations of the basic variables, i.e., d_a^2/U.

The programme reads m sets of data in the form of EB and the corresponding independent variables and places them in a matrix of the form

X_1	X_2	X_3	...	X_n	Y
X_{11}	X_{21}	X_{31}		X_{n1}	Y_1
X_{12}	X_{22}	X_{32}		X_{n2}	Y_2
⋮				⋮	
X_{1m}	X_{2m}	X_{3m}		X_{nm}	Y_m

The linear regression of Y on two or more independent variables is called the multiple linear regression. The general form of a multiple linear regression is:-

$$V_{Y.X} = \alpha_0 + \alpha_1 X_{1i} + \alpha_2 X_{2i} + \ldots \alpha_n X_{ni} \qquad [3.12]$$

where $V_{Y.X}$ is the mean of Y calculated from the regression, and

α_0, α_1, α_n ... α_n are described as population parameters

To indicate that the individual values of Y vary about the mean, it can be written as

$$Y_i = \alpha_0 + \alpha_1 X_{1i} + \alpha_2 X_{2i} \ldots \alpha_n X_{ni} + \varepsilon i \qquad [3.13]$$

Equation 3.13 implies that any Y value is due to the regression mean ($V_{Y.X}$) plus a deviation from the mean (εi).

The values of α_0, α_1 ... α_n cannot be obtained unless the whole population is measured. From a sample, taken from the population, the best estimates of these parameters are β_0, β_1 ... β_n. By the least squares principle these estimates are chosen to produce the least possible value for the sum of the squares of εi ($i = 1, 2 \ldots n$) when substituted for α_0, α_1 ... α_n, i.e.,

$$\sum_{i=1}^{n} \varepsilon i^2 = \min \sum_{i=1}^{n} (Y_1 - \beta_0 - \beta_1 X_{1i} - \beta_2 X_{2i} \ldots \beta_n X_{ni})^2 \qquad [3.14]$$

From Eq. 3.14 one can determine the approximate values of α_0, α_1 ... α_n by differentiating the equation first with respect to β_0, and then to β_1, β_2 ... and β_n. Solving for the values of β_0, β_1 ... β_n is done by matrix inversion carried out by the programme.

The programme has the facility to eliminate variables if the inversion causes the matrix to become singular. The programme also eliminates variables if their regression coefficient α_i causes their contribution to the value of Y_i to be negligible.

In order to select the best equation for predicting values of Y_i the programme provides calculations of the standard error of the estimate, residual variance, multiple correlation coefficient and variance ratio tests.

3.6 Pressure Drop through the Granular Bed

For a complete model of the granular bed it is necessary to be able to predict the pressure drop across it. Generally an equation of the Ergun[80] form has been found acceptable, where

$$\frac{\Delta P}{H} = a \frac{(1-\varepsilon)^2}{\varepsilon^3} \frac{\mu U}{d_c^2} + b \frac{(1-\varepsilon)}{\varepsilon^3} \frac{\rho_F U^2}{d_c} \qquad [3.15]$$

a and b are constants which lie in the ranges

$$710 > a > 120$$

$$4 > b > 0.8$$

The exact values of a and b depend on the shape of the collector particles and randomness of packing.

CHAPTER 4

EXPERIMENTAL WORK

4.1 Objectives of the Experimental Work

The experimental programme was designed to investigate the removal of aerosols suspended in a moving gas by a fixed granular bed and to generate data which could be readily analysed. Furthermore, it was hoped to develop equations from this data that could be used for future scale-up and design.

The specific objectives were to determine the effect on collection efficiency of (i) bed depth, (ii) gas velocity, (ii) aerosol size, (iv) collector size, and (v) direction of gas flow. Objective (i) is useful for testing the validity of Eq. 3.6, which can be written as

$$\ln(1 - EBT) = - 1.5(1 - \varepsilon)\, EB\, H/\varepsilon\, d_c \qquad [4.1]$$

Therefore a graph of $\ln(1 - EBT)$ versus H should be linear because for a given gas velocity voidage, single collector efficiency and collector diameter all remain constant for varying bed depths. Objective (v) would show whether gravity was a significant collection mechanism.

Many workers believed that electrical effects play a substantial role in collection[20,28,37], but were not sure how to quantify it. The present experiments were therefore designed to minimize all electrical effects by first passing the aerosol through a charge neutralizer. In addition, a column of copper was used to support the granular bed made up of metallic spheres. In this way the whole apparatus could be earthed. The electrical effects were therefore considered negligible and ignored.

4.2 Range of Variables Studied

The range of variables studied are summarized in Table VI.

TABLE VI. RANGE OF VARIABLES STUDIED

Variable	Range
Aerosol diameter	0.1 - 2.0 μm
Collector diameter	126 - 598 μm
Gas velocity	5 - 70 cm/sec
Bed depth	0.3 - 18 cm

4.3 Experimental Apparatus

Figure 4.1 gives a flow diagram of the equipment used for carrying out the experiments at superficial gas velocities ranging from 5 to 27 cm/sec. Details of purchased equipment are given in Table VII and of the particles and collectors in Table VIII.

After leaving the generator the aerosol was mixed with filtered bench air to produce the required gas flow through the granular bed. Because of the overall pressure drop throughout the system and the much higher flow of bench air, it was found that a back pressure was produced which prevented the flow of aerosol into the column. To remedy this, a small diaphragm pump was used to pass the aerosol into the main air flow.

The dusty gas was then passed through a neutralizer to remove residual electrical charges from the aerosol particles. The neutralizer was simply a chamber containing a radioactive source (1 millicurie of Krypton 85 gas). The Krypton gas was sealed in a stainless steel tube at atmospheric pressure.

The aerosol then passed through copper tubing to the column. To vary the flow rate through the bed, air could be bled off via a flow control valve before reaching the column. This removed the necessity of adjusting flow

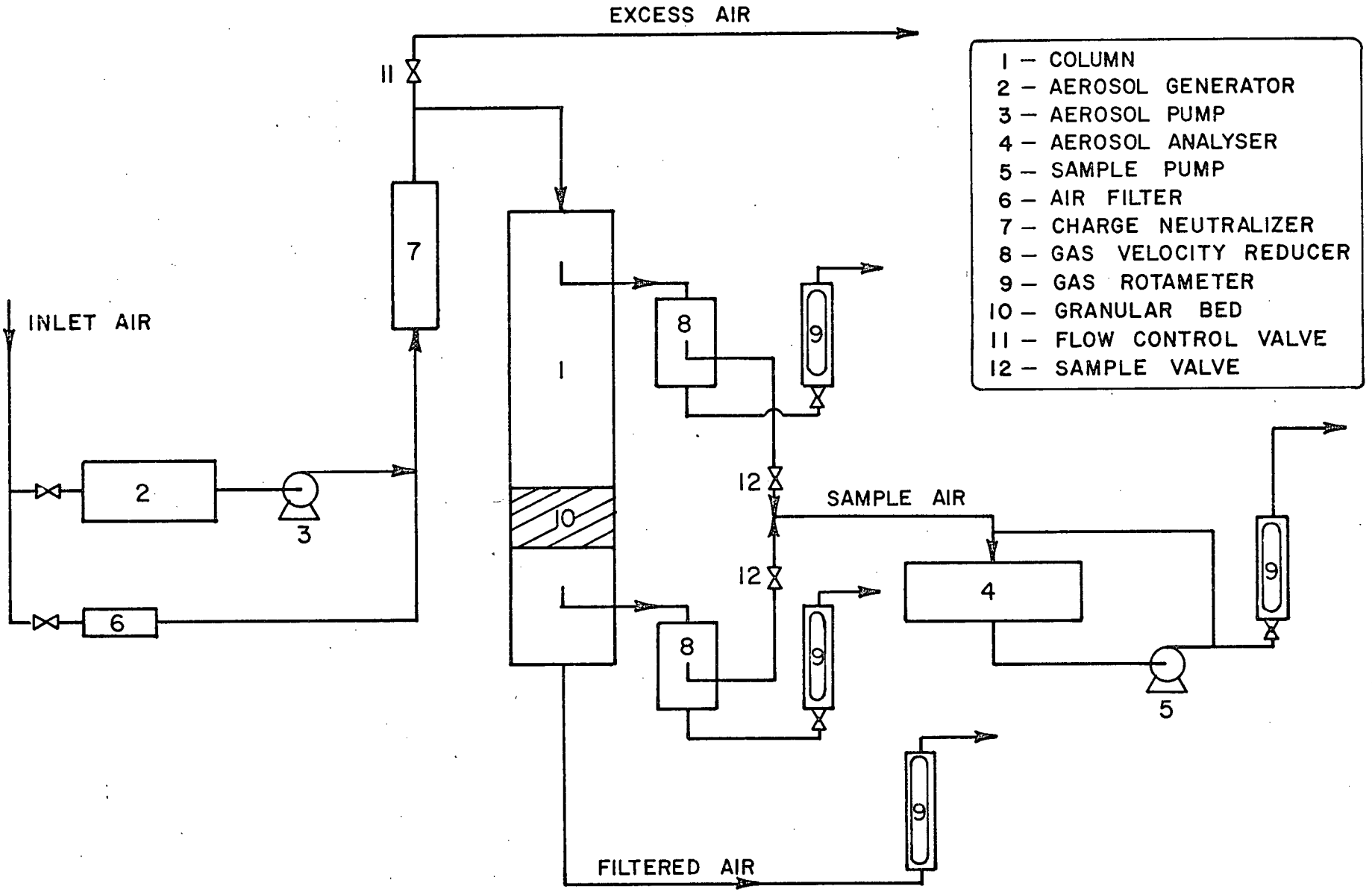

Fig. 4.1 Schematic Diagram of Equipment

TABLE VII. PURCHASED EQUIPMENT

Equipment	Manufacturer	Model
Aerosol particle generator	Royco	256
Aerosol particle sensor	Royco	241
Aerosol particle monitor	Royco	225
Digital display	Royco	264
Charge neutralizer	Sierra Instruments	7330
Hygrometer	Panametrics	2000
Oilless diaphragm pump	Gast Mfg. Corp.	DAA110
Vacuum pump	Gast Mfg. Corp.	0522-V4-G180DX

TABLE VIII. PARTICLES AND COLLECTORS

Aerosol Particle Size μm	Supplier	Material
0.109	Dow Chemical Co.	Polystyrene
0.500	Dow Chemical Co.	Polystyrene
0.600	Dow Chemical Co.	Polystyrene
0.804	Dow Chemical Co.	Polystyrene
1.011	Dow Chemical Co.	Polystyrene
2.020	Dow Chemical Co.	Polyvinyltoluene
Collector Size μm	**Supplier**	**Material**
598.1	Sherritt Gordon Mines Ltd.	Nickel powder
511.0	Sherritt Gordon Mines Ltd.	Nickel powder
363.9	Sherritt Gordon Mines Ltd.	Nickel powder
216.1	Sherritt Gordon Mines Ltd.	Nickel powder
126.0	Sherritt Gordon Mines Ltd.	Nickel powder
1800.0	Rona-B Lead Shot Ind.	Lead shot

rates at the aerosol generation section and ensured a constant aerosol concentration throughout each experiment.

Prior to venting, the gas flow was measured by a rotameter located downstream of the bed. Provisions were also made to measure the humidity of the vented gas.

4.3.1 The Column

This was basically a 7.6 cm diameter copper tube which could be easily separated into sections for introducing and removing the collector particles. The entering dusty gas was passed through a calandria to produce a uniform flow of gas before it entered the bed. The bed particles were supported on a fine wire mesh (approximately 64 μm aperture), which offered negligible resistance to the gas flow at the measured gas velocities. All the tubing from the neutralizer to the column was made of copper and the whole apparatus was earthed. Pressure taps were placed at the inlet and outlet of the bed and the pressure drop across the bed was measured by a mercury manometer. At the same level, but on the opposite side of the column, were placed the inlets for the sample probes (see Fig. 4.2).

The column was suspended at its centre and could easily be rotated in a vertical plane (see Fig. 4.4). This allowed the column to be operated in either the upflow or downflow mode by making some minor adjustments. These consisted of changing the position of the gauze bed support, rotating the column through 180° and altering the sampling and manometer tubing.

4.3.2 Sampling

The gas was sampled before and after the bed. Samples were removed in the direction of the gas flow via 0.9 cm diameter sharp edged probes located in the centre of the column.

The gas was continuously removed at a low rate into small chambers and out into the atmosphere via rotameters. From these chambers the gas could

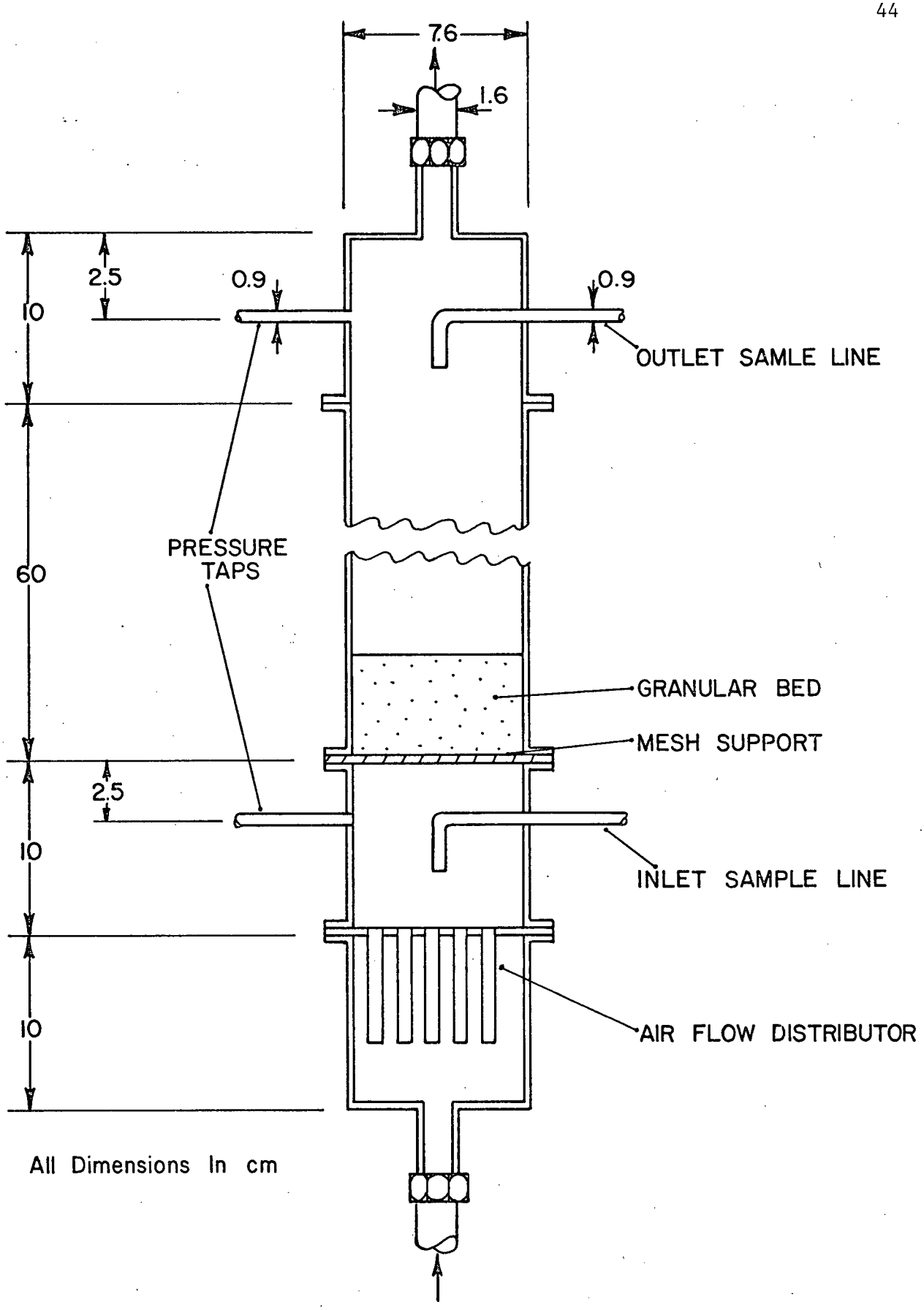

Fig. 4.2 Column Support for Granular Bed

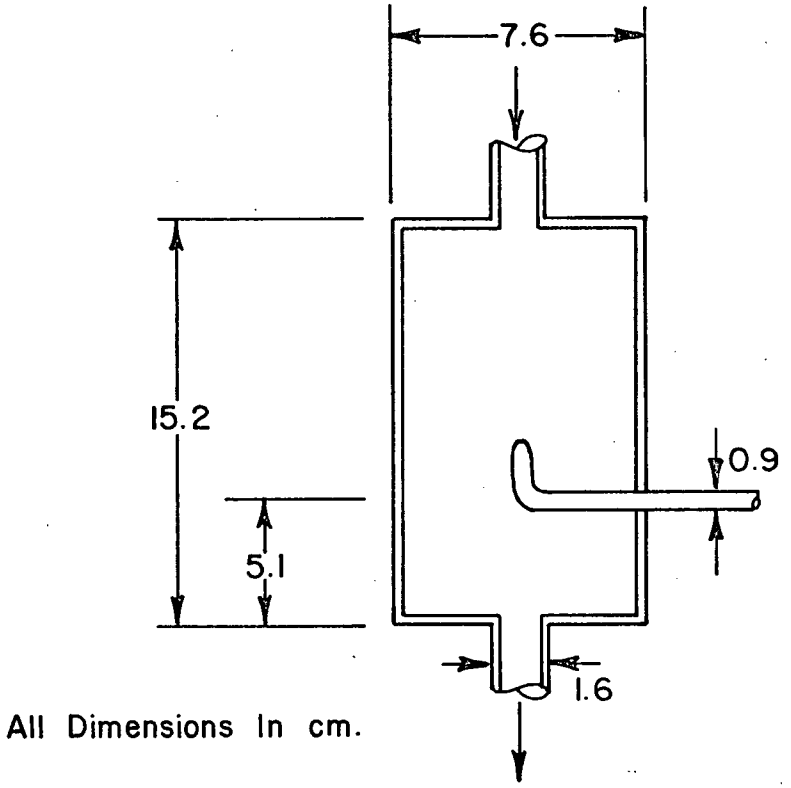

Fig. 4.3 Velocity Reducer

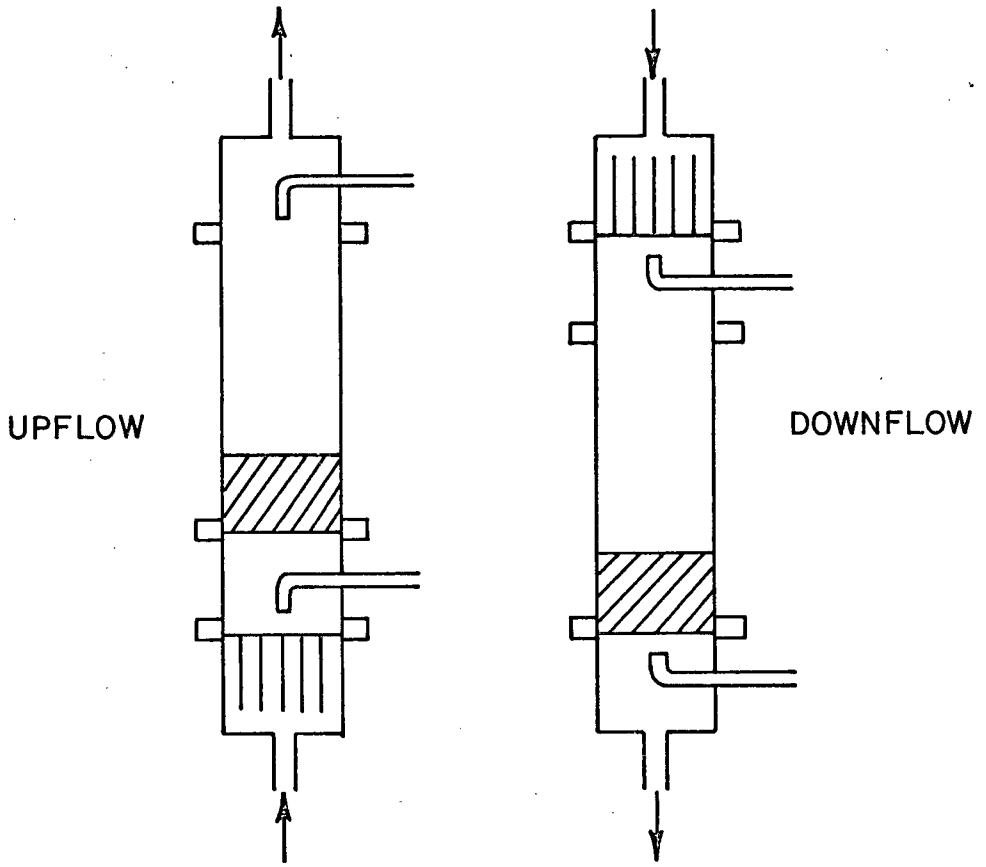

Fig. 4.4 Upflow and Downflow Operation of the Column

be sampled when necessary and directed to the particle counter. Samples could be obtained from either the gas entering the bed or exiting by opening the appropriate sample valve. The counter contained its own pump which allowed a larger volume of sheath air to be mixed with the sample before it entered the analyser cell. The discharge from the sample pump was measured by a rotameter and represented the sample flow.

No attempts were made to sample isokinetically as calculations suggested that the sampling rate had a negligible effect on the aerosol concentration for particles less than about 5 μm diameter[17]. This was also confirmed by a series of simple experiments.

The purpose of the velocity reducers (Fig. 4.3) was to dampen the variations in aerosol concentration within the column. These variations were caused by the aerosol generator and/or by deposited particles breaking away from the equipment walls.

The lines and probes were made as identical as possible for the inlet and outlet gas sampling trains. Errors inherent in the system would therefore be automatically eliminated when comparing aerosol counts.

4.4 Aerosol Particles

The aerosols used were of polystyrene latex with the exception of the 2.02 μm diameter aersol which was of polyvinyltoluene (provided by the Dow Chemical Company) and were generated by atomizing dilute suspensions of the latex particles. These particles were chosen because:

i) they are available in uniform sizes with low standard deviations (see electron micrographs Figs. 4.5 to 4.11)

ii) they could be generated and handled easily

iii) they could be generated at low concentrations which minimizes particle agglomeration and bed loading.

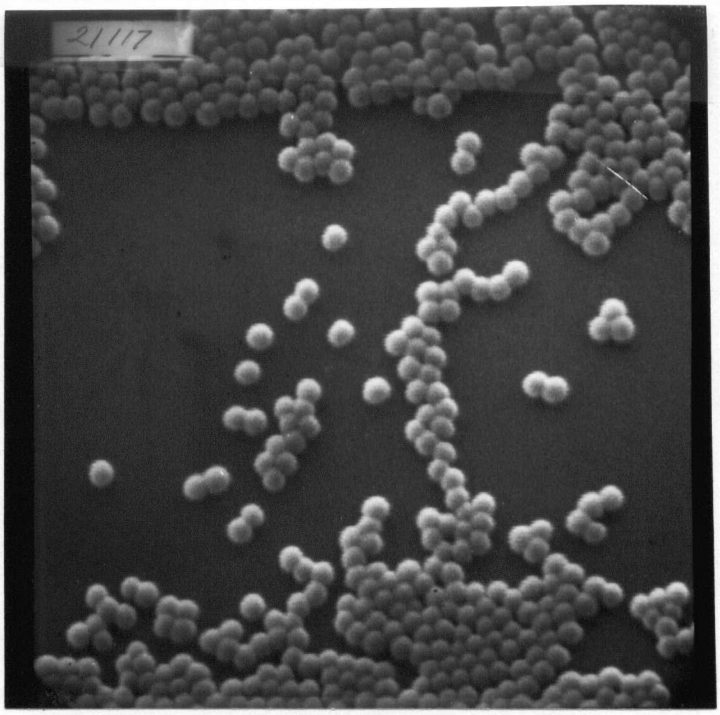

Fig. 4.5 Electron Micrograph of 0.109 μm diameter Latex Particles (Mag. 30,000 ×)

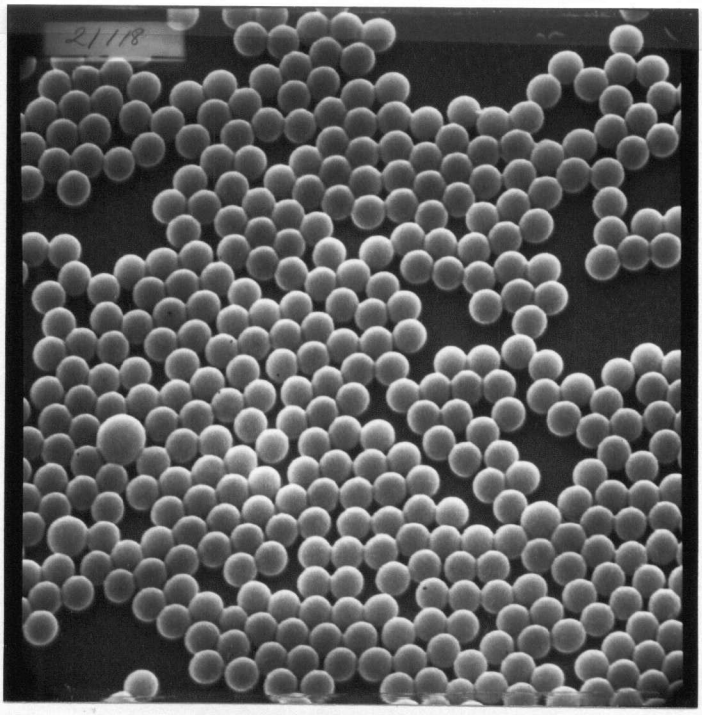

Fig. 4.6 Electron Micrograph of 0.50 μm diameter Latex Particles (Mag. 8,000 ×)

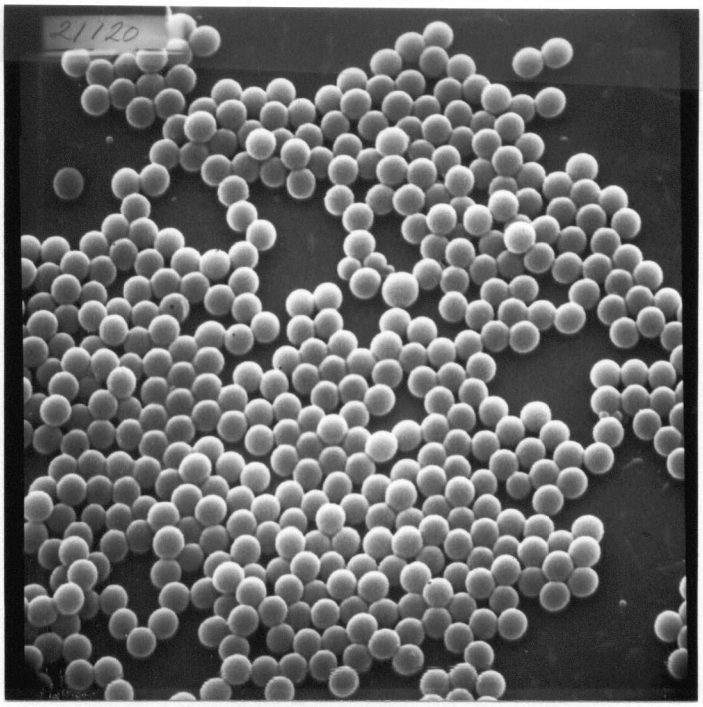

Fig. 4.7 Electron Micrograph of 0.60 μm diameter Latex Particles (Mag. 8,000 ×)

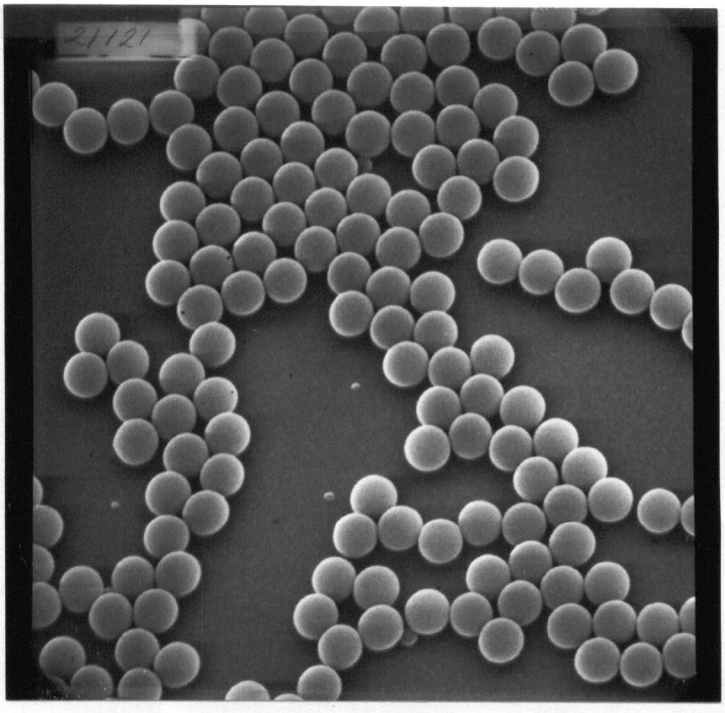

Fig. 4.8 Electron Micrograph of 0.804 μm diameter Latex Particles (Mag. 8,000 ×)

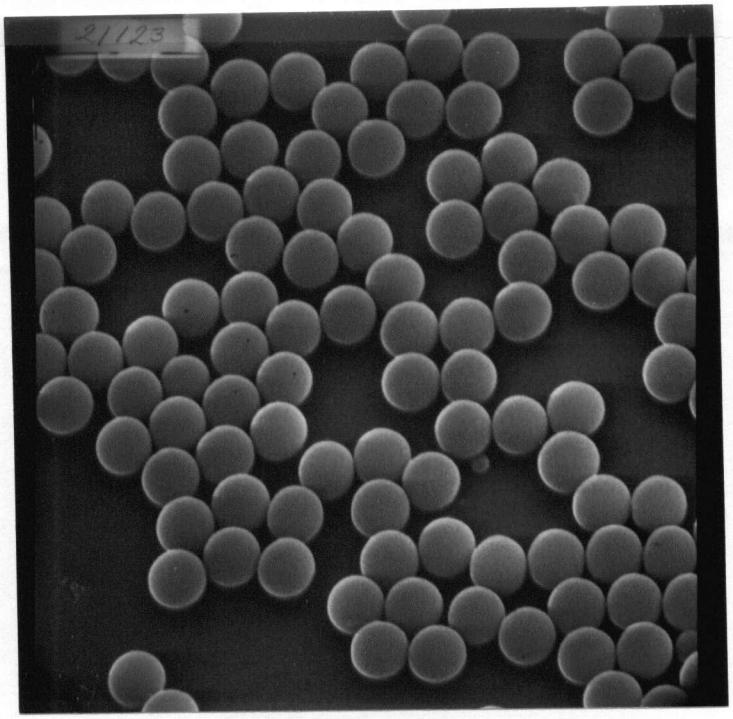

Fig. 4.9 Electron Micrograph of 1.011 μm diameter Latex Particles (Mag. 8,000 ×)

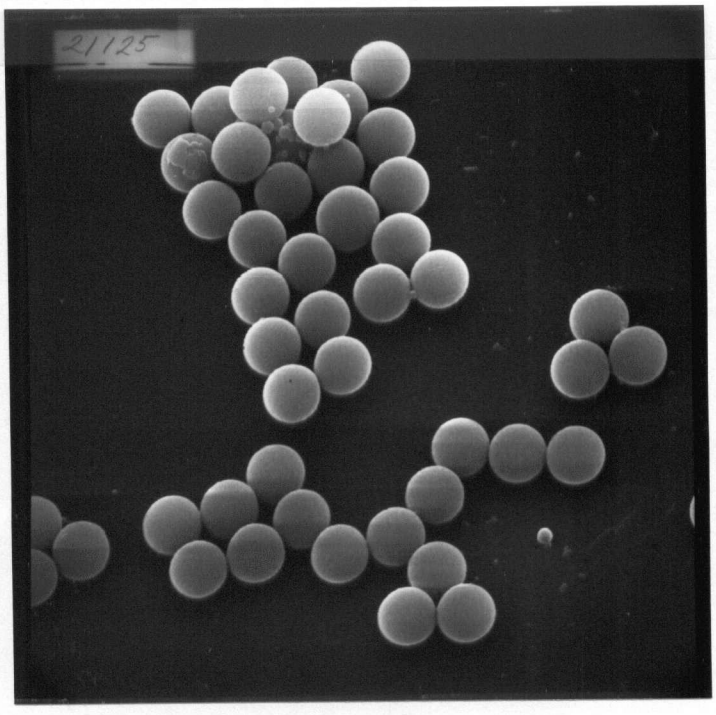

Fig. 4.10 Electron Micrograph of 2.02 μm diameter Latex Particles (Mag. 4,000 ×)

From the electron micrographs it can be seen that the particles are spherical, smooth and fairly uniform. However, in some cases (Figs. 4.8 and 4.10) a few very much smaller particles are also present. Properties of particles used are summarized in Table IX.

TABLE IX. PROPERTIES OF PARTICLES USED

Material	Diameter μm	Standard Deviation	Density gm/cc
Polystyrene	0.109	0.0027	1.05
Polystyrene	0.500	0.0027	1.05
Polystyrene	0.600	0.0030	1.05
Polystyrene	0.804	0.0048	1.05
Polystyrene	1.011	0.0054	1.05
Polyvinyltoluene	2.020	0.0135	1.027

4.5 Granular Bed Particles

Initial tests were carried out with 1.8 mm diameter lead shot. However, most experiments were performed with nickel shot obtained from Sherritt Gordon Mines Ltd. The sizes used are given in Table X.

Figures 4.11 to 4.16 are electron micrographs of each collector. It can be seen that they are fairly uniform and spherical. The surfaces are quite smooth but the larger collectors exhibit some surface irregularities which may increase their ability toccollect aerosols by providing more surface area.

4.6 Aerosol Generator

The aerosol was generated from a purchased hydrosol of latex particles after dilution with distilled water (about 0.1 ml of hydrosol to 30 ml of distilled water). The diluted hydrosol was atomized with clean air in a Royco aerosol generator model 256. The atomizer consisted essentially of a

TABLE X. CHARACTERISTICS OF NICKEL SHOT

Sieve Analysis μm	% Material Retained on the Sieve				
Collector	1	2	3	4	5
+ 600	45.8	9.7	0.1		
-600 + 500	54.1	90.1	10.7		
-500 + 300	0.1	0.2	86.1	0.8	
-300 + 150			3.1	97.8	6.0
-150 + 106				1.9	89.2
- 106					4.8
Vol. Av. diameter μm	598.1	511.0	363.9	216.1	126.0
Voidage	0.416	0.398	0.425	0.415	0.425

small neutralizer (or jet pump) (see Fig. 4.17). The input air causes a partial vacuum over the jet that protrudes into the diluted hydrosol, so that water is forced out of the jet to be dispersed into vapour. The water vapour and standard particles then flow out of the atomizer into the aerosol mixer tube. The aerosol then has to be dried to remove any water droplets. In the mixer tube air, which has been dried over anhydrous calcium sulphate and filtered, is added at two points in a direction that causes the air to flow in a helical pattern around the humid air from the atomizer. The tube has a number of constrictions so that the atomizer air and drier air are thoroughly mixed. At the end of the tube dehumidified air and suspended particles are drawn off.

For normal operation of the aerosol generator the drier air flow rate was set at $\tilde{\sim}$ 20 l/min and the atomizer air pressure at 5 p.s.i. Thus the maximum aerosol supply pressure was only 5 p.s.i. The aerosol concentration was set to about 10^7 particles/m^3 but could easily be varied by changing

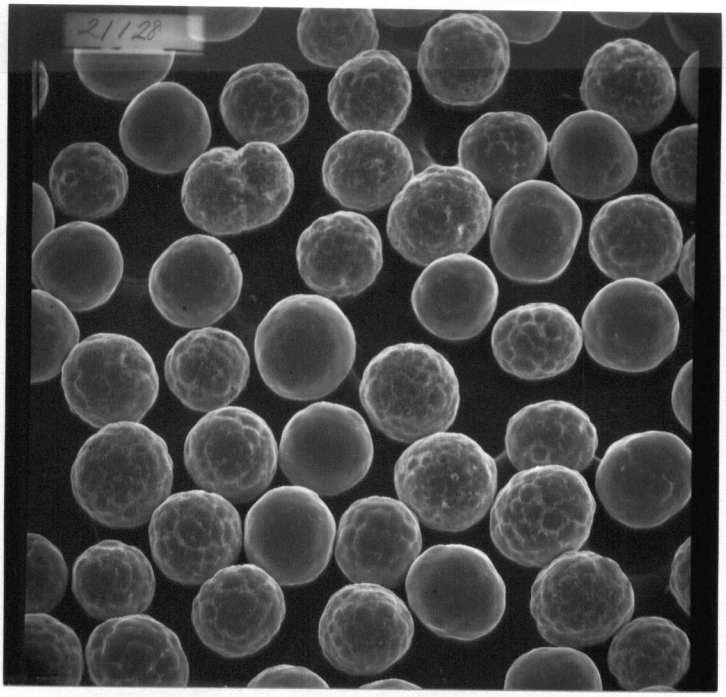

Fig. 4.11 Electron Micrograph of 598 μm diameter Nickel Shot (Mag. 15 ×)

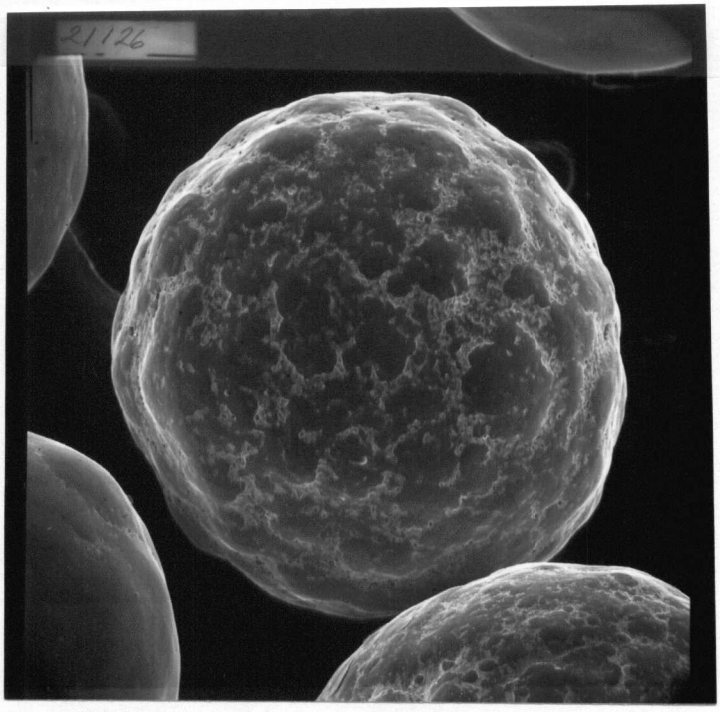

Fig. 4.12 Close up of a 598 μm diameter Nickel Shot (Mag. 80 ×)

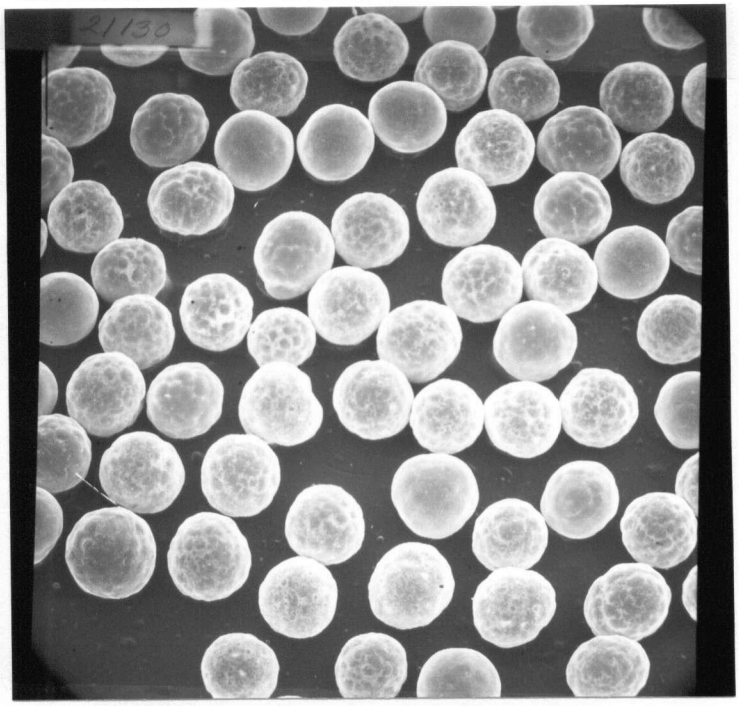

Fig. 4.13 Electron Micrograph of 511 μm diameter Nickel Shot (Mag. 15 ×)

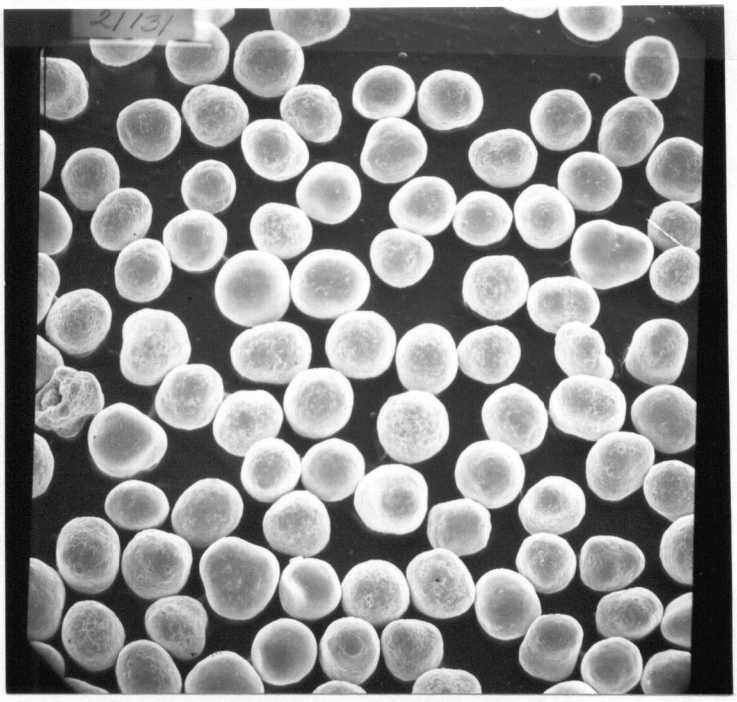

Fig. 4.14 Electron Micrograph of 363 μm diameter Nickel Shot (Mag. 20 ×)

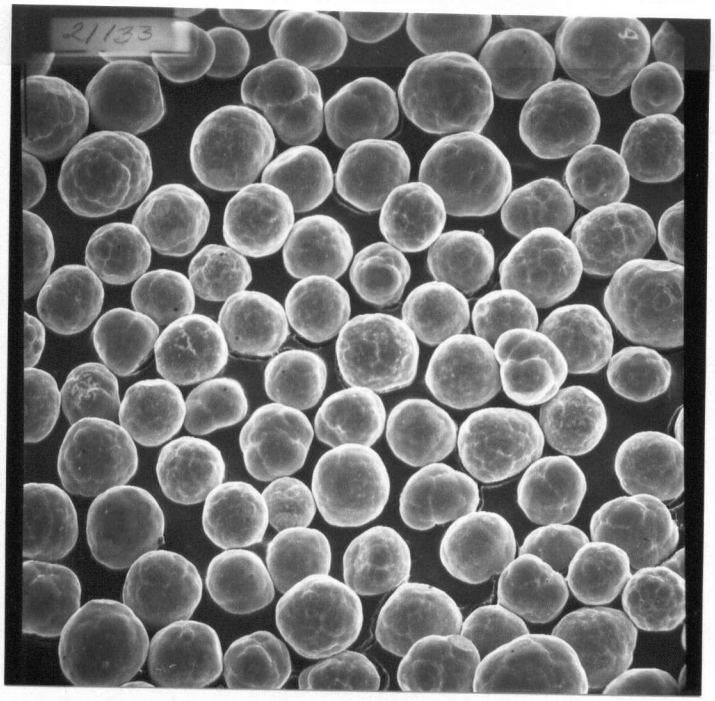

Fig. 4.15 Electron Micrograph of 216 μm diameter Nickel Shot (Mag. 40 ×)

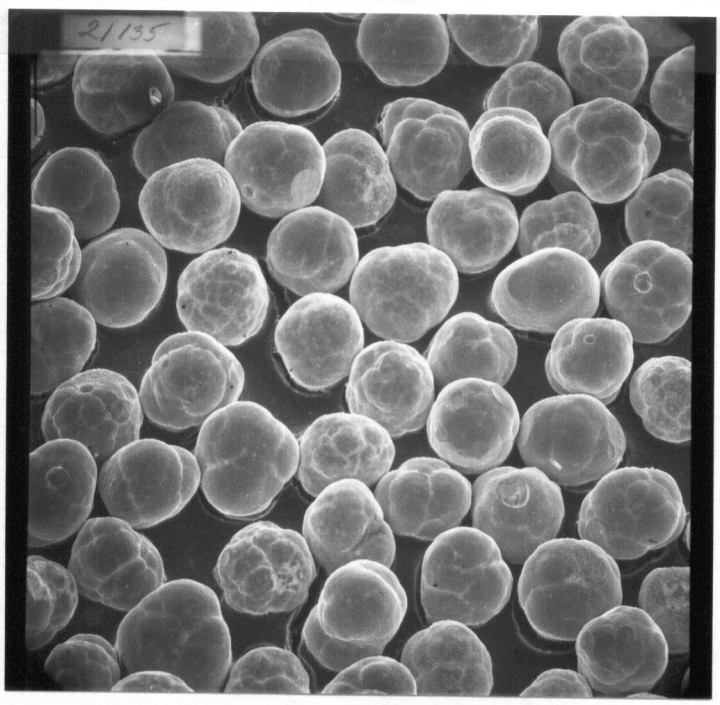

Fig. 4.16 Electron Micrograph of 126 μm diameter Nickel Shot (Mag. 80 ×)

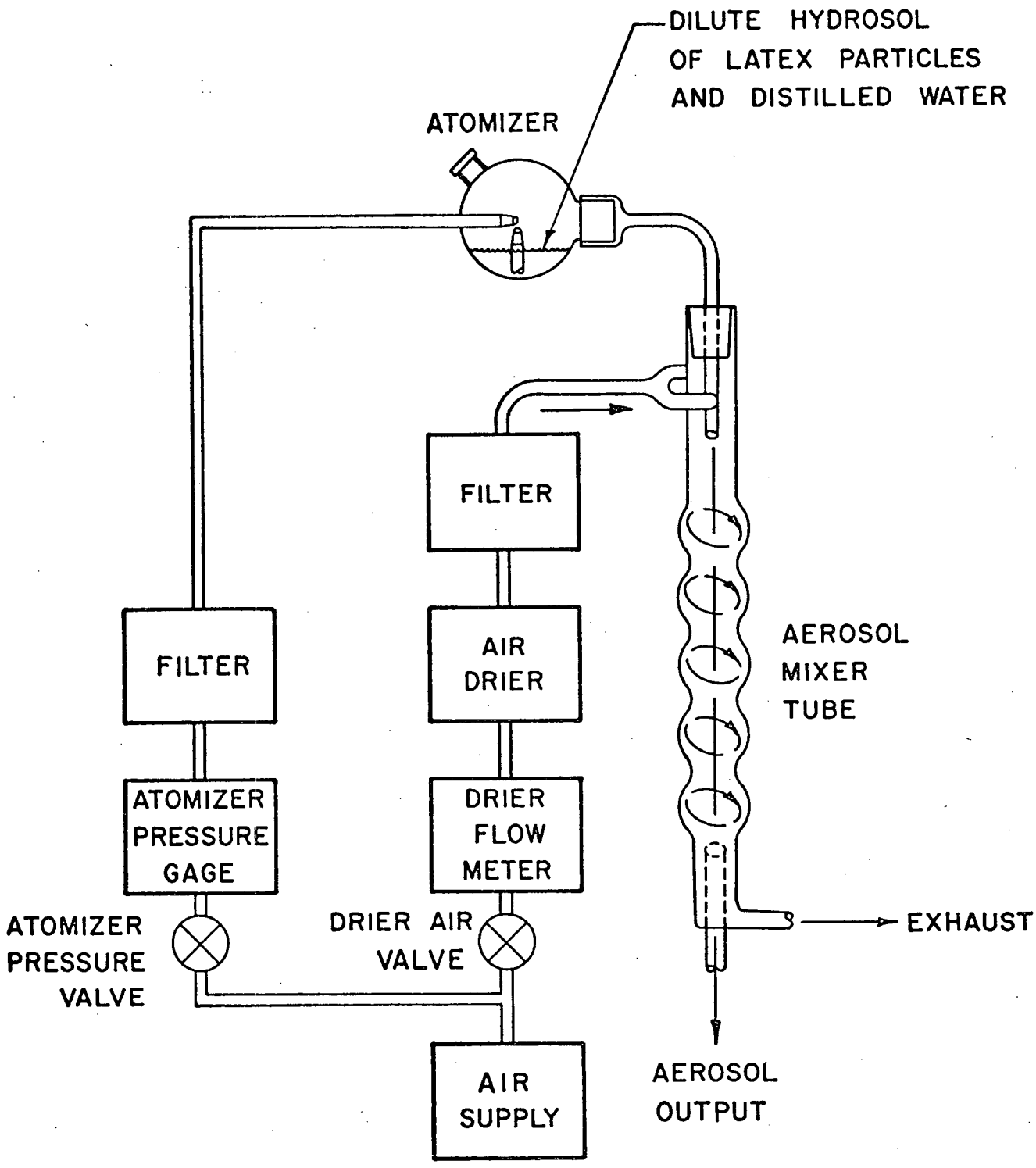

Fig. 4.17 Block Diagram of Aerosol Generator

(i) the drier air flow, (ii) the atomizer pressure, or (iii) the hydrosol concentration.

4.7 Aerosol Detector

It was necessary to be able to count the number of aerosol particles in a given volume of gas in order to determine the collection efficiency of the granular bed.

The counter used was a Royco sensor model 241, which operates on the principle of forward light scattering. A sharply defined beam of light is focused onto a small sensitive volume called the sample cell ($\sim$0.5 × 1.0 × 4 mm). All aerosol particles entering the sensor are passed through the cell (see Fig. 4.18). If no particles are present, all the light passes through to the light trap where it is absorbed. If a particle is present, light is scattered and is able to by-pass the light trap. By means of two collecting lenses the forward scattered light is focused onto a photomultiplier which generates a current pulse to drive a digital counter.

Coincidence errors arise when more than one particle enters the cell at any one time. In the case of the Royco counter this occurs at aerosol concentrations greater than about 10^{10} particles/m^3.

4.8 Minor Modifications and Additional Equipment

After several experiments had been carried out it was realized that it would be necessary to increase the gas flow through the column. This required changing the rotameter floats and recalibrating them.

Further modifications were made when it was noted that the aerosol diaphragm pump was acting as a filter and prevented the passage of sufficient amounts of 1 and 2 μm aerosol particles. Hence, instead of pumping the air through the system, the air was drawn through it by means of a vacuum pump (see Fig. 4.19). This arrangement presented some sampling problems and all

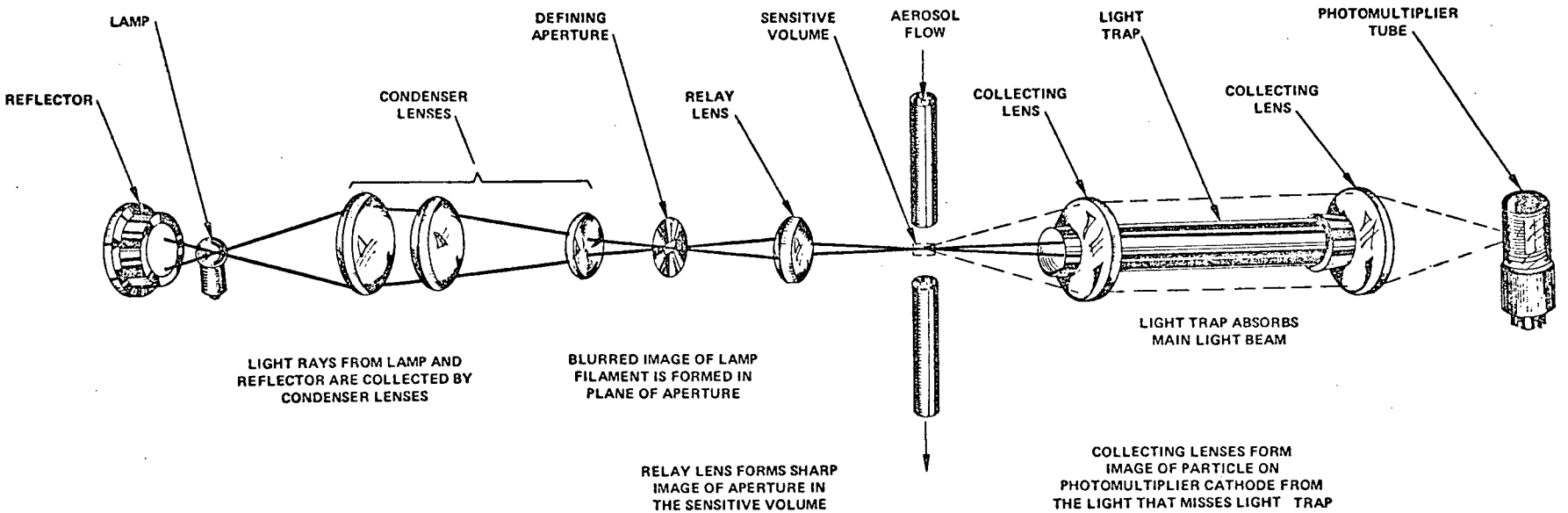

Fig. 4.18 Layout of Optics for Aerosol Analyser

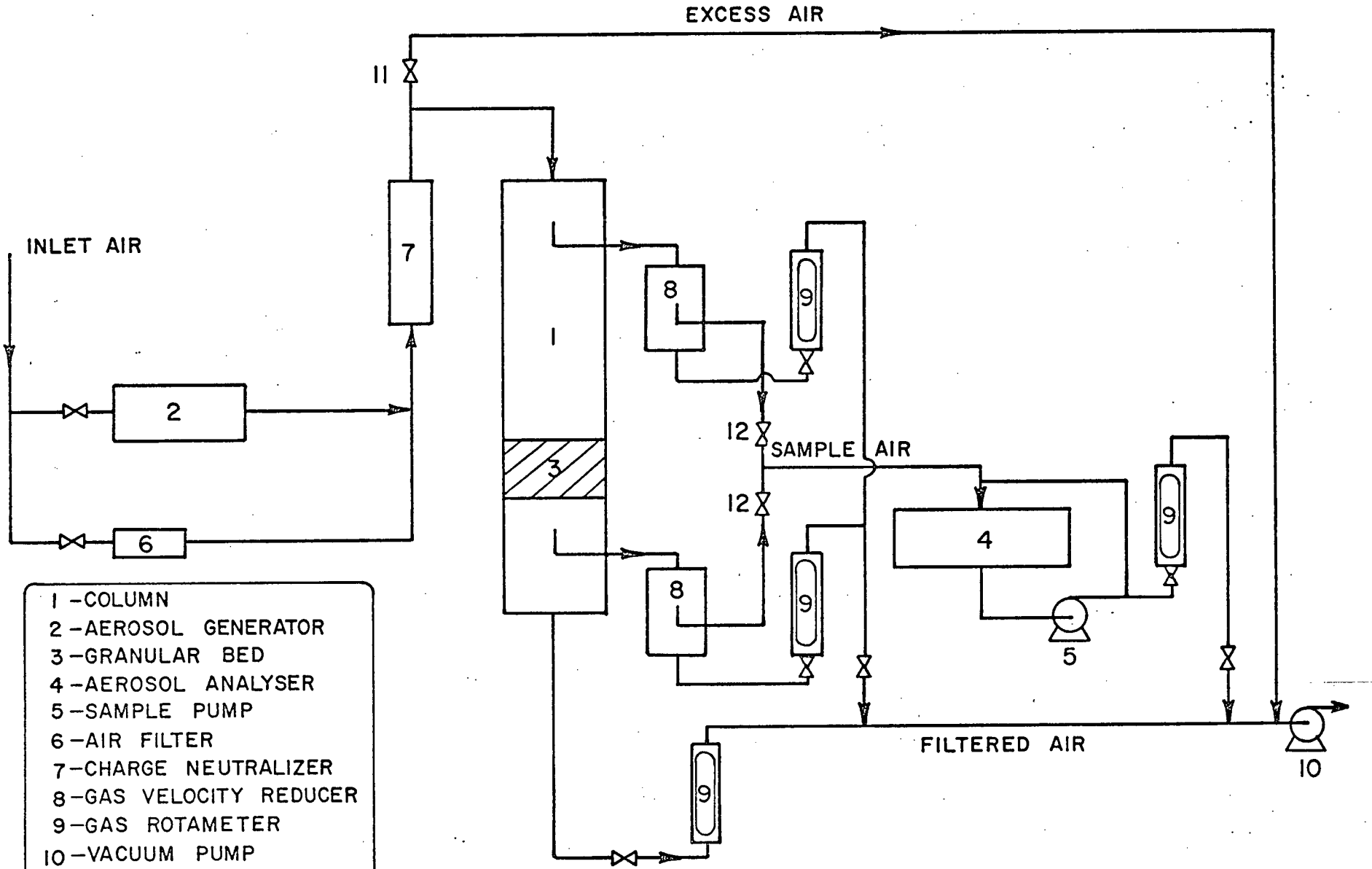

Fig. 4.19 Schematic Diagram of Modified Equipment

the outlet lines had to be connected to the pump. As the sample pump in the aerosol counter was not powerful enough to draw samples from the equipment, its discharge line was also connected to the vacuum pump. Set up in this manner, the operation of the equipment was virtually the same as before.

Additional equipment was used to generate humidified air. To vary the humidity a simple spray nozzle was added to the inlet gas supply. Water was sprayed into the main air flow and the damp air and water droplets passed into a cyclone. Water droplets were removed from the base of the cyclone and the humidified air passed through a filter before being mixed with the aerosol flow (see Fig. 4.20). The humidity of the gas was measured by a Panametrics hygrometer (model 2000) with the probe inserted into the gas leaving the column.

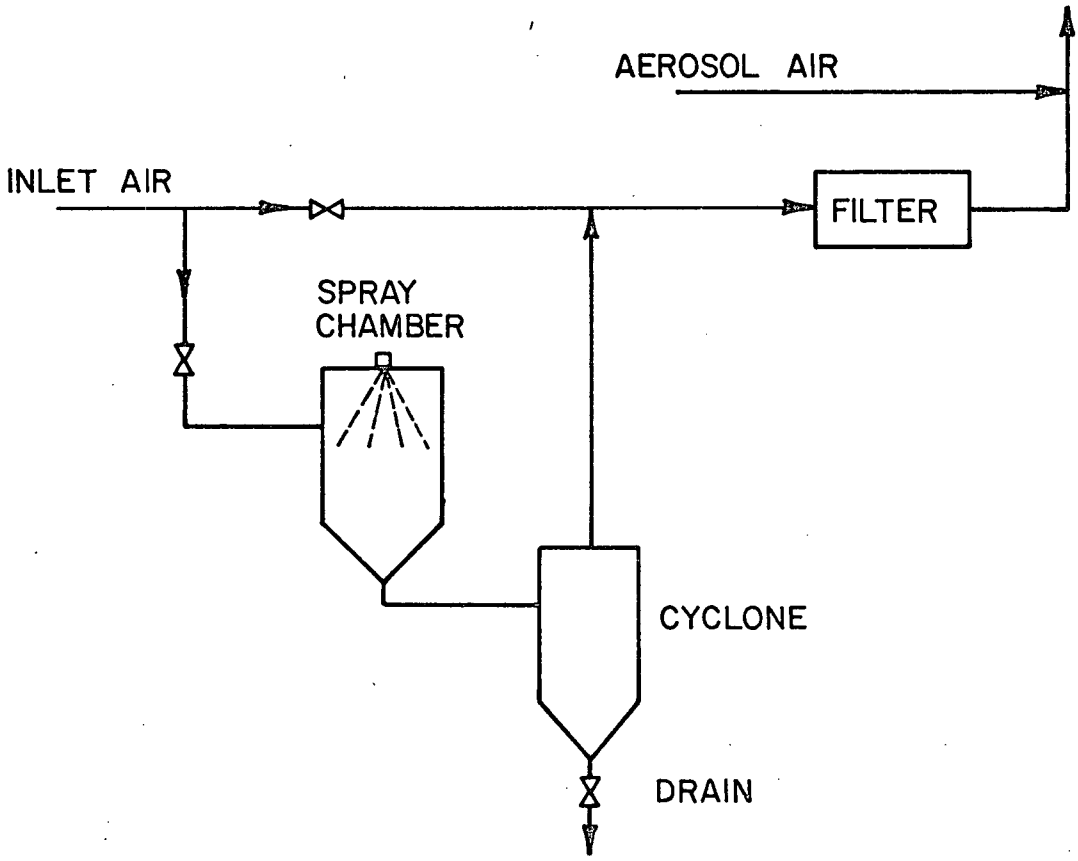

Fig. 4.20 Humidifying Equipment

CHAPTER 5

PRELIMINARY EXPERIMENTS

A series of experiments was carried out to develop a consistent experimental procedure and to become familiarized with the equipment.

5.1 The Effect of Humidity on Collection Efficiency

If electrical charges were present in the equipment or on the aerosol particles, then changes in humidity should affect the collection efficiency. For instance, if electrical charges were helping collection then damp air, which would more easily disperse these charges, would produce a lower collection efficiency than dry air.

However, based on several tests (see Tables XI and XII) no significant difference in collection efficiency could be detected by changes in humidity.

These results suggest that the aerosols and collectors are electrically neutral and that the electrical effects may be ignored.

It was realized that humidity could also affect the retention forces between the particle and the collector by altering the nature of the absorbed film of water on the collector surface. The humidity was therefore recorded at the beginning and end of all subsequent experiments.

5.2 Bed Ageing or Loading

It has been reported[23] that a build up of dust in the interstices of granular beds increases the collection efficiency as well as the pressure drop across the bed. These effects usually occur at aerosol concentrations very

TABLE XI. COLLECTION EFFICIENCY OF 598.1 μm NICKEL SHOT AT VARIOUS HUMIDITIES (Bed depth = 4.5 cm; Aerosol diameter = 0.5 μm)

Gas Velocity cm/sec	Collection Humidity Relative Humidity 38%	45%	70%
5.24	38.2	37.9	34.6
11.16	29.6	28.2	27.4
16.97	28.8	28.0	27.8
22.37	26.9	28.4	27.4
27.08	26.5	23.9	26.4

TABLE XII. COLLECTION EFFICIENCY OF 511.0 μm NICKEL SHOT AT VARIOUS HUMIDITIES (Bed depth = 9.1 cm; Aerosol diameter = 0.5 μm)

Gas Velocity cm/sec	Collection Efficiency Relative Humidity 18%	38%	64%
5.24	43.0	41.9	42.1
11.16	32.9	35.1	35.0
16.97	31.9	32.3	32.8
22.37	31.2	31.9	32.0
27.08	30.3	32.5	31.5

much higher than 10^7 particles/m^3, which were used in the present work. Thus in all experiments the bed loading was extremely small. For example, it would take about two years for one gram of 2.02 μm particles to be deposited assuming typical operating conditions and a 100% removal efficiency. Nevertheless, long term tests were conducted on each collector and Tables XIII and XIV summarize the results performed with two collectors.

As can be seen, no significant change in collection efficiency was observed.

TABLE XIII. BED AGEING TESTS ON 598 μm NICKEL SHOT
(Bed depth = 9.1 cm;
Aerosol diameter = 0.500 μm)

Gas Velocity cm/sec	Collection Efficiency Time Hours 0	3	5	8	9.5	12	14	16	18
5.24	46.3	44.7	40.9	40.2	41.9	43.5	41.3	43.0	45.2
11.16	37.1	37.8	36.1	35.3	34.5	35.7	32.8	32.9	39.2
16.97	36.7	38.3	31.3	32.3	32.9	33.0	32.8	32.9	35.0
22.37	32.1	34.4	32.9	30.7	31.5	30.9	35.7	31.2	31.0
27.08	33.7	38.0	32.5	32.6	33.0	32.8	33.7	30.3	33.4

TABLE XIV. BED AGEING TESTS ON 216.0 μm NICKEL SHOT
(Bed depth = 2.27 cm;
Aerosol diameter = 0.500 μm)

Gas Velocity cm/sec	Collection Efficiency Time Hours 0	3	6	9
5.24	88.2	86.5	85.5	86.2
11.16	80.1	77.2	78.0	80.5
16.97	76.3	75.9	74.9	75.9
22.37	72.3	71.8	71.4	74.3
27.08	71.6	68.1	69.0	70.1

5.3 Collection by the Empty Column and Bed Support

Several empty column tests were carried out to determine the removal of particles on the bed support and walls of the column. As can be seen from Table XV, the removal was found to be less than 1%.

TABLE XV. COLLECTION BY THE EMPTY COLUMN

Gas Velocity cm/sec	Collection Efficiency Aerosol diameter μm 0.109	0.500	0.600	0.804
5.24	0.80	1.00	0.90	0.60
11.16	0.40	0.90	0.80	0.80
16.97	0.33	0.80	0.80	0.50
22.37	0.35	0.25	0.80	0.90
27.08	0.00	0.35	0.40	0.65

Since the aerosol removal of the empty column was so low, no correction to the measured bed collection efficiency was made.

5.4 Background Count

The background counts were readings recorded by the aerosol counter during normal operation of the equipment but with no aerosol generation. The background count could be caused by dust in the system from (i) particles depositing in the inlet tubing and subsequently breaking away, (ii) incomplete filtration of the bench and aerosol drier air, (iii) impure distilled water (used in dilution of the latex hydrosol), (iv) leaks of air into the equipment, or (v) electrical noise generated within the aerosol detection equipment. Prior to each experiment background counts were therefore determined. The counts usually varied between 20-40 particles/minute which is negligible in comparison with counts of about 2,000-8,000 recorded when the aerosol generator was operating.

It was also possible that during normal operation of the equipment water droplets (caused by atomization of the diluted latex hydrosol) were carried into the column. If this was the case, then the presence of the droplets would modify the measured collection efficiency of the bed. Tests were therefore performed to determine if this was taking place. This was simply done by running the aerosol generator with distilled water only. Table XVI shows some of the recorded counts and it can be seen there is no detectable difference from the background count.

TABLE XVI. BACKGROUND COUNTS FOR THE EMPTY COLUMN
(Gas velocity = 27 cm/sec)

Aerosol generator not used	Aerosol generator used with only distilled water
39	42
40	27
21	34
28	29
33	30
Av. 32	Av. 32.4

5.5 Sampling Counts and Changeover Time

Due to the unsteady performance of the aerosol generator several counts had to be taken before reproducible counts could be recorded. Once the system was reasonably steady (i.e., the several successive counts fell within ± 5% of each other) then 4-8 readings were taken and averaged.

After sampling the inlet gas flow to the bed, the aerosol concentration was determined for the outlet flow. However, it was necessary to decide how long to wait for the system to stabilize before counts could be recorded after each changeover. Waiting for 1, 2, 5 and 10 minutes between each changeover gave no noticeable difference in measured counts. A waiting time

of one minute between changeovers was therefore adopted.

5.6 Reproducibility

Several tests were repeated three to four months later and were found to agree well within ± 5%. Also with the changeover of pumping to drawing the gas through the equipment (which allowed tests with 1 and 2 μm diameter aerosols to be performed), tests with 0.8 and 0.5 μm diameter aerosols were repeated. Again the results obtained were in good agreement with those of previous tests. When the equipment was modified for higher gas flows, several measurements were repeated to check for consistency. This was done by overlapping the two velocity ranges with the low velocity tests covering 5 to 27 cm/sec and the high velocity tests covering 16 to 67 cm/sec.

5.7 Errors

These were very difficult to quantify owing to the nature of the equipment and the filtration process.

The largest single source of errors was probably the aerosol generator which tended to behave rather erratically. For example, counts of the sampled gas flow could jump from 2,000 to 4,000 counts per minute for no apparent reason and remain there for the rest of the experiment. Alternatively the counts would increase steadily from 2,000 to 6,000 over the course of the experiment and later perhaps fall back to 4,000. Thus errors were introduced by the aerosol generator which could not be overcome.

Re-entrainment and bounce-off could substantially affect the overall aerosol deposition and hence the collection efficiency of the bed. If these effects were taking place, then the recorded efficiencies would be lower than their true value. It was possible to check to see if re-entrainment was occurring by shutting off the aerosol generator at the end of an experiment and measuring the aerosol concentration of the gas

downstream from the bed. It was noted that the counts rapidly fell to the background value after the aerosol generator was shut off which implies that little, if any, re-entrainment was taking place. However, bounce-off is a different phenomena. It occurs when a particle collides with a collector but is not retained. This effect is usually only observed with dry, solid aerosols. Using sticky, liquid aerosols such as dioctyl phthalate (D.O.P.) bounce-off could be eliminated. Thus it would be possible to determine if bounce-off was occurring by comparing results of tests conducted with dry and liquid aerosols. This was not done in this study as the available aerosol generator was not capable of producing liquid aerosols.

Further small errors are summarized below.

i) Aerosol counter:-As mentioned before, errors could be introduced by the 'interference' effect or by particles depositing on the optical surfaces of the analyser. This would usually occur at high aerosol concentrations. The period for counting the aerosols was set electronically with the digital counter being stopped automatically after one minute and therefore timing errors were negligible.

ii) Gas flow:-Small errors could be caused by incorrectly reading the rotameters. Also fluctuations in the bench air supply could cause errors and could contribute to the erratic behaviour of the aerosol generator.

iii) Non isokinetic sampling:-This could cause a small error in the measured counts but is most unlikely, especially with aerosols below 2 μm in diameter. Errors within the sampling equipment were minimized by making the inlet and outlet sampling trains as identical as possible.

5.8 Experimental Programme

5.8.1 Procedure

From the preliminary experiments a test procedure was developed. Each experiment involved the measurement of collection efficiency for various superficial gas velocities at different bed depths and was repeated for a range of aerosol and collector sizes.

Details of a typical run, which took about 2-3 hours are presented below.

i) The aerosol counter was switched on and allowed to warm up for about half an hour.

ii) A measured volume of specific collector particles was charged to the column and fluidized to give a loosely packed bed. If necessary the surface was levelled without compressing the bed.

iii) The column was set up in an upflow or downflow mode (see Chapter 4).

iv) A dilute hydrosol mixture of a specific aerosol was charged to the aerosol generator.

v) With the aerosol generator isolated, all pumps and gas flows were turned on and adjusted to give maximum flow.

vi) Particle counts were taken to measure the background count.

vii) The aerosol generator and pump were turned on and the humidity of the exit gas from the column was measured. Also the air temperature was noted.

viii) The particle counts/minute were monitored for the inlet air until steady and then 4 to 8 readings were taken.

ix) The sample flow was then changed to the outlet gas and one minute allowed for stabilization. Further 4 to 8 readings were taken.

x) The sample flow was changed back to the inlet gas to check the counts for consistency.

xi) The pressure drop across the column was measured for each gas velocity.

xii) The gas velocity was then reduced and steps (viii) to (xii) repeated.

5.8.2 Programme

For each collector the tests summarized in Table XVII were carried out.

TABLE XVII. SUMMARY OF EXPERIMENTAL TESTS

Test	Aerosol diameter μm					
	0.109	0.500	0.600	0.804	1.011	2.020
Downflow:						
Low velocity	×	×	×	×	×	×
High velocity		×		×	×	
Upflow:						
Low velocity		×		×	×	
High velocity		×		×		
Bed depth	×	×	×	×		
Humidity test		×				
Ageing test		×				

Low velocity configuration:-5 to 27 cm/sec

High velocity configuration:-16.33 to 67.0 cm/sec

Bed depth test:-For aerosols 0.109, 0.600 and 0.804 μm in diameter only two depths were used; for 0.500 μm aerosol four to five depths were used.

Humidity test :-This involved comparing the collection of 0.500 μm aerosol with dry and damp air. All other tests were carried out at ∿ 30-40% relative humidity.

Ageing test :-This involved runs of up to 18 hours duration and measuring the collection efficiency every two hours for each gas velocity.

CHAPTER 6

EXPERIMENTAL RESULTS AND DISCUSSION

6.1 Introduction

A summary of all experimental conditions and results can be found in Appendix A. When tests were duplicated, the shown results are averaged values. Unless otherwise stated, all the figures in this section show results for experiments conducted in the downflow mode.

6.2 The Effect of Superficial Gas Velocity on Bed Collection Efficiency

Figs. 6.1 to 6.10 show the collection efficiency of the granular beds as a function of superficial gas velocity for various collectors and aerosol particles. Figs. 6.1 to 6.5 refer to the low velocity tests only. Figs. 6.6 to 6.10 refer to both the high and low velocity tests for upflow and downflow.

The characteristic shape of the efficiency curve (see Fig. 2.1) was not observed in the initial low velocity tests. Figs. 6.1 to 6.5 show a steady decrease in collection efficiency with no subsequent rise due to increasing inertial effects. Therefore, additional high velocity tests were performed in order to study particle collection in the inertia dominated region.

From Figs. 6.6 to 6.10, which cover the full range of velocities tested, it is clear that the efficiency curves can be divided into two regions. At low velocities the collection efficiency decreases with increasing gas velocity due to the reduced diffusional effect and, perhaps, gravitational

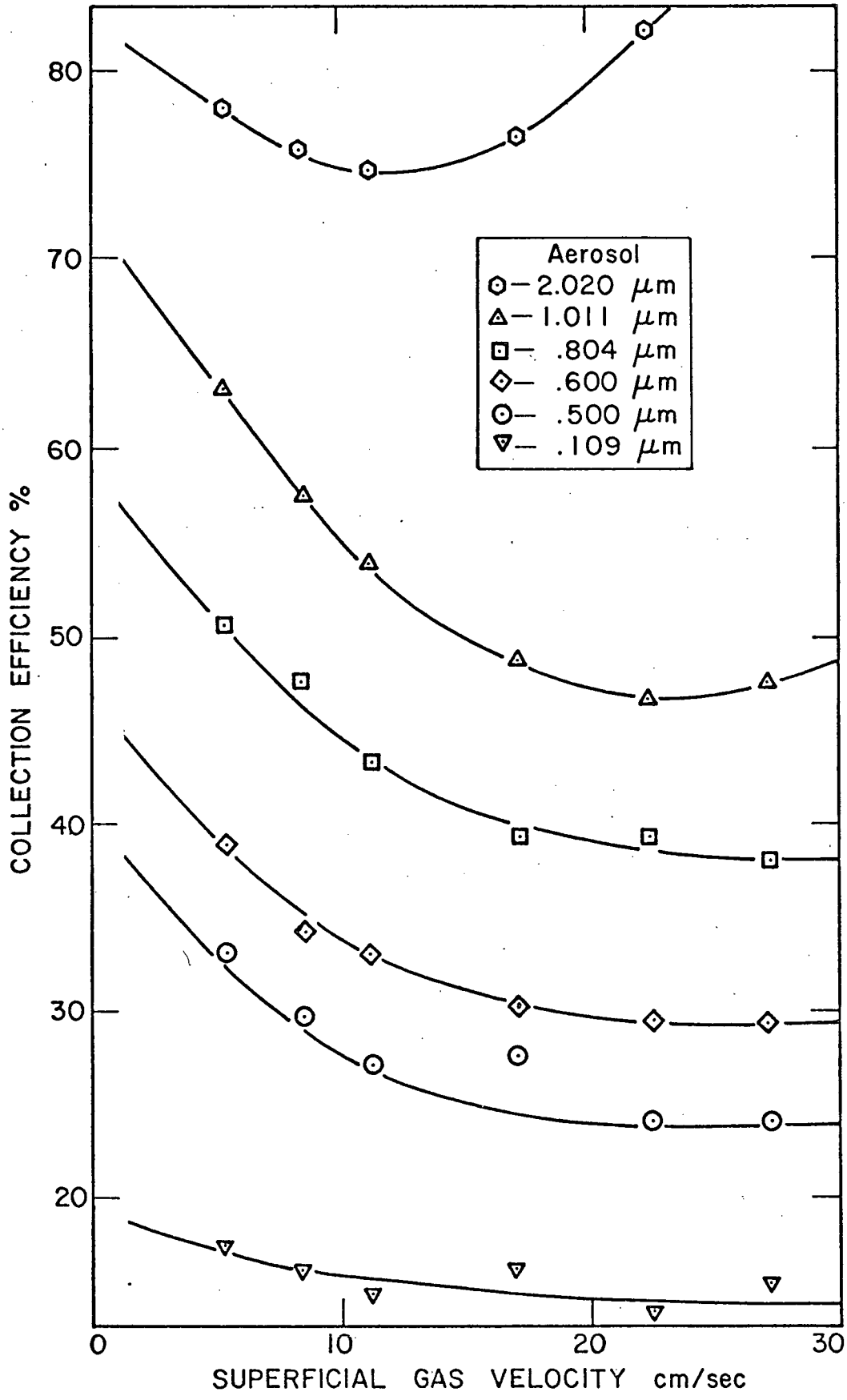

Fig. 6.1 Collection Efficiency as a Function of Gas Velocity (Bed depth = 4.54 cm; collector diameter = 598.1 μm)

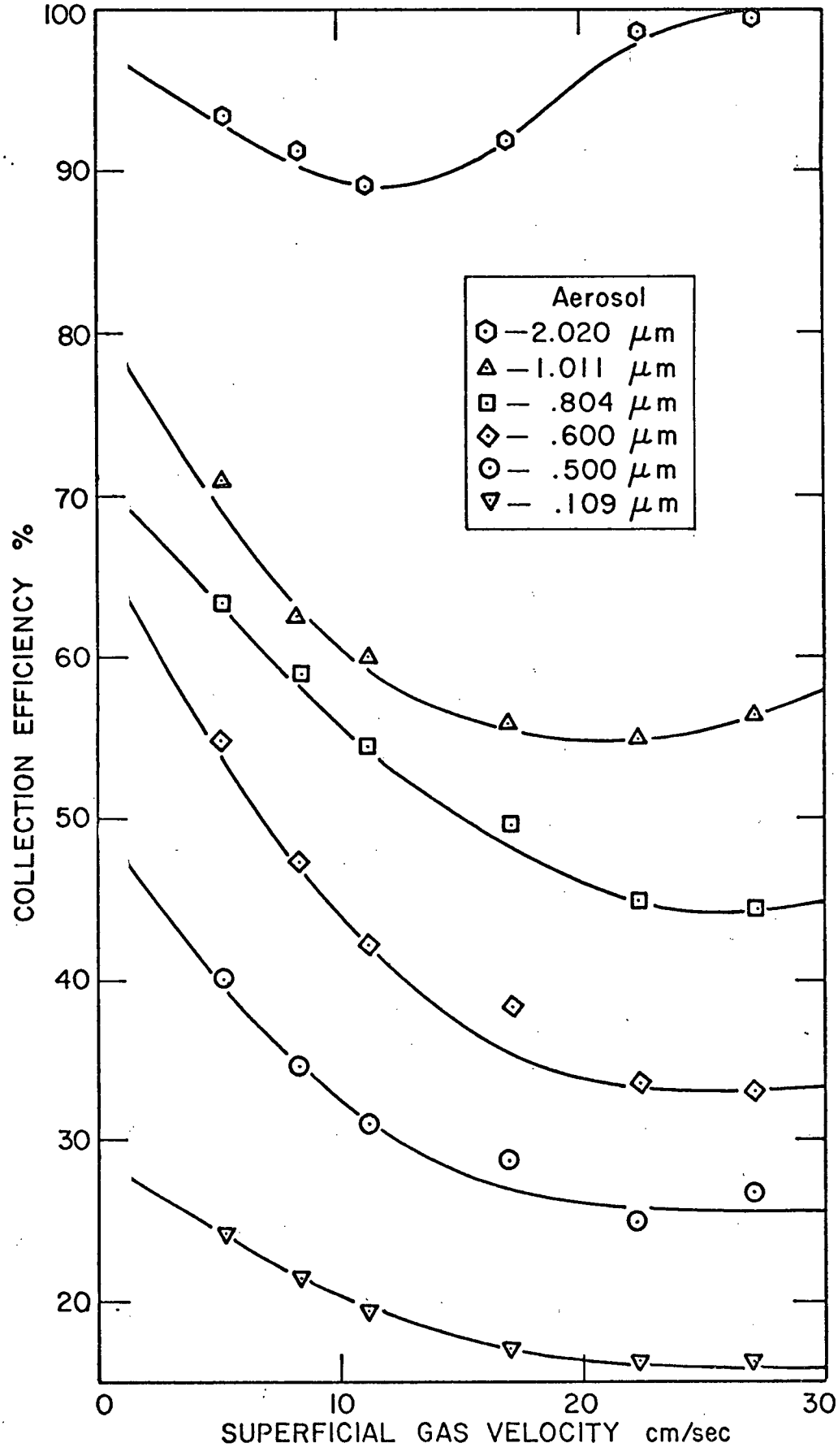

Fig. 6.2 Collection Efficiency as a Function of Gas Velocity (Bed depth = 4.54 cm; collector diameter = 511 μm)

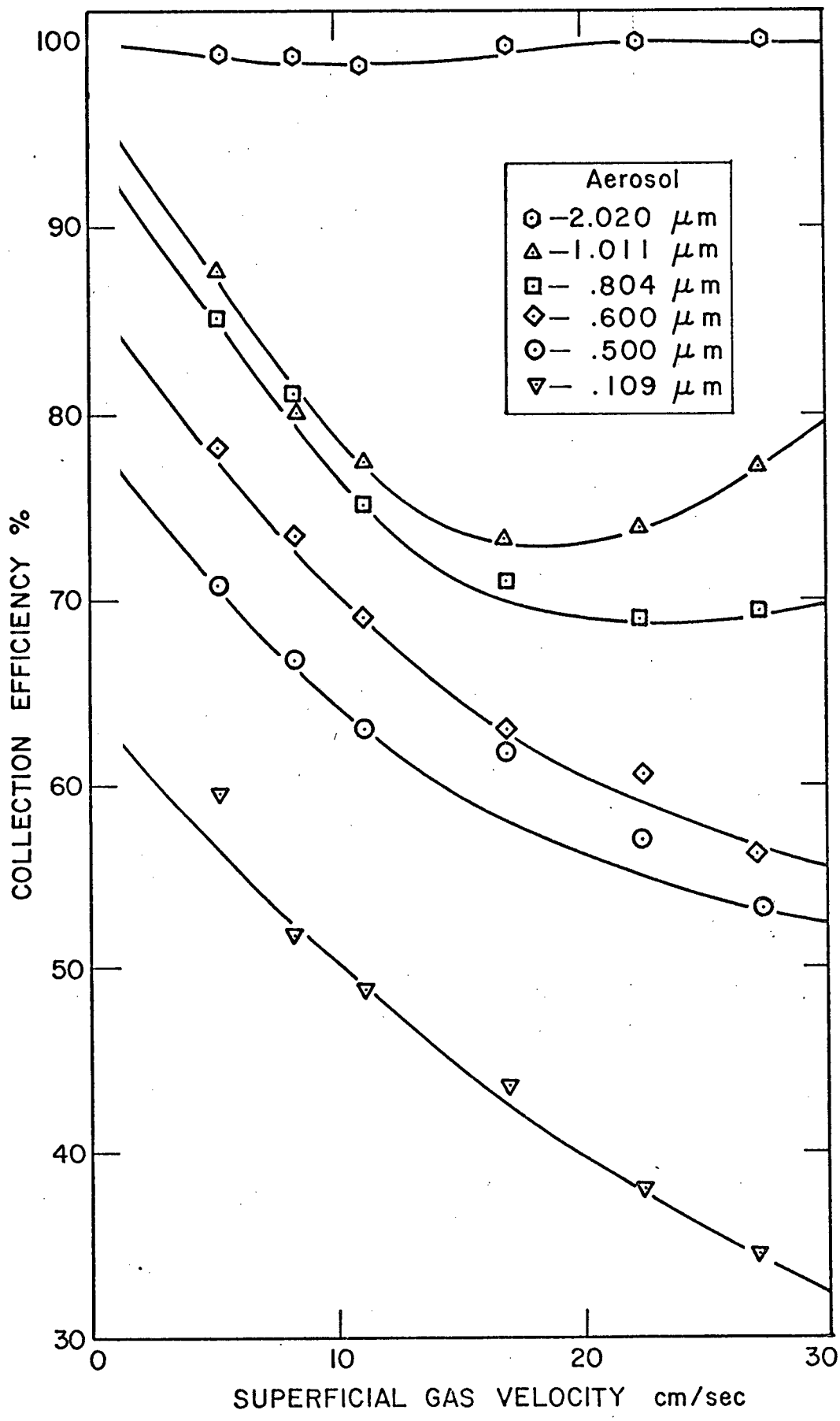

Fig. 6.3 Collection Efficiency as a Function of Gas Velocity (Bed depth = 4.54 cm; collector diameter ≐ 363 μm)

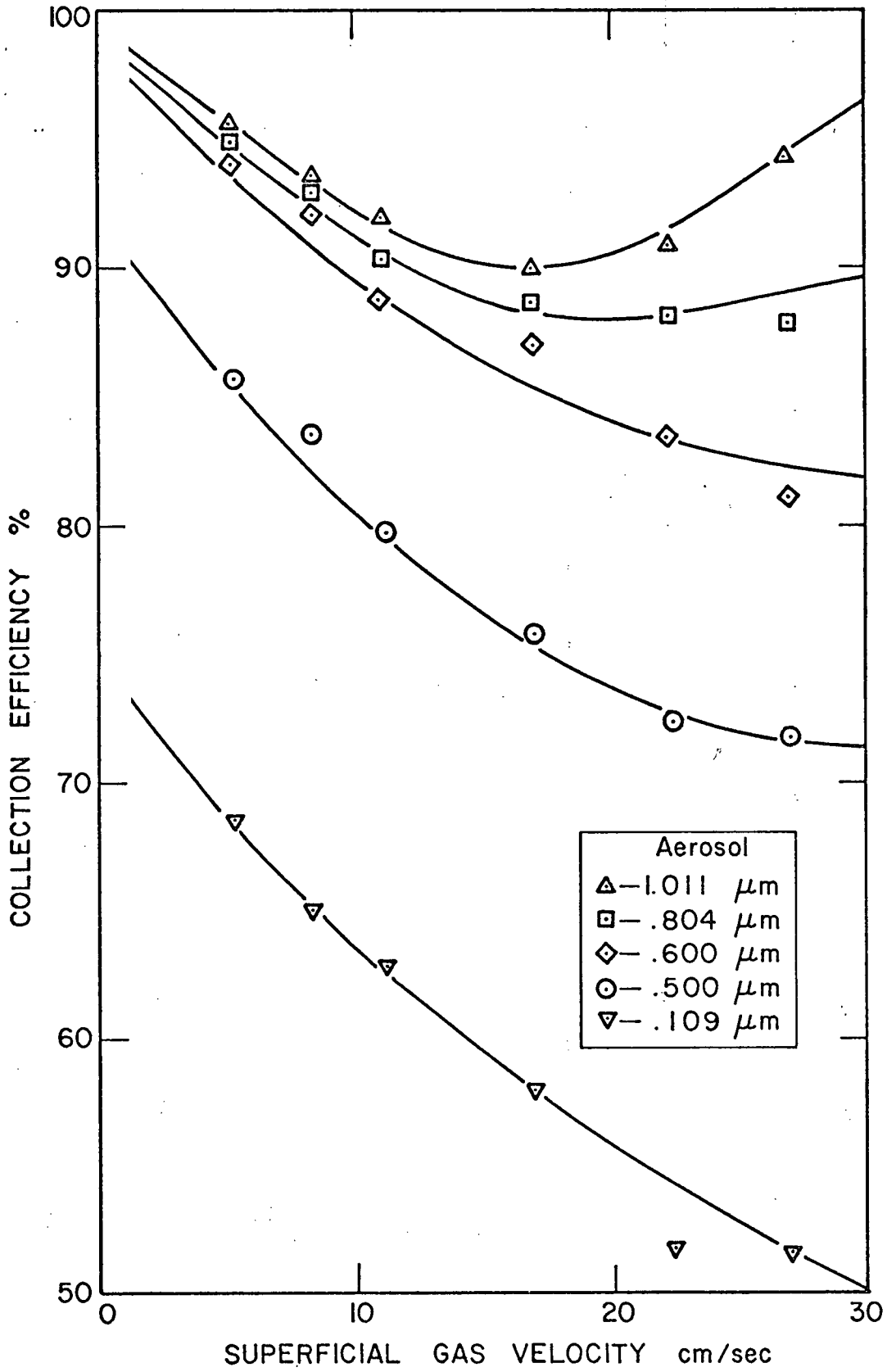

Fig. 6.4 Collection Efficiency as a Function of Gas Velocity (Bed depth = 2.27 cm; collector diameter = 216 μm)

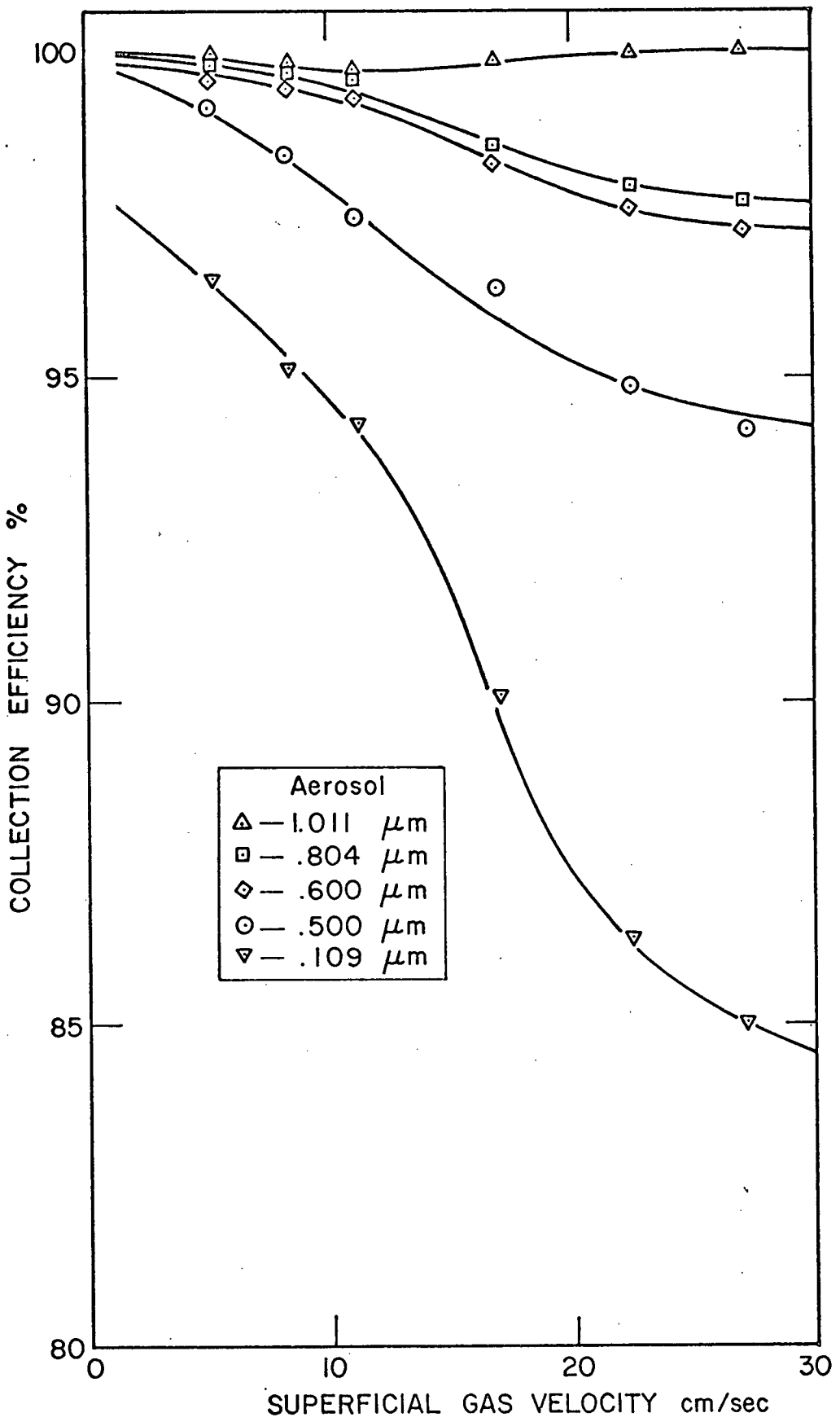

Fig. 6.5 Collection Efficiency as a Function of Gas Velocity (Bed depth = 2.27 cm; collector diameter = 126 μm)

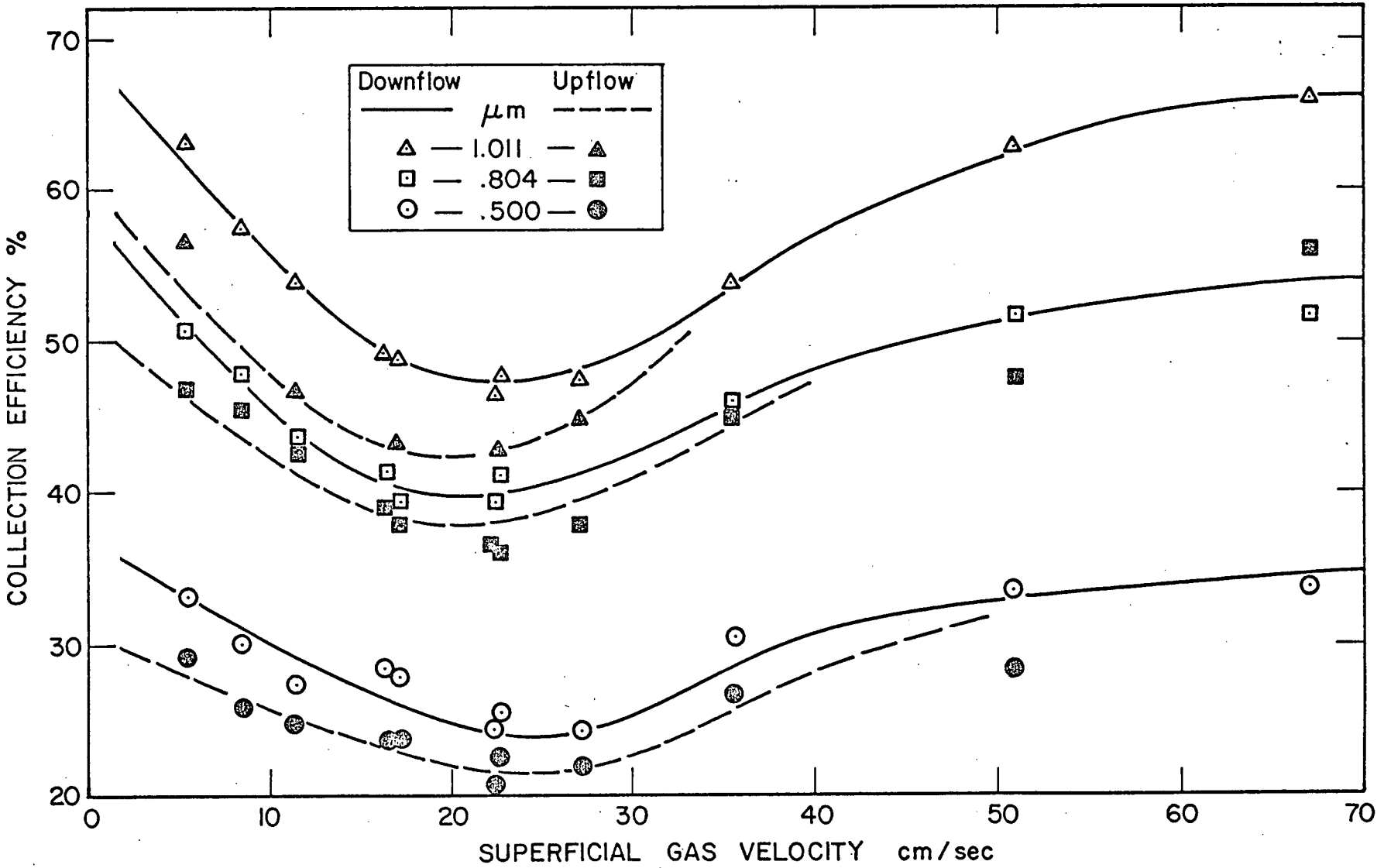

Fig. 6.6 Collection Efficiency as a Function of Gas Velocity
(Bed depth = 4.54 cm; collector diameter = 598 μm)

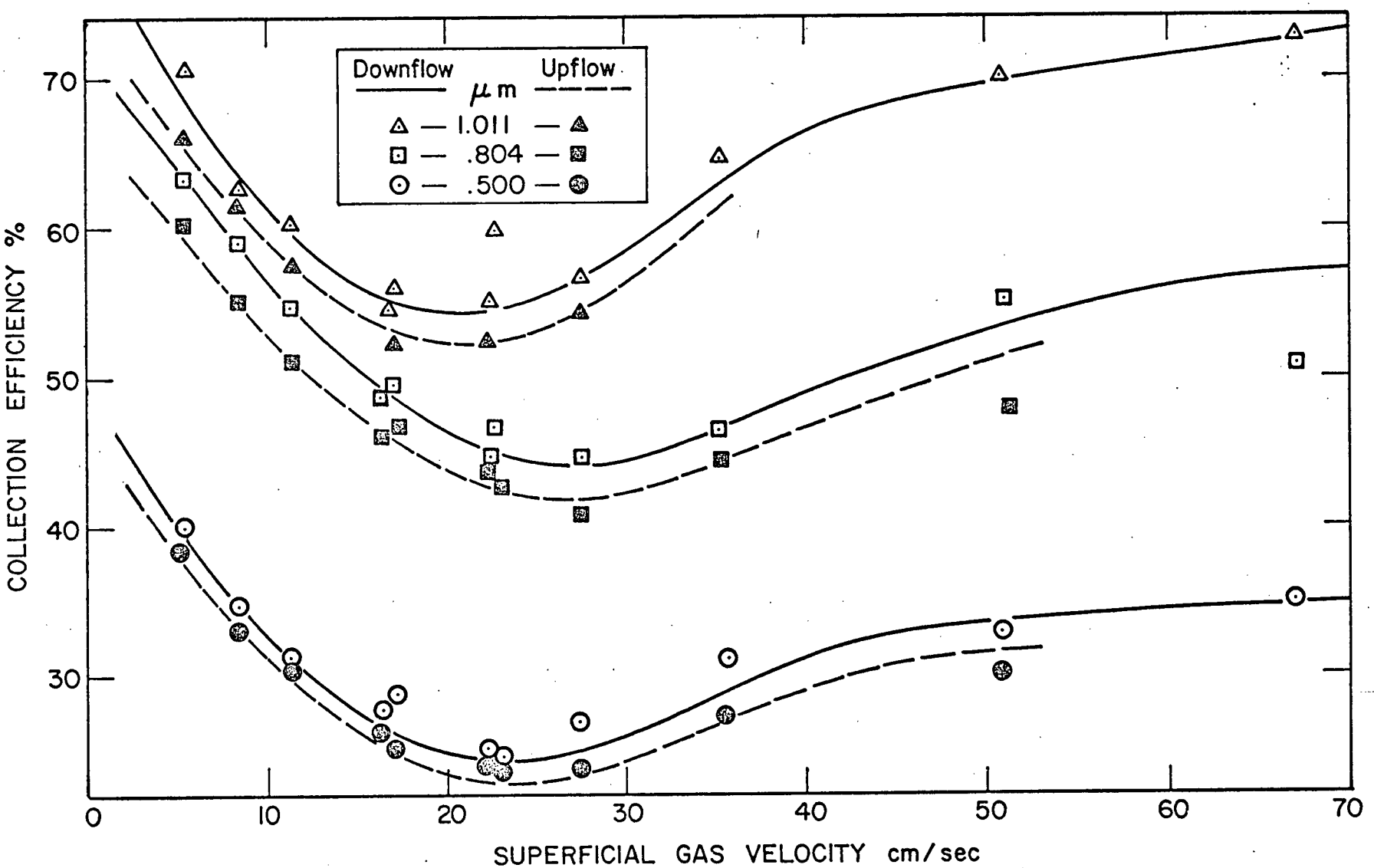

Fig. 6.7 Collection Efficiency as a Function of Gas Velocity
(Bed depth = 4.54 cm; collector diameter = 511 μm)

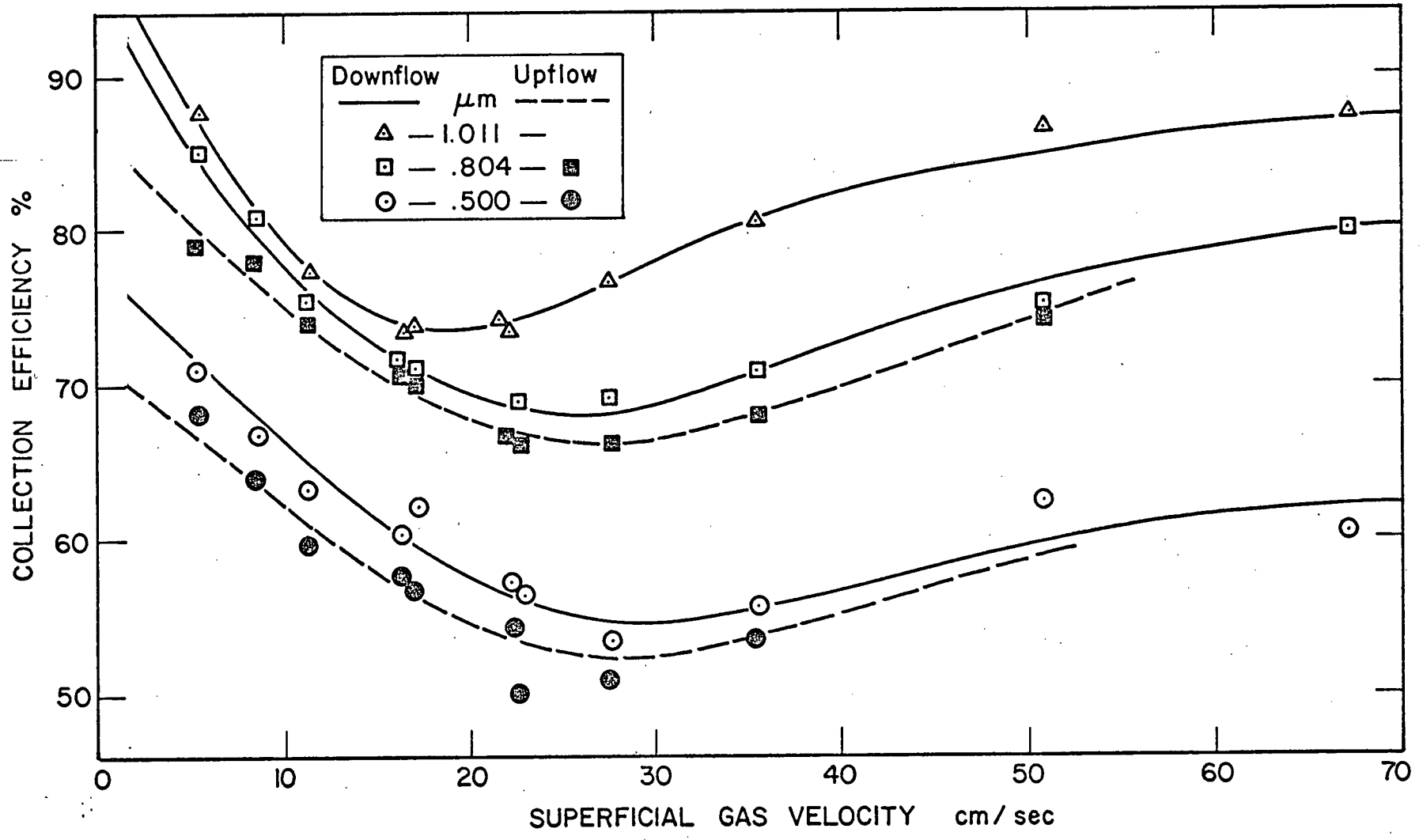

Fig. 6.8 Collection Efficiency as a Function of Gas Velocity
(Bed depth = 4.54 cm; collector diameter = 363 μm)

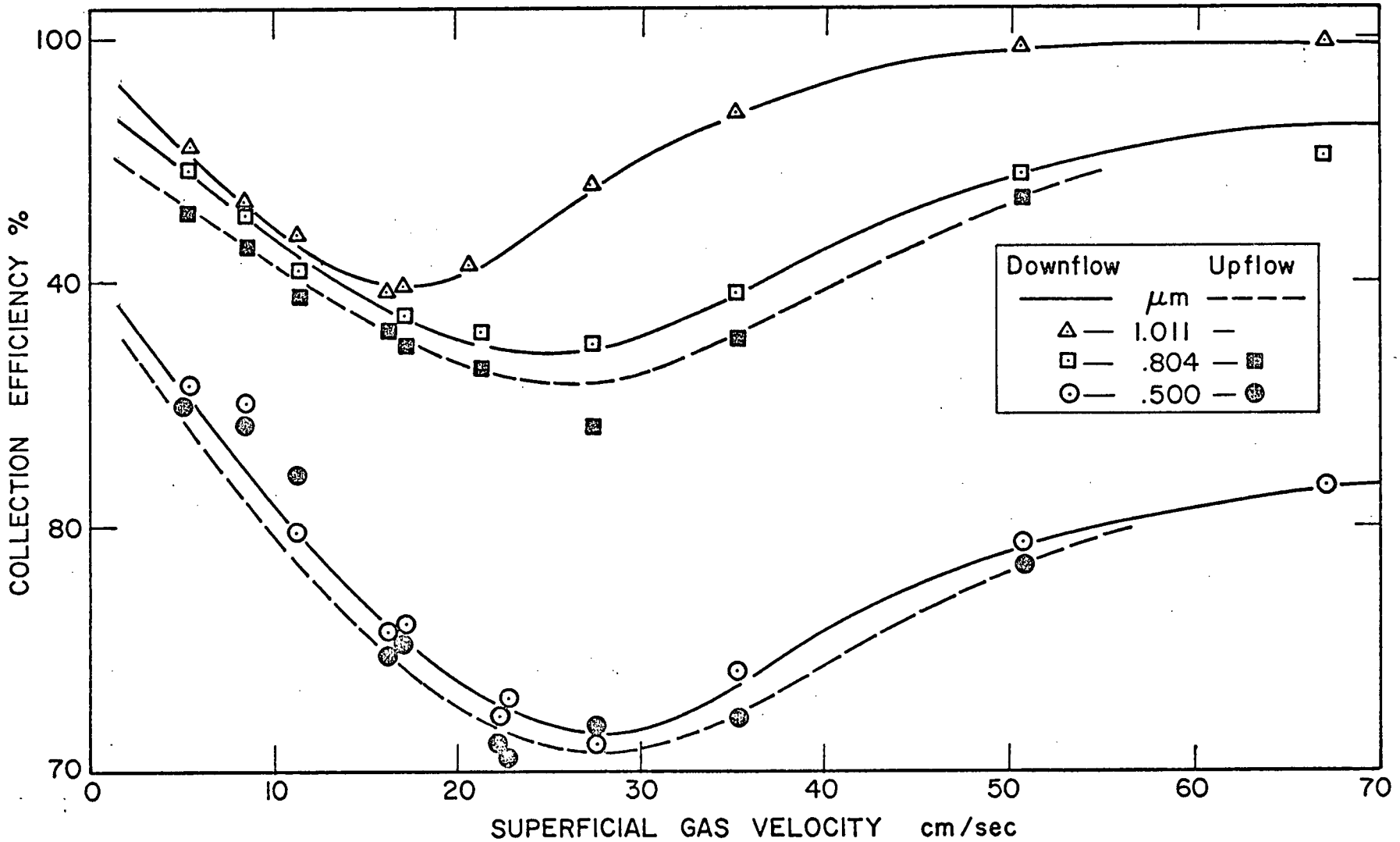

Fig. 6.9 Collection Efficiency as a Function of Gas Velocity
(Bed depth = 2.27 cm; collector diameter = 216 μm)

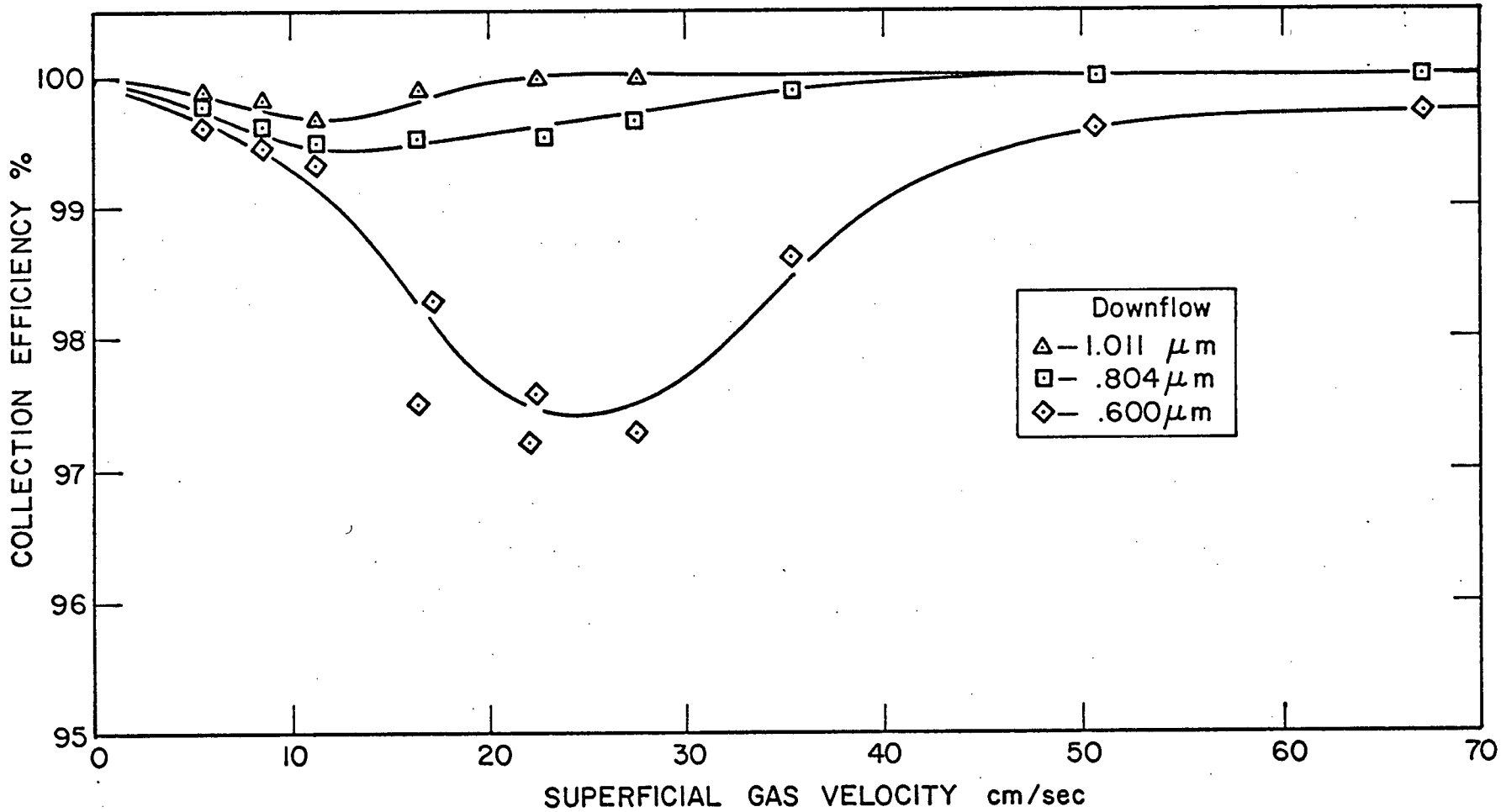

Fig. 6.10 Collection Efficiency as a Function of Gas Velocity
(Bed depth = 2.27 cm; collector diameter = 126 μm)

effect for the larger aerosol particles. Minimum collection occurs at gas velocities between about 15 and 20 cm/sec where both the diffusional and inertial effects are weak. As the gas velocity increases the collection efficiency starts to rise again because the inertial effect becomes dominant. It may be noted that, as the aerosol size increases, the velocity of minimum collection decreases. For example, in case of 598.0 μm diameter nickel shot the velocity for minimum collection is about 12 cm/sec for 2 μm diameter aerosol particles and 25 cm/sec for 0.5 μm diameter aerosol particles.

At velocities greater than about 45 cm/sec the collection efficiency was usually found to level off or decline. This phenomena may be caused by bounce-off because re-entrainment is unlikely for reasons mentioned in Section 5.8.

6.3 The Effect of Flow Direction on Bed Collection Efficiency

Figs. 6.6 to 6.10 also show the results for the upflow (dashed lines) as well as downflow (solid lines) experiments. There is a substantial decrease in collection efficiency at the lower velocities in the upflow mode especially for the 1.01 μm aerosols. The difference in collection becomes negligible at high gas velocities. Also, the smaller the aerosol particle the smaller the difference between upflow and downflow results. Since the direction of flow only influences the gravitational collection mechanism it can be concluded that gravity is playing a significant role in collection especially at low gas velocities and for large aerosols.

6.4 The Effect of Aerosol Diameter on Bed Collection Efficiency

As seen from Figs. 6.1 to 6.10, the collection efficiency usually decreases with aerosol size. Many workers[27,28,29] have pointed out that this trend stops at a certain aerosol size after which the collection

efficiency starts to increase again due to the enhanced diffusional effect. Figure 6.11 shows that no minimum in the efficiency-aerosol size curves was detected in this work. This may have been due to the lack of experimental results at low gas velocities and small aerosols. Chen[29] has pointed out that the minimum only occurs at gas velocities less than about 4 cm/sec.

6.5 The Effect of Collector Size on Bed Collection Efficiency

As expected the collection efficiency increases with decreasing collector diameter due to the reduced interstitial spaces. The smaller void spaces increase the effects of inertial, diffusional and gravitational collection because the aerosol particles need to travel smaller distances to reach the collector surface. It is unlikely that sieving plays a significant role in collection even for the larger aerosol particles (2.02 μm in diameter) and the smallest collector particles (126 μm in diameter).

6.6 The Effect of Bed Depth on Collection Efficiency

Figs. 6.12 to 6.16 summarize the results of varying the bed depth for 0.5 μm diameter aerosol particles and different gas velocities. As suggested by Eq. 3.6, the data are plotted as log(100 - % collection efficiency) versus bed depth (H). The results follow straight lines, which pass approximately through the point of zero collection efficiency at zero bed depth. This is in agreement with Eq. 3.6 whose validity is therefore confirmed.

At large bed depths some deviation from the straight line behaviour occurs and Eq. 3.6 overpredicts the collection efficiency. The deviation is accentuated by the log scale and only occurs when the efficiencies exceed about 90%. The effect may be due to the presence of a small fraction of undersize aerosol particles in the aerosol. The electron micrographs (Figs. 4.8 and 4.10) show that several smaller particles are found together with the larger aerosol. The collection efficiency for these smaller sized

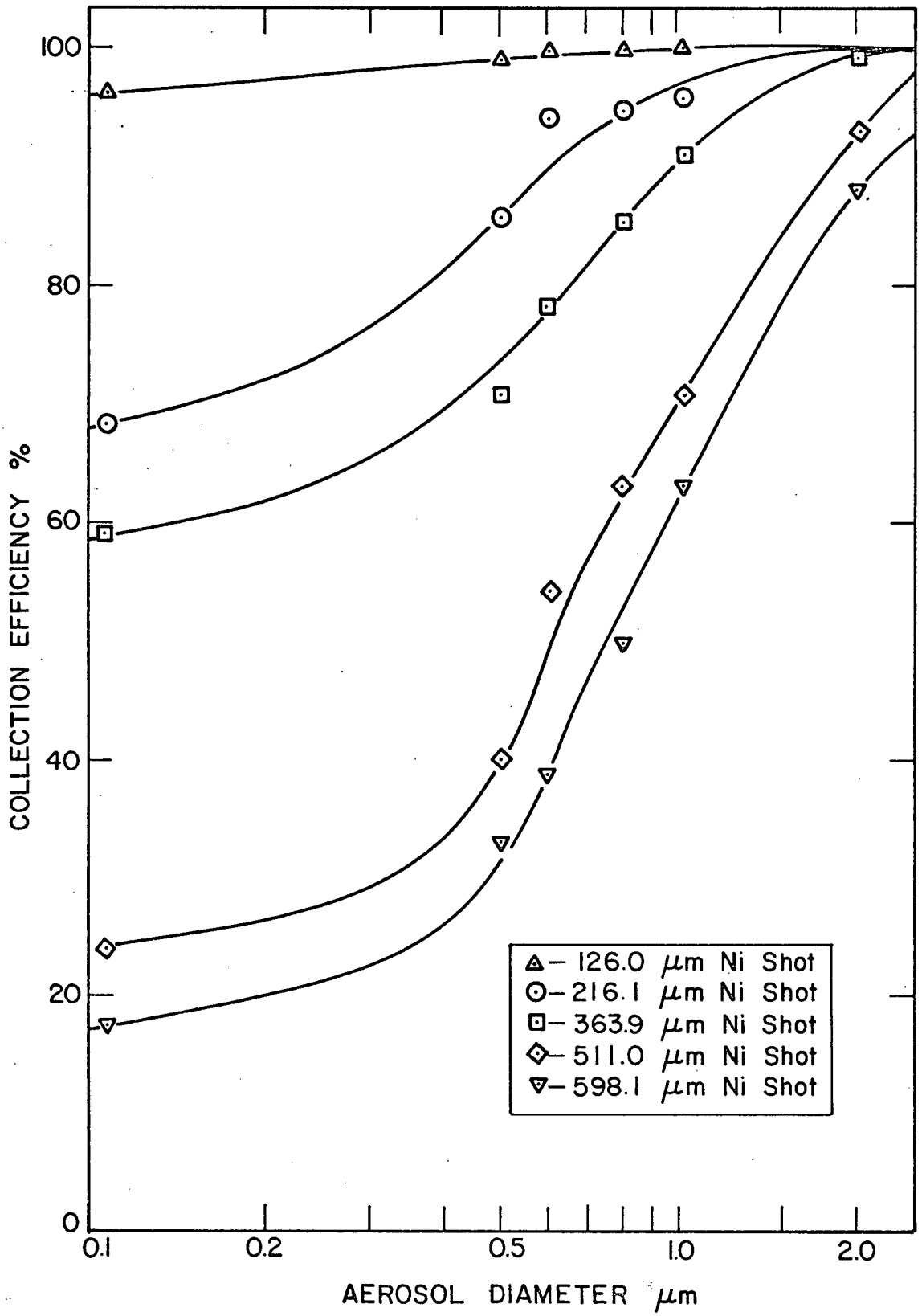

Fig. 6.11 Collection Efficiency as a Function of Aerosol Diameter at a Superficial Gas Velcoity of 5.24 cm/sec.

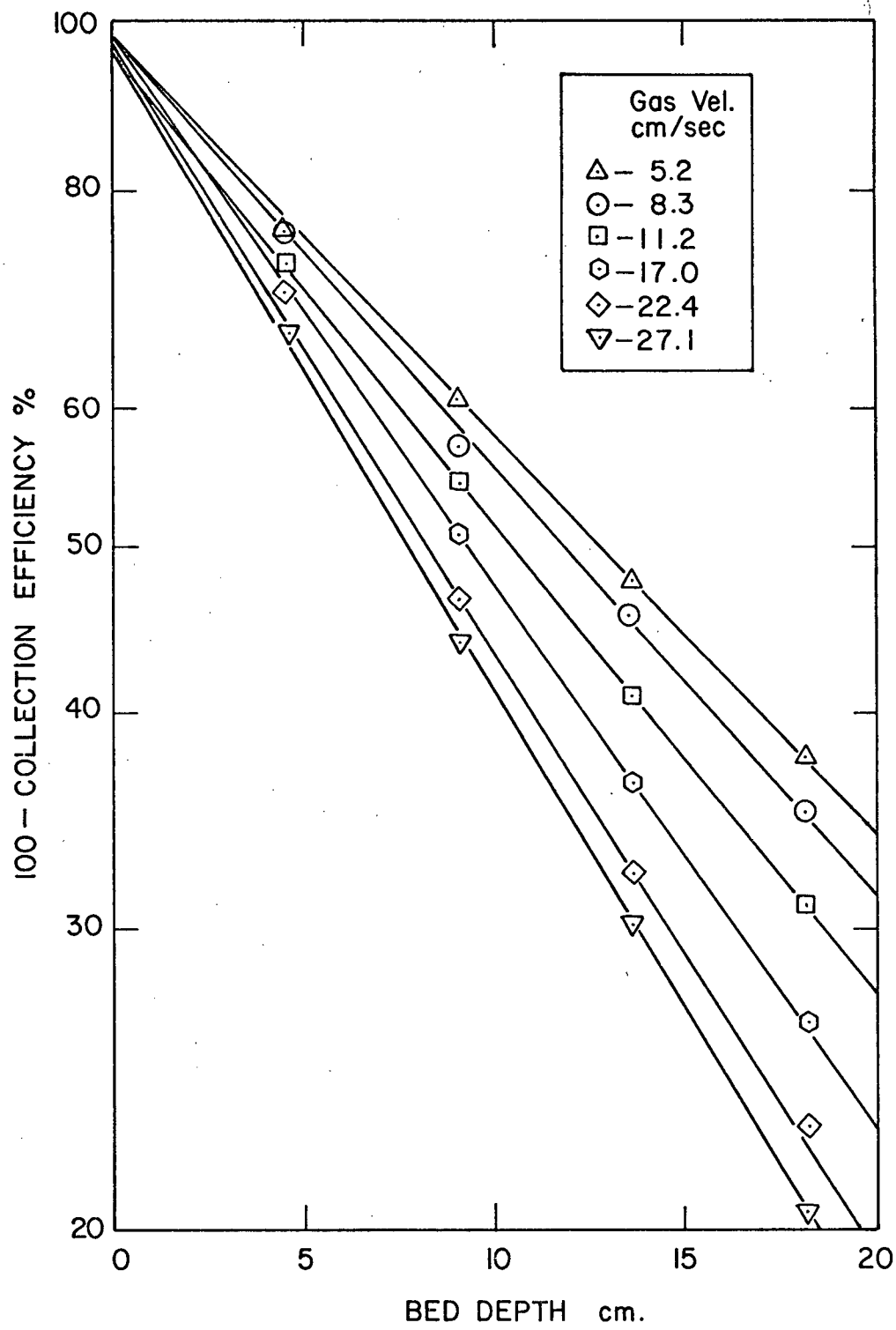

Fig. 6.12 Collection Efficiency as a Function of Bed Depth
(Collector diameter = 598 μm, aerosol diameter = 0.5 μm)

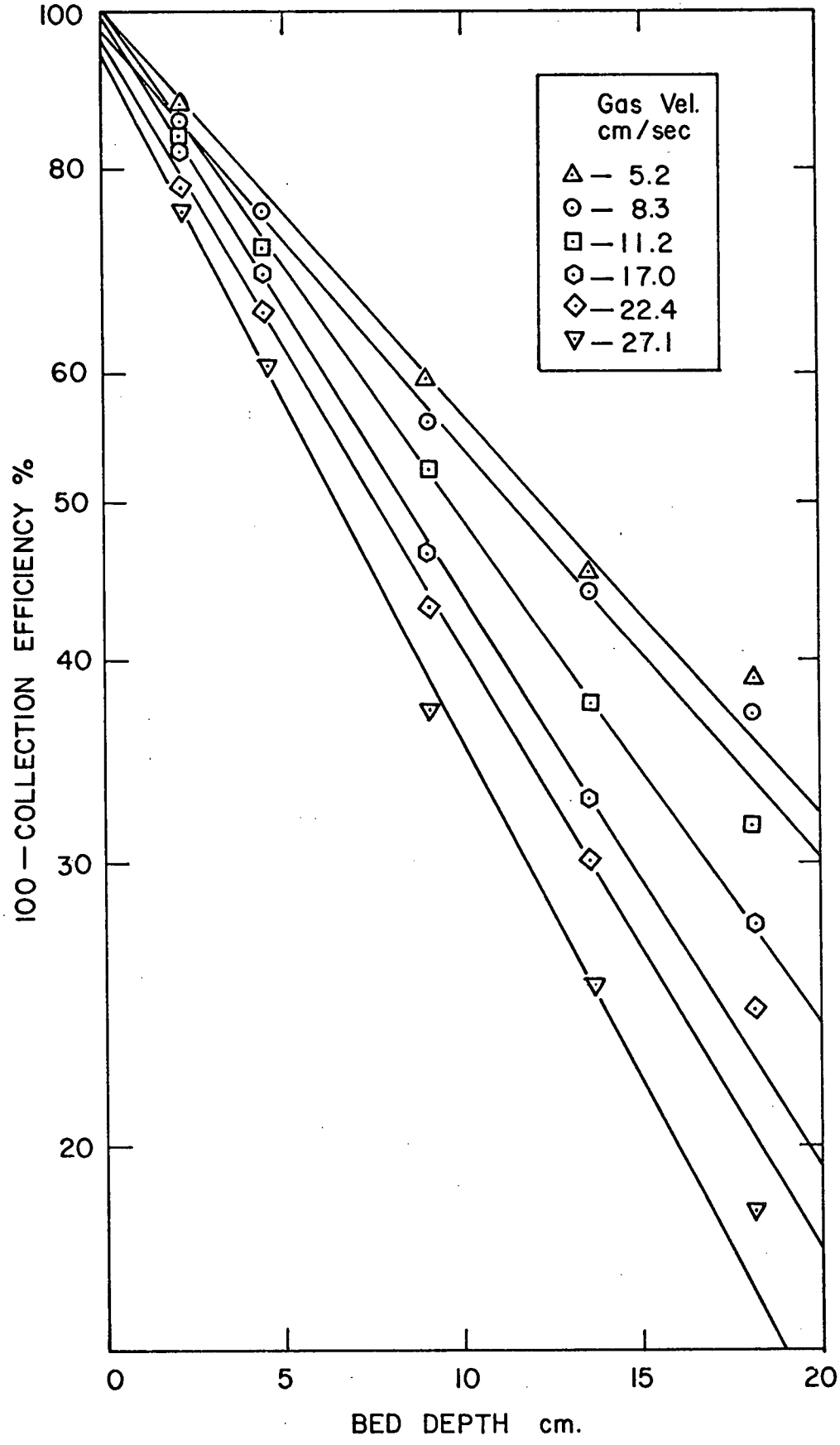

Fig. 6.13 Collection Efficiency as a Function of Bed Depth
(Collector diameter = 511 μm, aerosol diameter = 0.5 μm)

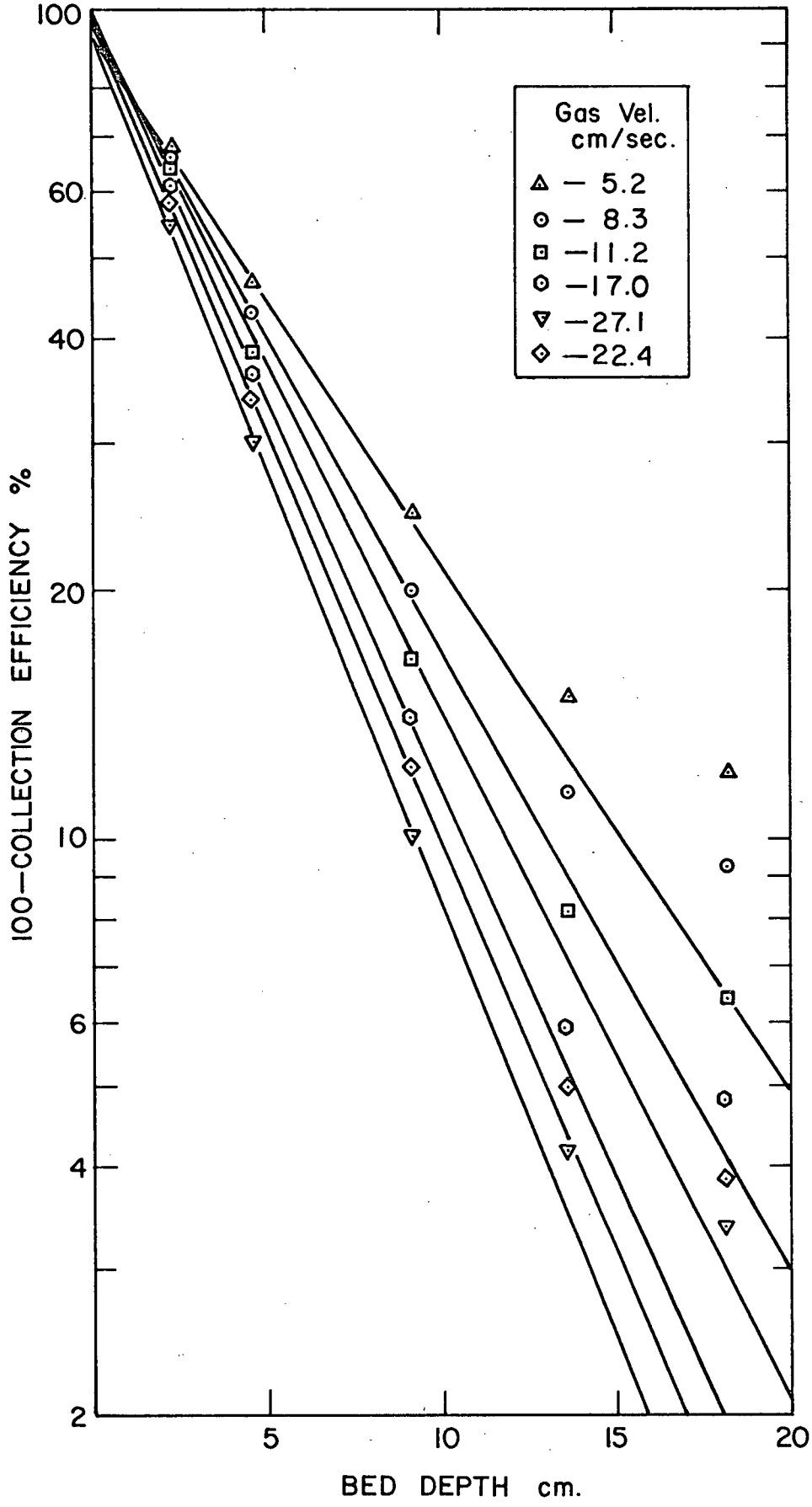

Fig. 6.14 Collection Efficiency as a Function of Bed Depth
(Collector diameter = 363 μm, aerosol diameter = 0.5 μm)

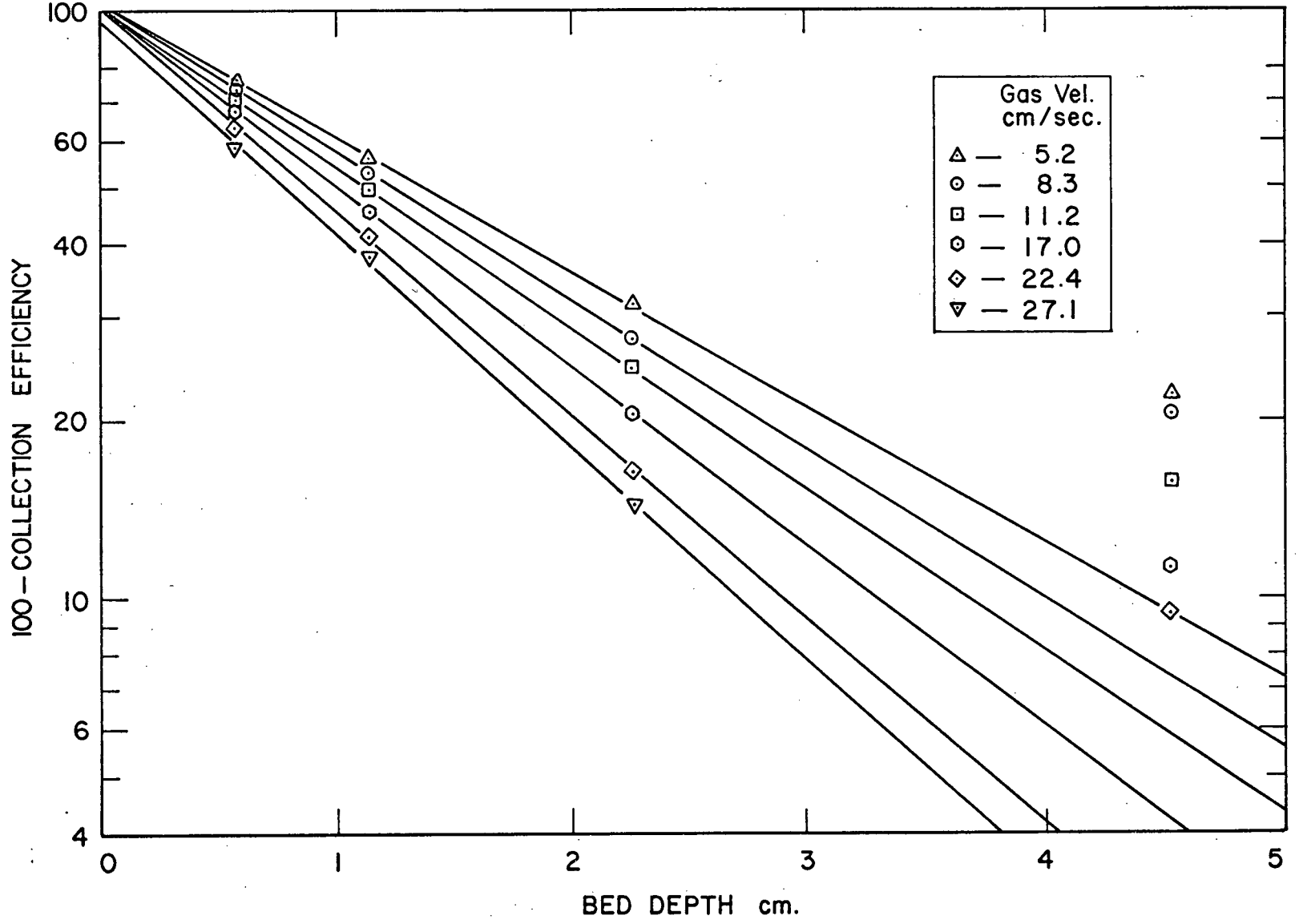

Fig. 6.15 Collection Efficiency as a Function of Bed Depth
(Collector diameter = 216 μm, aerosol diameter = 0.5 μm)

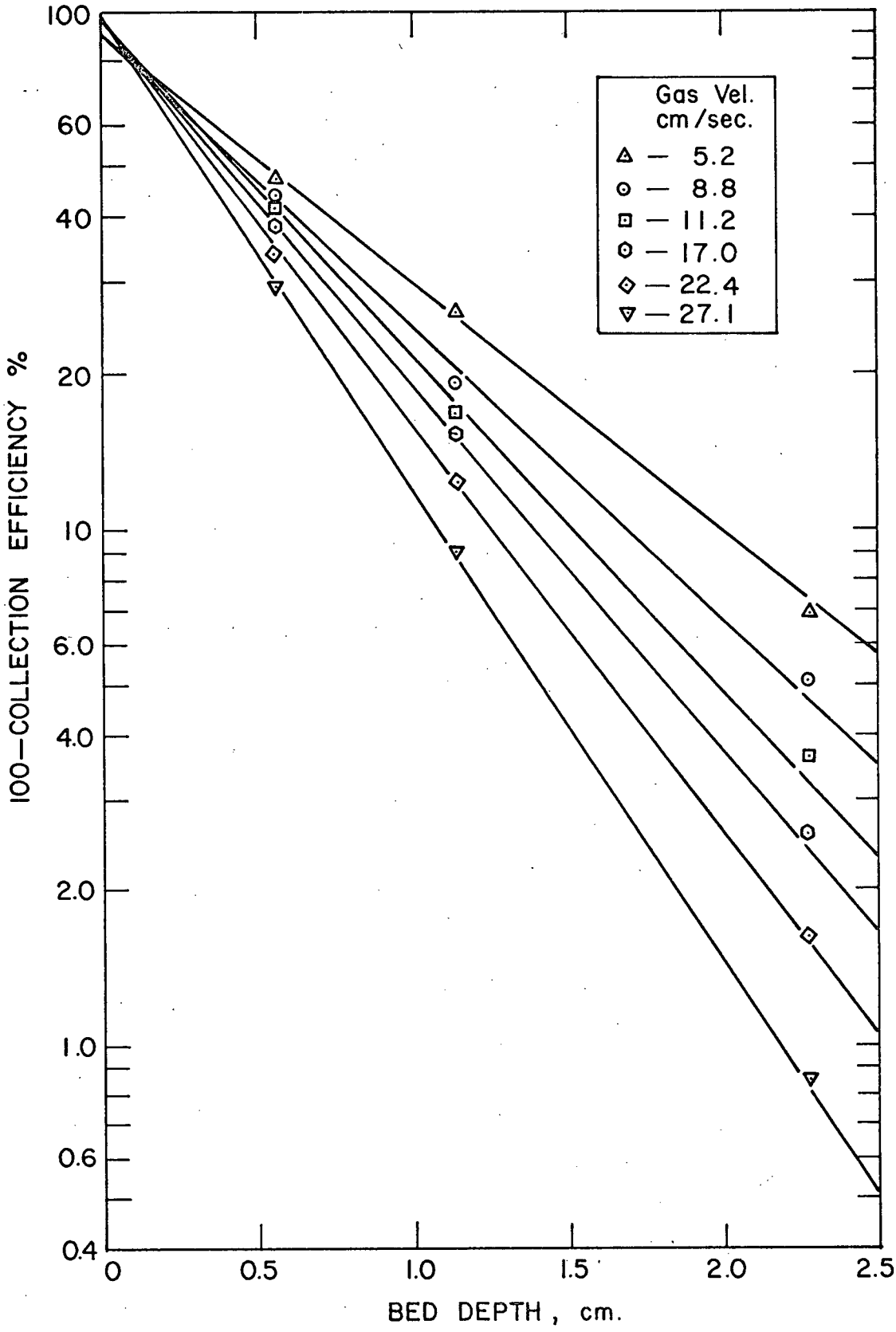

Fig. 6.16 Collection Efficiency as a Function of Bed Depth (Collector diameter = 126 μm, aerosol diameter = 0.5 μm)

aerosols would be much lower than that of the main aerosol. Thus their presence would result in a reduced, overall collection efficiency especially at high removal rates.

6.7 Pressure Drop across the Granular Bed

Pressure drops across the granular beds were measured for each gas velocity and the detailed results are given in Appendix A. From Fig. 6.17 it can be seen that there is a good linear relationship between $\Delta P/H$ and gas velocity. The results fit an Ergun[80] type equation of the following form:

$$\frac{\Delta P}{H} = 316 \frac{(1 - \varepsilon)^2}{\varepsilon^3} \frac{\mu U}{d_c^2} + 1.73 \frac{(1 - \varepsilon)}{\varepsilon^3} \frac{\rho_F U^2}{d_c} \qquad [6.1]$$

where the variables have the following units:

$\Delta P/H$ = dynes/cm^2 cm

d_c = cm

U = cm/sec

ρ_F = gm/cc

μ = gm cm/sec

The coefficients 316 and 1.73 lie within the range observed by others[80]. For the velocity range tested, viscous force dominates in the granular bed as compared to inertial effects. The pressure drop was attributable mainly to viscous energy losses.

6.8 Summary of Experimental Results

i) At low gas velocities (less than about 10 cm/sec) the collection efficiency decreases with increasing gas velocity, probably due to decreasing diffusional and gravitational effects.

ii) A minimum is observed in collection efficiency versus gas velocity curves when diffusional and inertial effects are both weak.

iii) The larger the aerosol size the lower the gas velocity at which this minimum collection occurs.

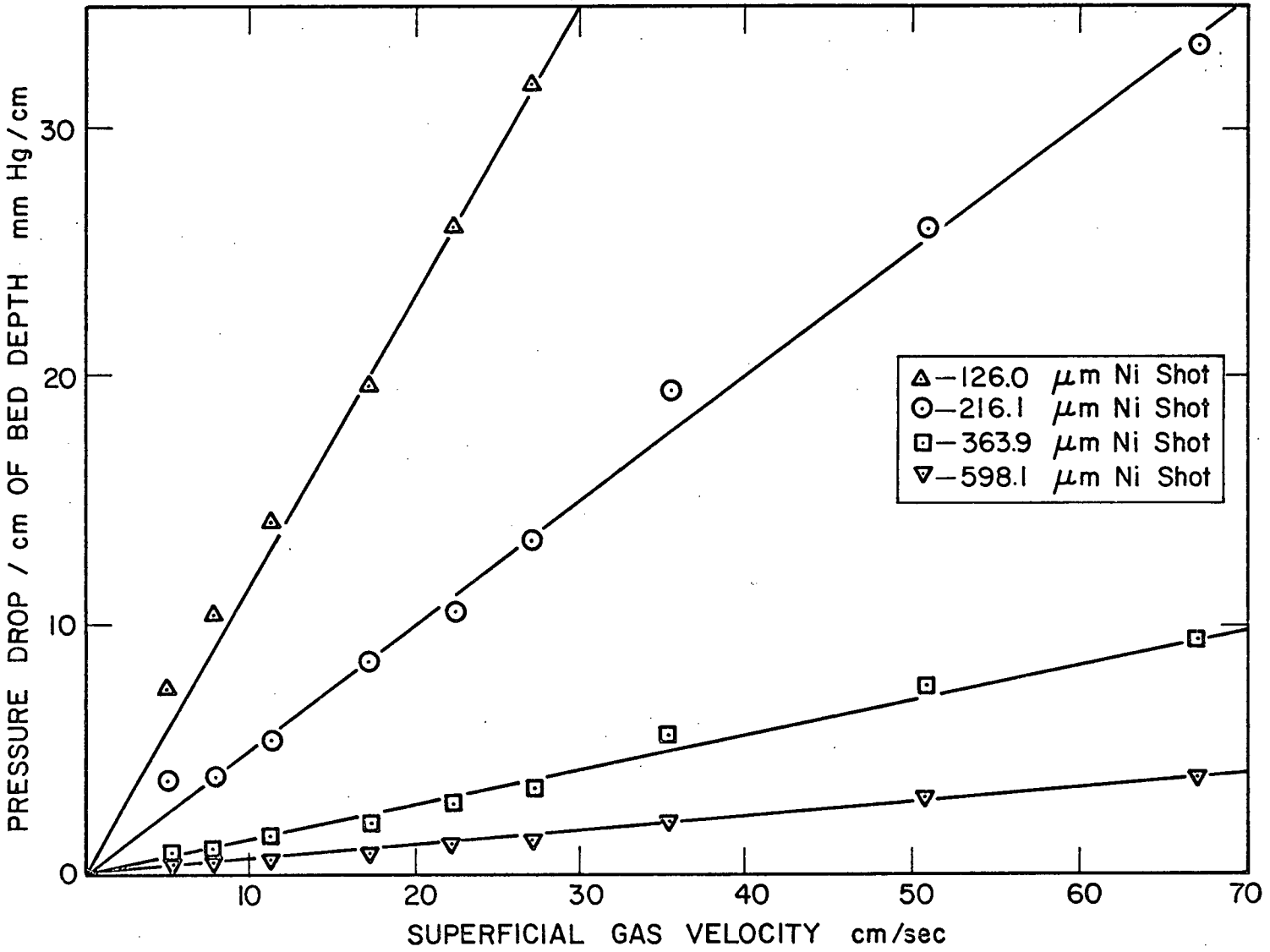

Fig. 6.17 Pressure Drop as a Function of Gas Velocity

iv) At higher gas velocities (greater than about 20 cm/sec) collection efficiency increases with gas velocity because inertial effects become dominant.

v) The collection efficiency increases with increasing aerosol size and decreasing collector size.

vi) The collection efficiency increases with bed depth as predicted by Eq. 3.6.

vii) As the collection efficiency for downflow is always greater than upflow at low gas velocities, it is evident that gravitational settling was playing a role in the filtration.

viii) For the range of conditions studied, direct interception played no role in the filtration.

CHAPTER 7

STATISTICAL ANALYSIS

7.1 Introduction

From the experimental results it was hoped to develop an empirical and, possibly, a theoretical model to predict aerosol collection in granular beds. The model would be based on variables such as bed depth, gas velocity, aerosol properties and collector dimensions.

The overall bed collection efficiencies (EBT), which were determined experimentally, were first reduced to single collector efficiencies (EB) by means of Eq. 3.6. Since EB is independent of bed depth, the single particle efficiencies calculated for different bed depths, but otherwise identical conditions, could be averaged.

As discussed in Chapter 1, the following dimensionless groups govern particle collection in granular beds and were calculated for each set of experimental conditions: Reynolds number (Re); Stokes number (St); Interception number (NR); Peclet number (Pe); and Gravity number (NG).

These dimensionless groups and single collector efficiencies are tabulated in Appendix B.

7.2 Evaluation of Various Empirical Equations

Most workers have concentrated on calculating the individual collection efficiencies due to inertia, diffusion, gravity and interception, and summed them to give an overall single collector efficiency. Others have calculated the various dimensionless numbers and combined them in such a manner as to

produce the single particle efficiency. As pointed out before, neither method is entirely correct, especially when working in a region where the magnitude of the effects of several collection mechanisms are comparable.

The equations developed by other workers were fitted to the present experimental data using a multiple regression programme. Other equations, such as polynomials based on the gas velocity, as well as aerosol and collector diameters were also tested.

The results of all regression analyses are summarized in Appendix C. In general, these equations gave relatively good fits when predicting the collection efficiency for a single collector or aerosol size. However, the overall fit for all the experimental data was quite poor. Consequently there was a need to develop a more general equation.

7.3 Identification of the Best Empirical Equation

The best fit of the experimental data was obtained with an equation of the type:

$$EB = a\left(\frac{d_a}{d_c}\right)(d_a U) + b\,\frac{d_a}{d_c}(d_a U)^{-2/3} + c\,\frac{d_a^2}{U} \qquad [7.1]$$

with constants a = 660, b = 0.0148, c = 400,000, and a multiple correlation coefficient (R) of 0.972. (The development of this equation is given in Appendix D together with a comparison of the experimental and predicted collection efficiencies.)

Equation 7.1 satisfactorily predicts the minimum in the collection efficiency versus gas velocity curves and the effect of gravity. Some disagreement, however, arises at high velocities, which could be due to bounce-off which is not taken into account.

The fit is worst for the 0.109 μm diameter aerosols which suggests that the diffusive effect is not properly represented. However, it should be noted that the experimental results obtained with 0.109 μm diameter aerosols

may be somewhat unreliable since the particle counter was used as its limit of detection. (The manufacturer recommends its use only for particles greater than 0.3 μm in diameter.)

Figs. 7.1 to 7.6 provide a comparison between some predicted (using Eqs. 3.6 and 7.1) and experimental bed collection efficiencies. Fig. 7.7 is a scatter plot of all calculated efficiencies versus experimental efficiencies and the agreement is within ± 10% for most cases.

The initial experimental results obtained by using granular beds of lead shot were not used in the development of Eq. 7.1. However, the collection efficiencies predicted by Eq. 7.1 agree with the lead shot results to within ± 1.5%. Also listed in Appendix D are comparisons of the predicted bed collection efficiencies and the experimental results of other researchers.

Comparisons were made with Figueroa's[20] data based on experiments with 7000 μm diameter sand. His other experimental results were not compared since they were obtained with plastic bed particles susceptible to electrical effects. The predictions of Eq. 7.1 agree well with Figueroa's results and especially the measurements made with 0.5 μm diameter aerosols.

Further comparisons were made with the results of Doganoglu[23]. He used 110 and 600 μm diameter glass beads as collector particles and D.O.P. aerosol particles. Equation 7.1 is rather poor in predicting the collection efficiencies of the 600 μm collectors, except at the higher velocities of 30 cm/sec. The predictions are better for the 110 μm collectors especially for the removal of 1.75 μm diameter aerosols. The poor predictions of Doganoglu's results could be due to the fact that he used liquid D.O.P. aerosol particles whereas Eq. 7.1 is based on dry, solid aerosol particles. However, this does not explain why in general the prediction of Eq. 7.1 are higher than the experimental values; using liquid aerosols should in fact improve the collection efficiency of the bed.

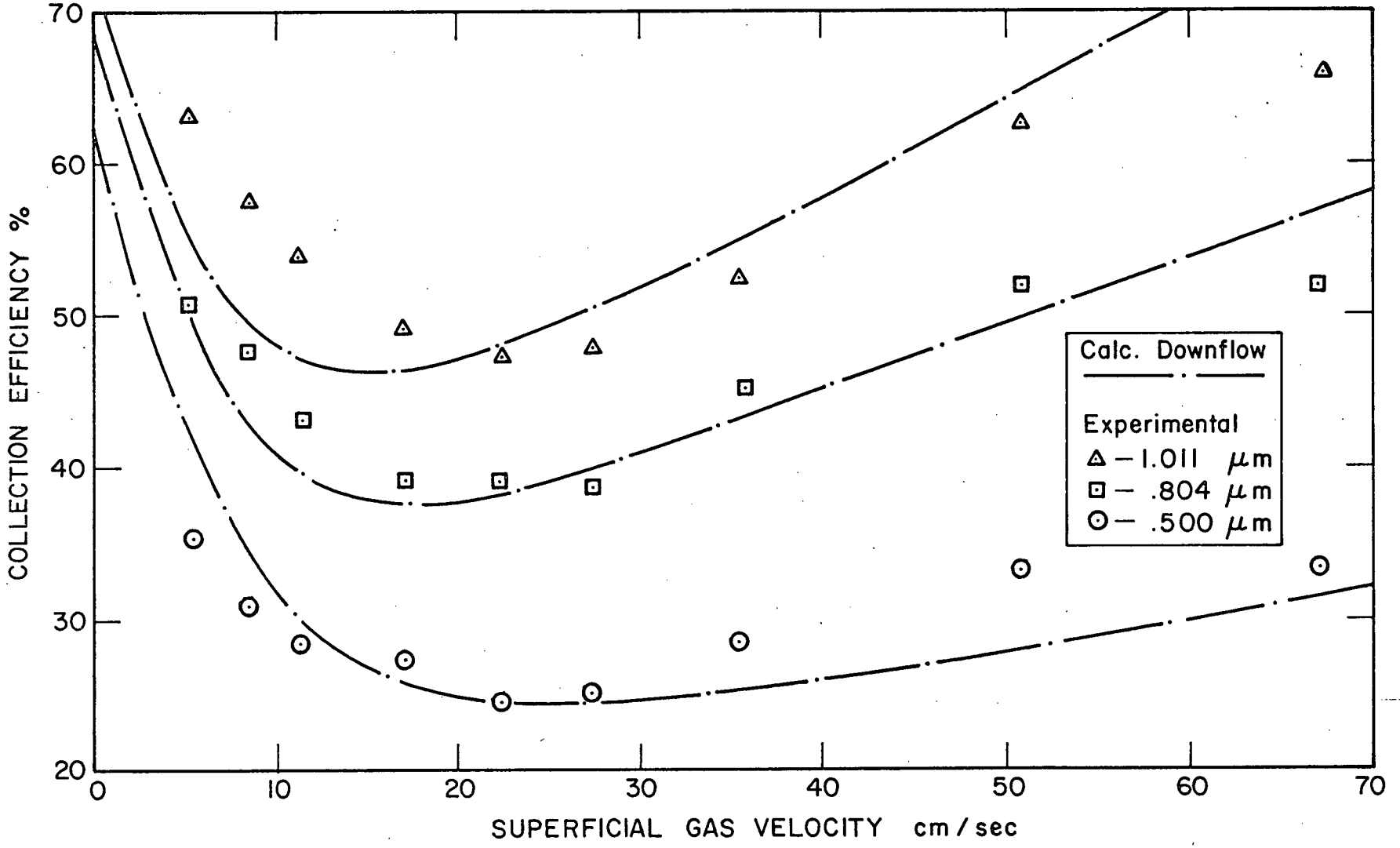

Fig. 7.1 Comparison of Experimental and Calculated Collection Efficiencies (Collector diameter = 598.1 μm)

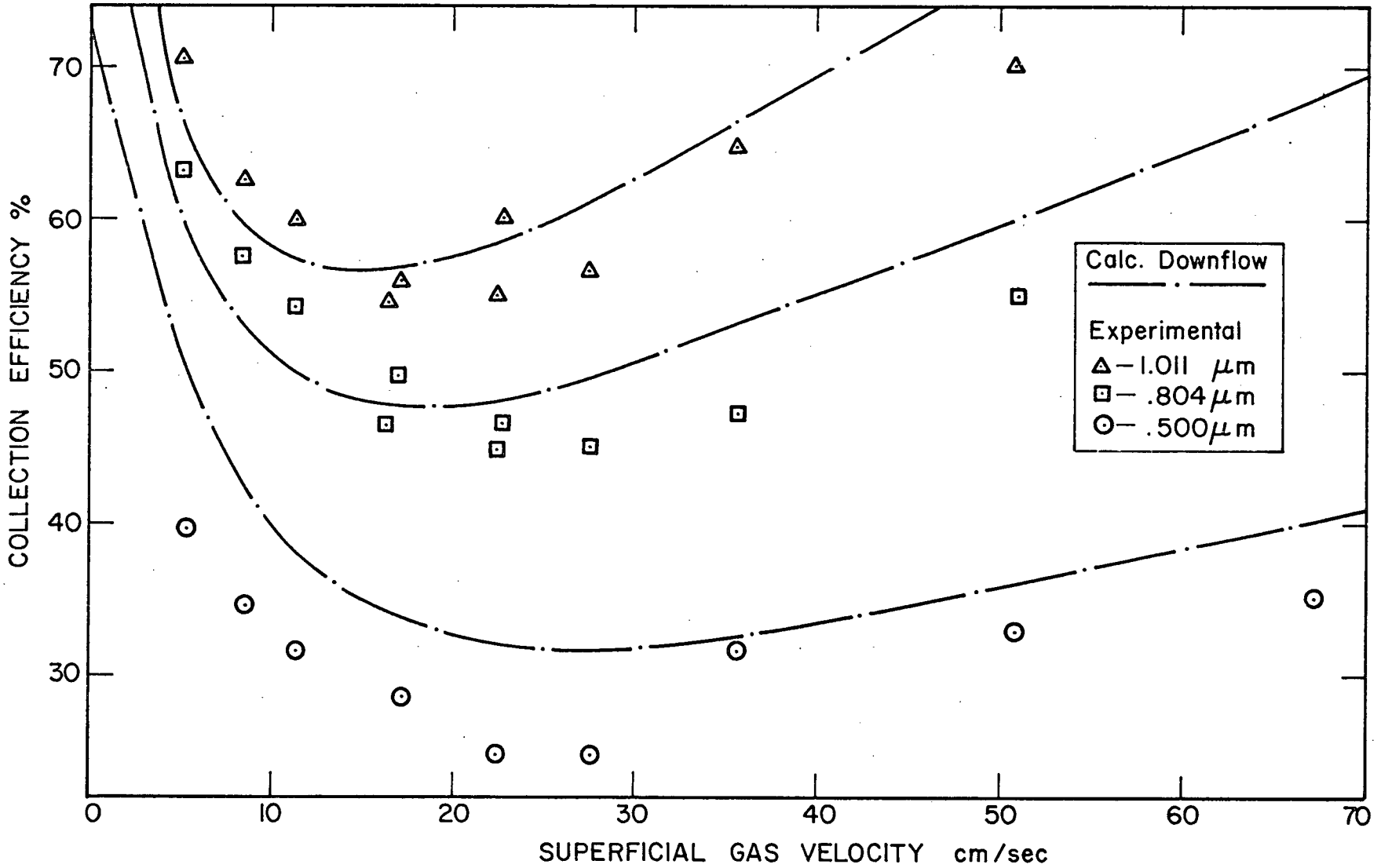

Fig. 7.2 Comparison between Experimental and Calculated Collection Efficiencies (Collector diameter = 511.0 μm)

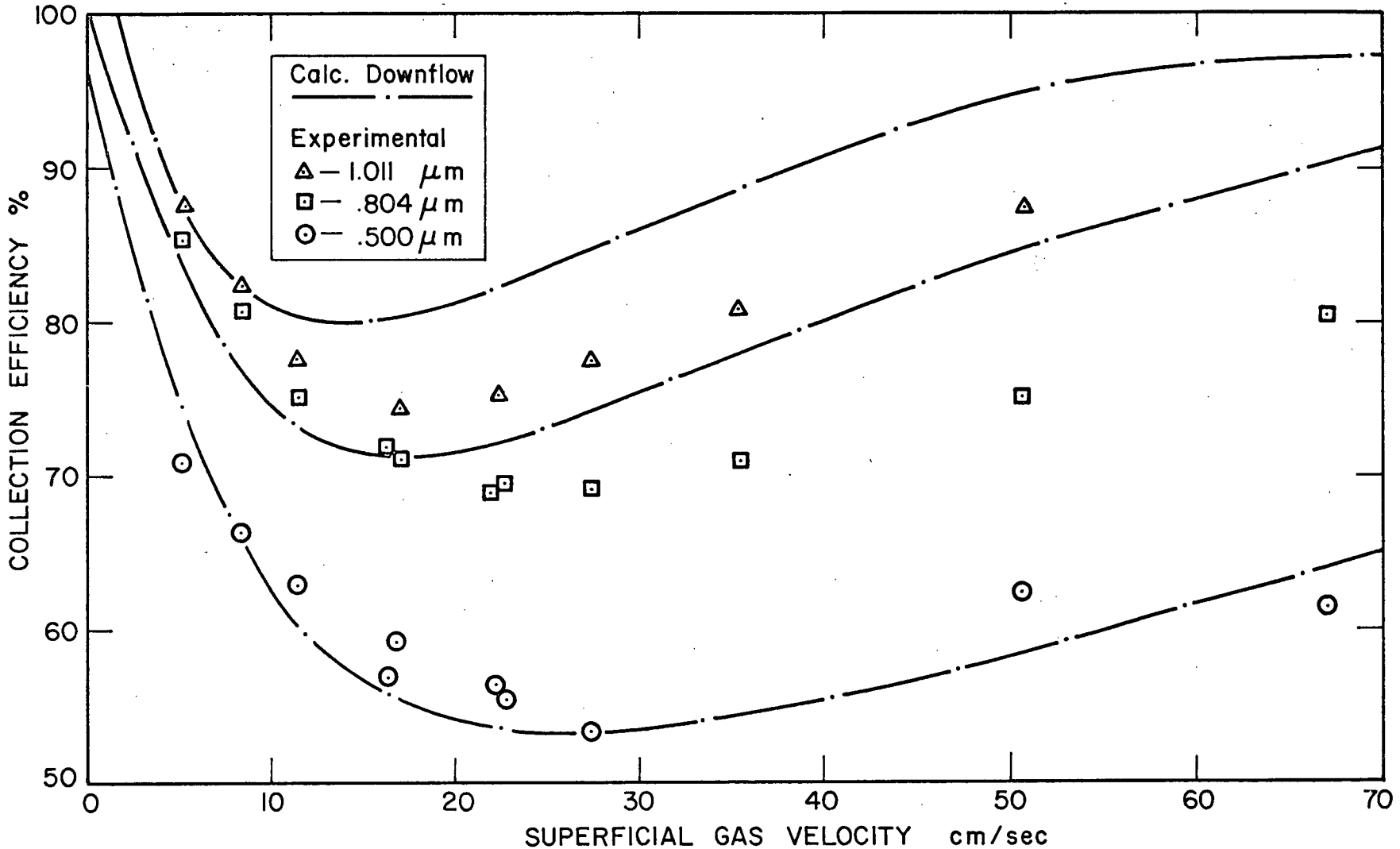

Fig. 7.3 Comparison Between Experimental and Calculated Collection Efficiencies (Collector diameter = 363.9 μm)

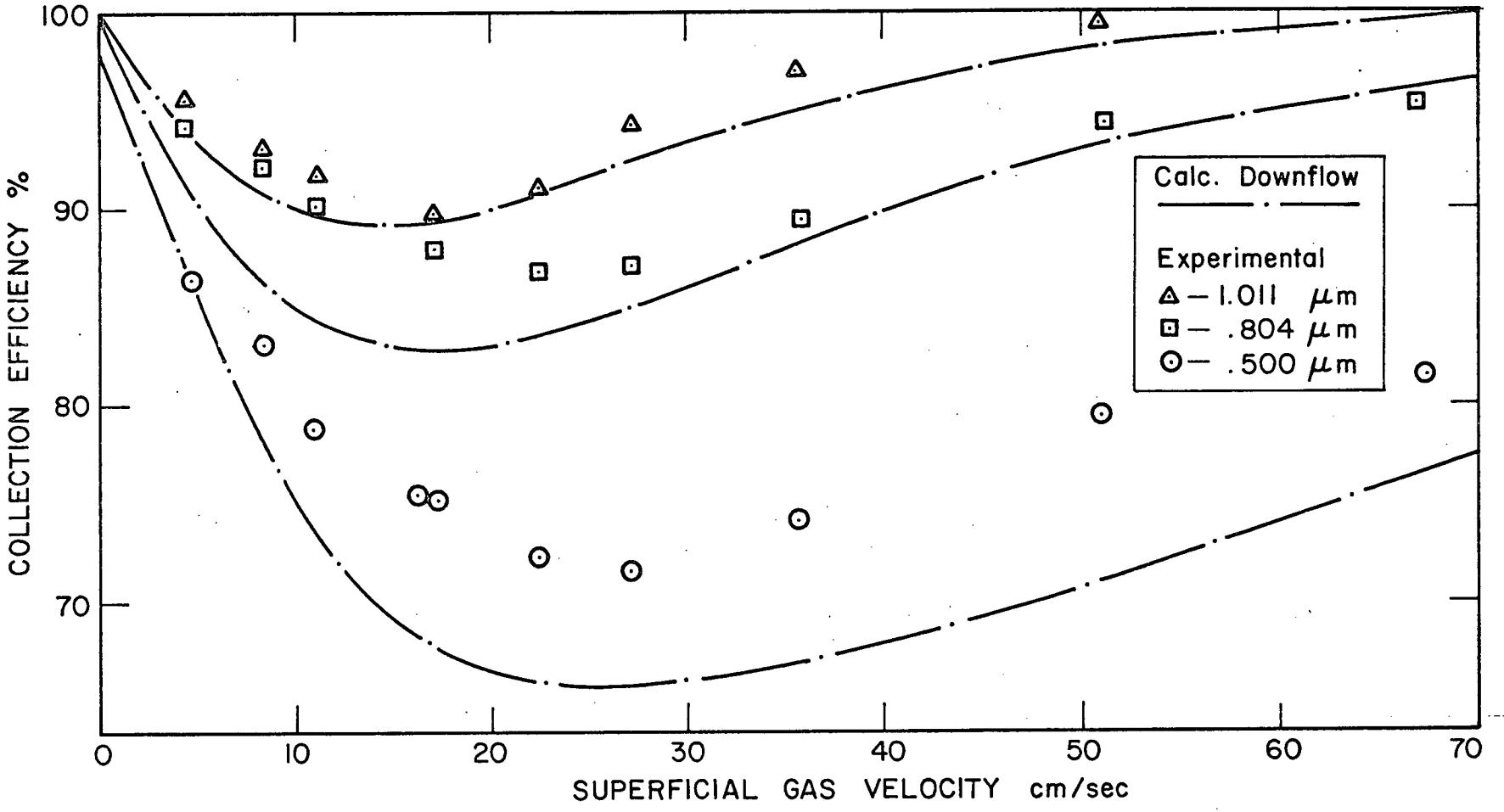

Fig. 7.4 Comparison of Experimental and Calculated Collection Efficiencies (Collector diameter = 216.0 μm)

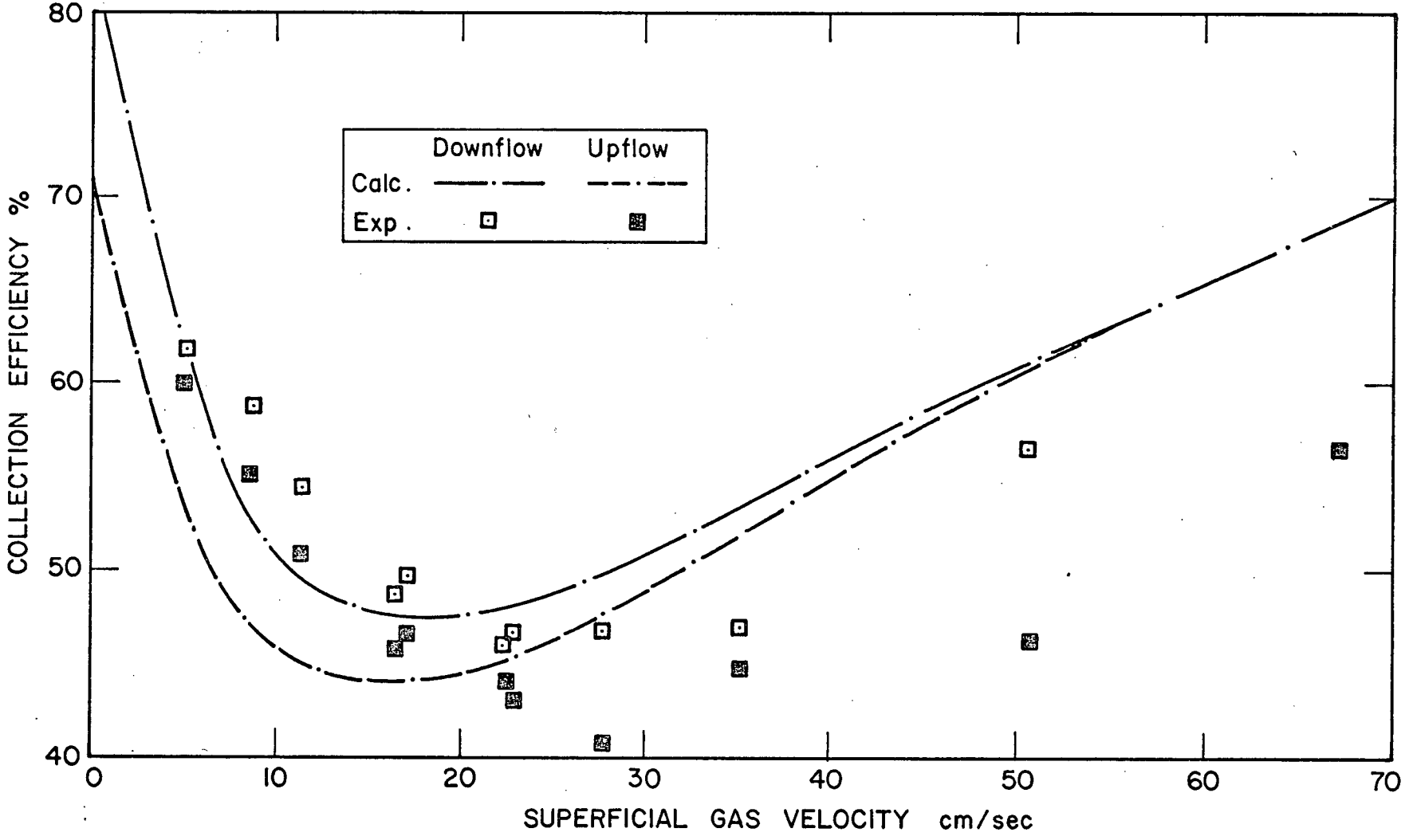

Fig. 7.5 Comparison of Experimental and Calculated Collection Efficiencies (Upflow and downflow; aerosol diameter = 0.804 μm; collector diameter = 511.0 μm)

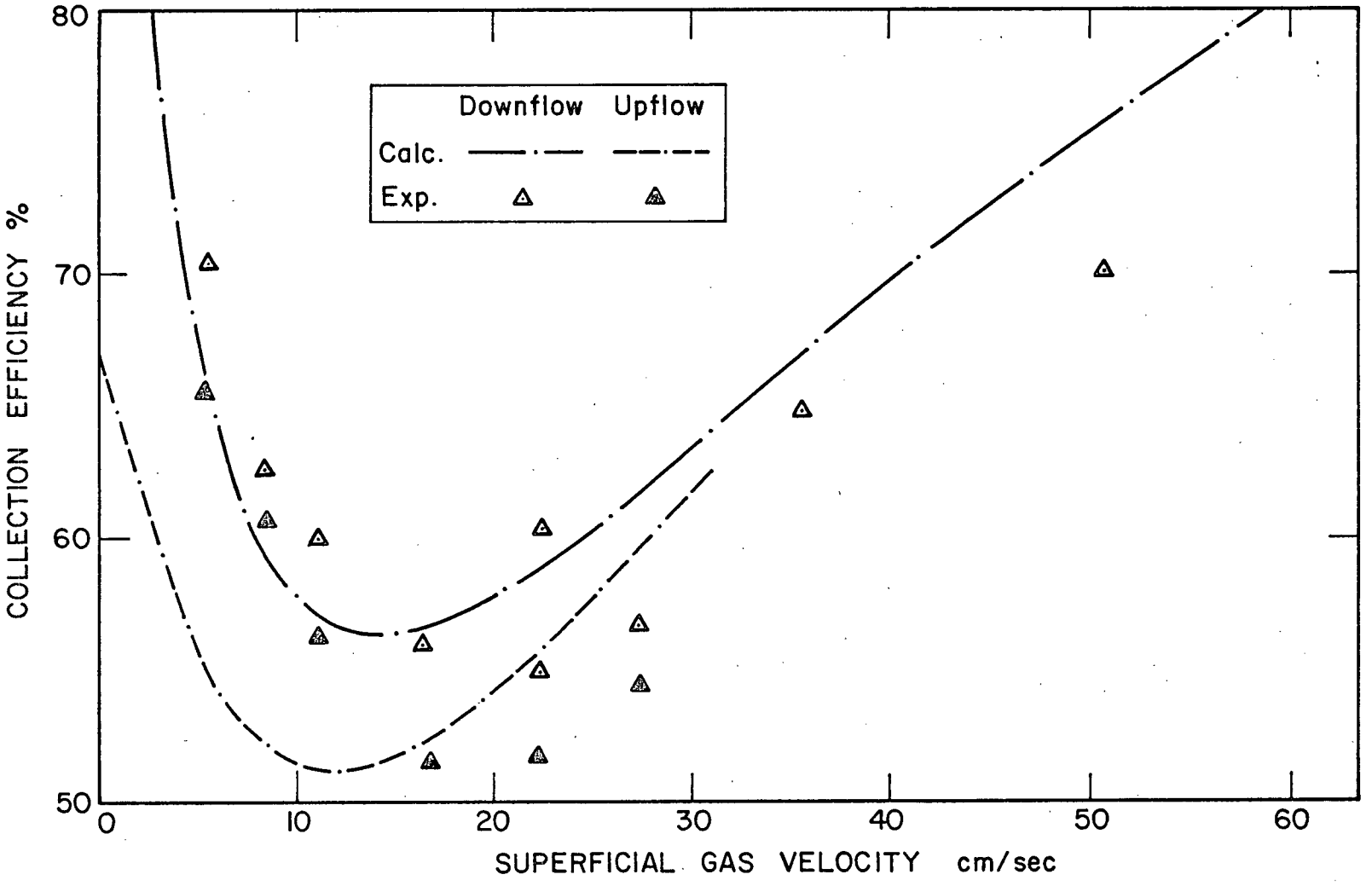

Fig. 7.6 Comparison of Experimental and Calculated Collection Efficiencies (Upflow and downflow; aerosol diameter = 1.011 μm; collector diameter = 511.0 μm)

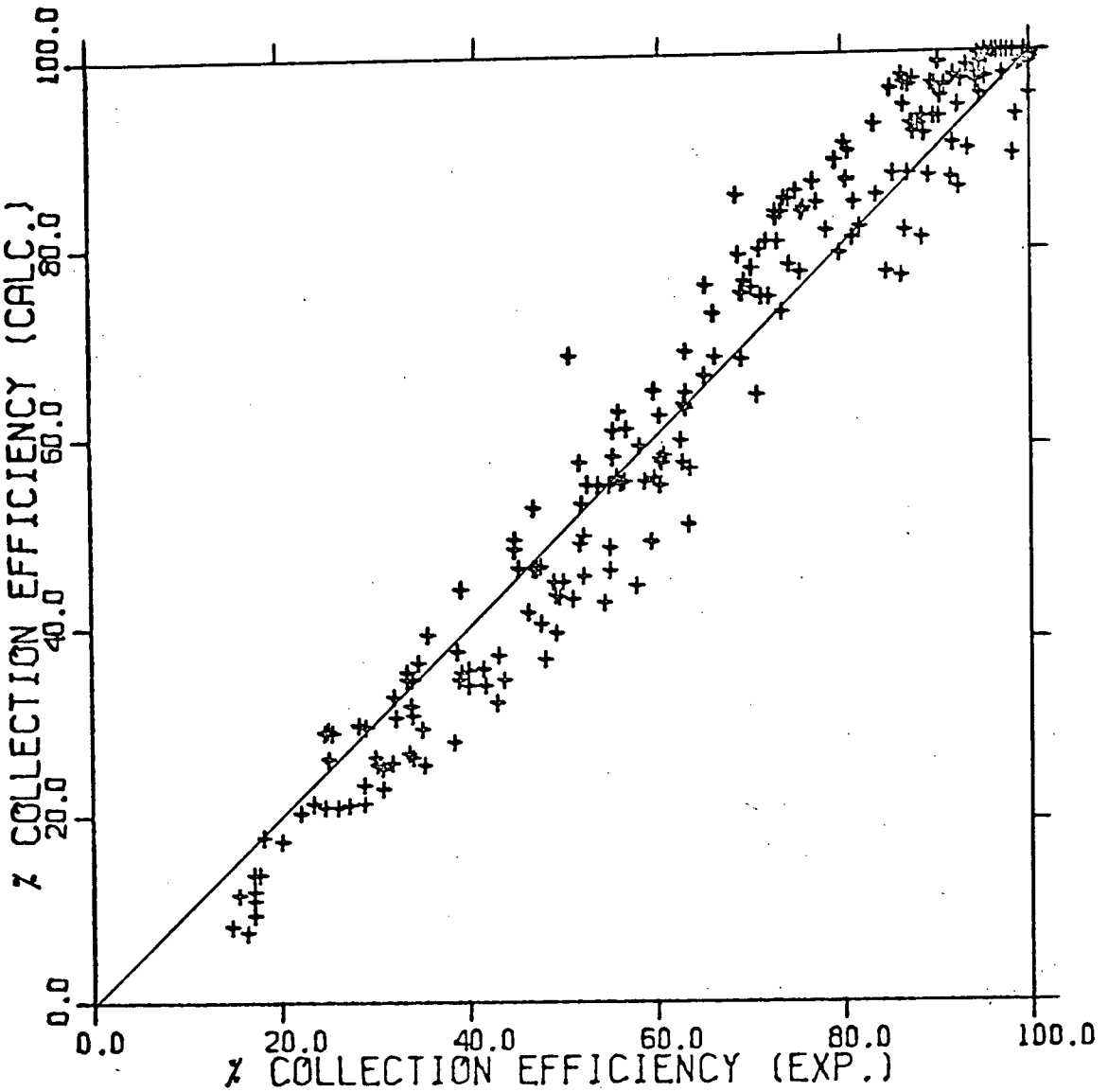

Fig. 7.7 Scatter Plot of Experimental and Calculated Collection Efficiencies (using Eqs. 3.6 and 7.1)

7.4 Interpretation and Modification of Equation 7.1

By considering the fluid properties of the dispersion medium it is possible to reduce Eq. 7.1 to dimensionless form. Thus the first term on the right hand side becomes a Stokes number (St) and the third term becomes a gravity number (NG).

1st term:
$$\frac{d_a^2}{d_c} U \equiv \frac{\rho_F}{9\mu} \left(\frac{d_a^2}{d_c} U\right) \equiv St$$

3rd term:
$$\frac{d_a^2}{U} \equiv \frac{\rho_a g}{18\mu} \left(\frac{d_a^2}{U}\right) \equiv \frac{U_s}{U} = NG$$

The second term is more difficult to simplify and does not reduce easily to dimensionless form. Thus Eq. 7.1 becomes

$$EB = 1.018\ St + 0.0148\ NR(d_a\ U)^{-2/3} + 1.25\ NG \qquad [7.2]$$

The efficiency equation therefore consists of three terms. The first and third terms represent the inertial and gravitational effects, respectively. The gravity term being positive for downflow and negative for upflow. The contribution of the gravity term to EB is usually very small and only becomes significant for low gas velocities and large or dense aerosols. The contributions of the first and second terms are highly dependent on gas velocity. The main contribution to EB is due to the second term at low velocities and the first (inertial) term at high velocities. It is interesting to note that the interception term was eliminated from all the equations by the regression analysis. Thus it can be concluded that direct interception was playing a negligible role in the aerosol filtration of this work.

It is rather difficult to explain the second term in Eq. 7.1, which may be due to diffusion even though it cannot be reduced to a Peclet number or a similar dimensionless group. It is probably a combination term reflecting both diffusion and inertia.

7.4.1 Modification of the Second Term in Equation 7.1

An attempt was made to introduce the Peclet number into the second term of Eq. 7.1. It is simple to show that

$$\frac{d_a}{d_c} (d_a U)^{-2/3} = (\frac{d_a}{d_c})^{1/3} (d_c U)^{-2/3}$$

Now the Peclet number is defined as $(d_c U/D_a)$ where the diffusivity of the aerosol particle is denoted by D_a. Fig. 7.8 shows that $D_a^{-2/3}$ is proportional to d_a for the range $0.1 < d_a < 2.02$ μm. Hence

$$(\frac{d_a}{d_c})^{1/3} (d_c U)^{-2/3} \propto \frac{d_a}{D_a^{-2/3}} (\frac{d_a}{d_c})^{1/3} (d_c U)^{-2/3}$$

$$\propto \frac{d_a^{4/3}}{d_c^{1/3}} (\frac{d_c U}{D_a})^{-2/3}$$

$$\propto \frac{d_a^{4/3}}{d_c^{1/3}} (Pe)^{-2/3}$$

To render the term completely dimensionless, it could be divided by d_a or d_c. Dividing by d_c was found to give the best results for predicting EB. Thus Eq. 7.1 could be rewritten as

$$EB = a.St + b.NR^{4/3} Pe^{-2/3} + c.NG \qquad [7.3]$$

and fitted to the experimental data by regression analysis. The following values were found for the constants: a = 1.0; b = 150,000; and c = 1.5.

Equation 7.3 gave equally good predictions of EB as Eq. 7.1, having a multiple correlation coefficient (R) of 0.94. Fig. 7.9 shows a scatter plot of the calculated versus experimental collection efficiencies using Eq. 7.3.

In the present experiments $NR^{4/3} >> 1$, and the second term in Eq. 7.3 may be rewritten as:

$$b\ Pe^{-2/3} [1 - \exp\{- NR^{4/3}\}]$$

or

$$b\ Pe^{-2/3} - b\ Pe^{-2/3} \exp\{- NR^{4/3}\}$$

The term $b\ Pe^{-2/3}$ represents the diffusional effects whereas $b\ Pe^{-2/3} \exp\{- NR^{4/3}\}$ reflects the interaction between diffusion and inertia.

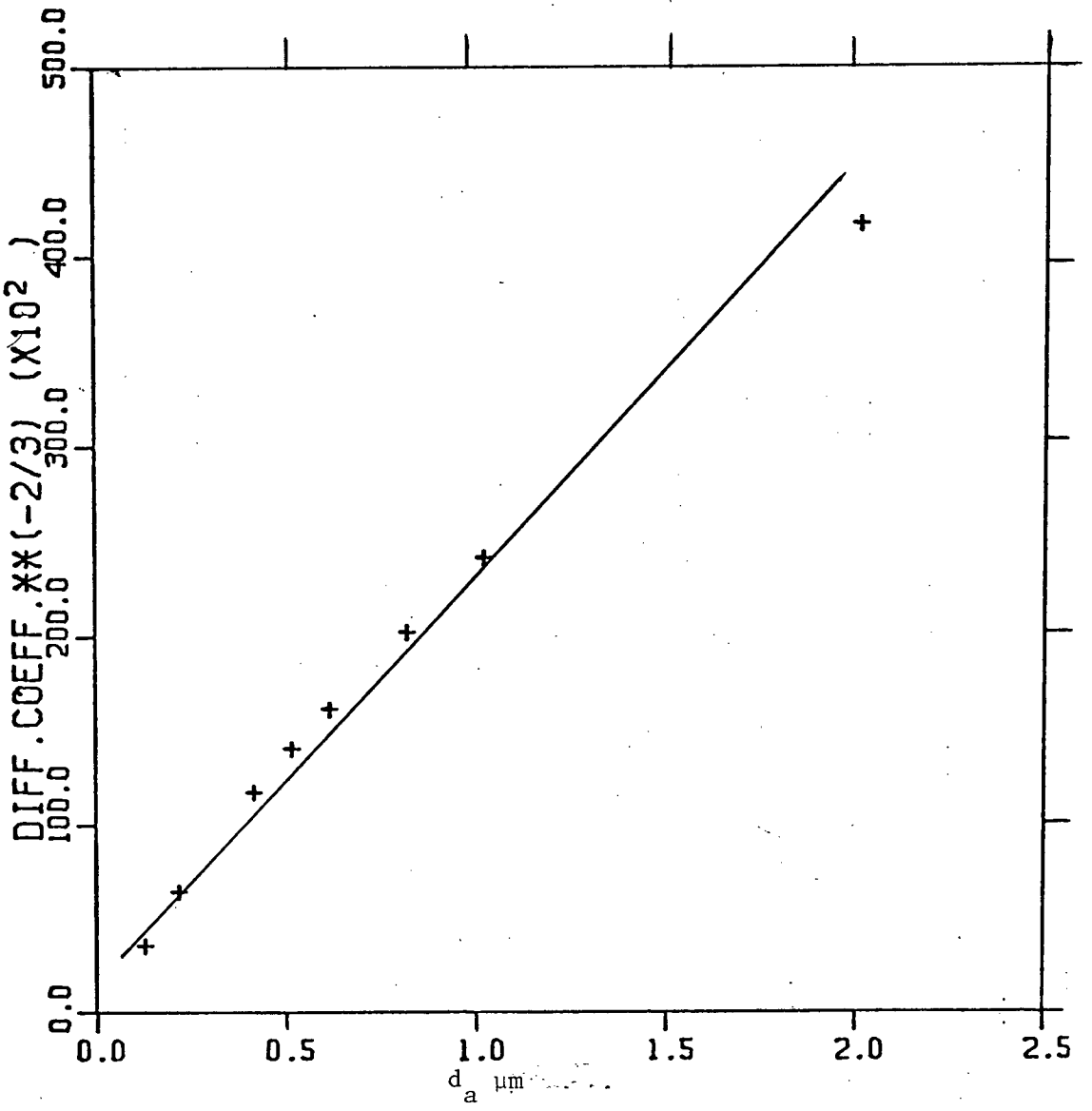

Fig. 7.8 Diffusion Coefficient (D_a) as a function of Aerosol Diameter (d_a)

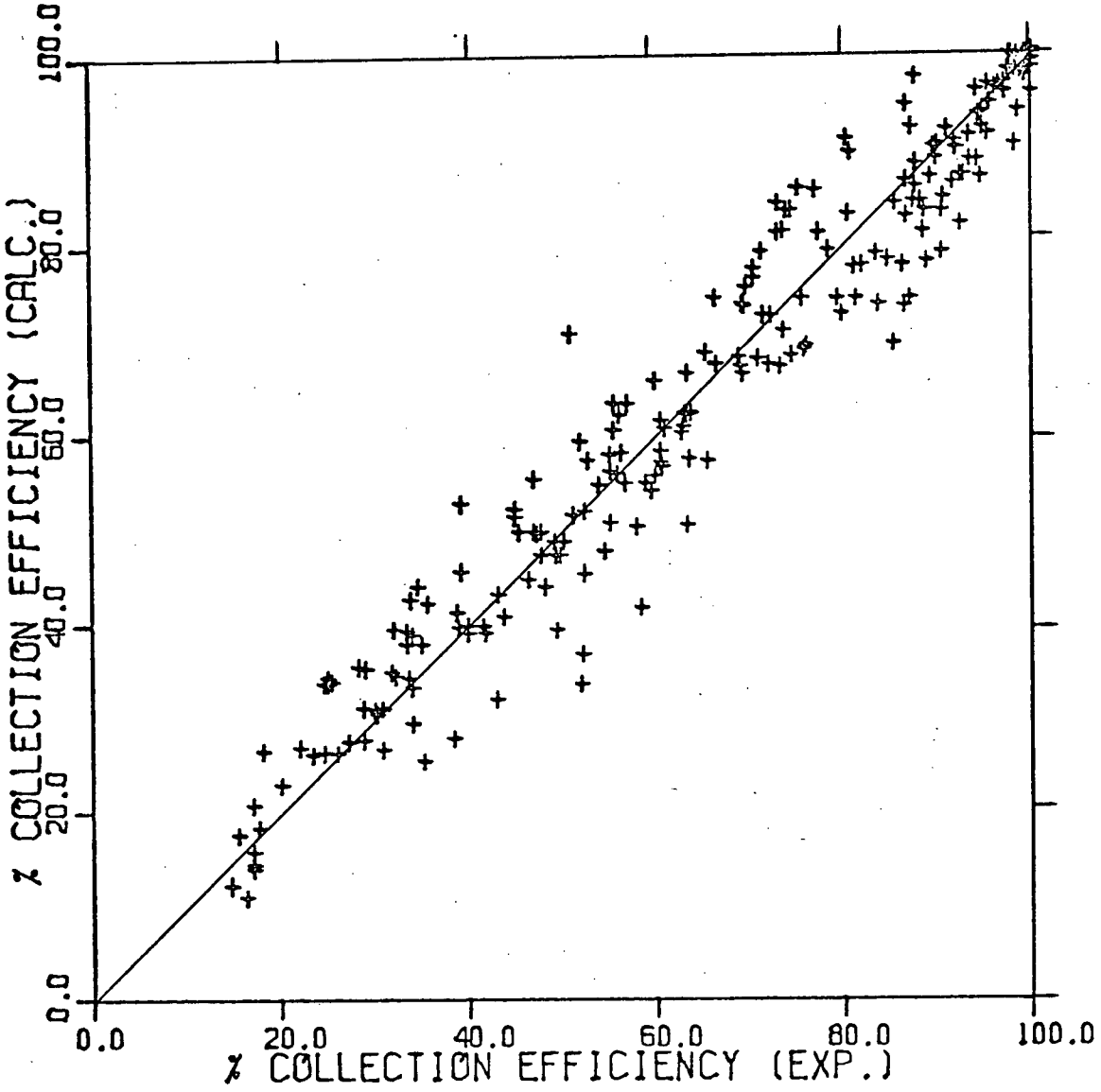

Fig. 7.9 Scatter Plot of Experimental and Calculated Collection Efficiencies (using Eqs. 3.6 and 7.3)

Although Eq. 7.3 adequately predicts the collection efficiencies observed in the present experimental work, it does not predict a minimum collection efficiency with respect to aerosol diameter. However, as noted by several workers, this minimum collection efficiency is only observed at low gas velocities, i.e., less than 4 cm/sec. Therefore Eq.7.3's only limitation is it cannot be used for prediction of EB at gas velocities below about 5 cm/sec. For lower gas velocities aerosol capture is dominated by the diffusional mechanism and equations developed for purely diffusional deposition[63,32,81] may be used instead.

A recent paper by Schmidt[69] discusses the use of an equation of the type:

$$EB = 3.97\ St + (8\ Pe^{-1} + 2.3\ Re^{1/8}\ Pe^{-5/8}) + 1.45\ NR + NG \quad [7.4]$$

This equation predicts a minimum in EB with respect to aerosol diameter and it was therefore fitted to the present experimental data. The following equation was obtained by multiple regression:

$$EB = 0.8\ St + 8\ (8\ Pe^{-1} + 2.3\ Re^{1/8}\ Pe^{-5/8}) + 1.25\ NG \quad [7.5]$$

However Eq. 7.5 proved only applicable to aerosols in the 0.5 to 1.0 μm diameter range; the fit for 0.109 and 2.02 μm diameter aerosols was considerably poorer. Fig. 7.10 shows a scatter plot for aerosols in the 0.5 to 1.0 μm diameter range. It is clear that the fit is much poorer than that obtained by Eq. 7.1 or 7.3.

7.5 Conclusion

An equation (Eq. 7.3) has been developed which predicts the collection of 0.1 to 2.02 μm latex aerosols by beds of spherical collectors in the range of 100 to 600 μm in diameter. The predictions of this equation match the present experimental results better than expressions proposed by previous workers. Equation 7.3 has the advantage of simplicity and wide range of

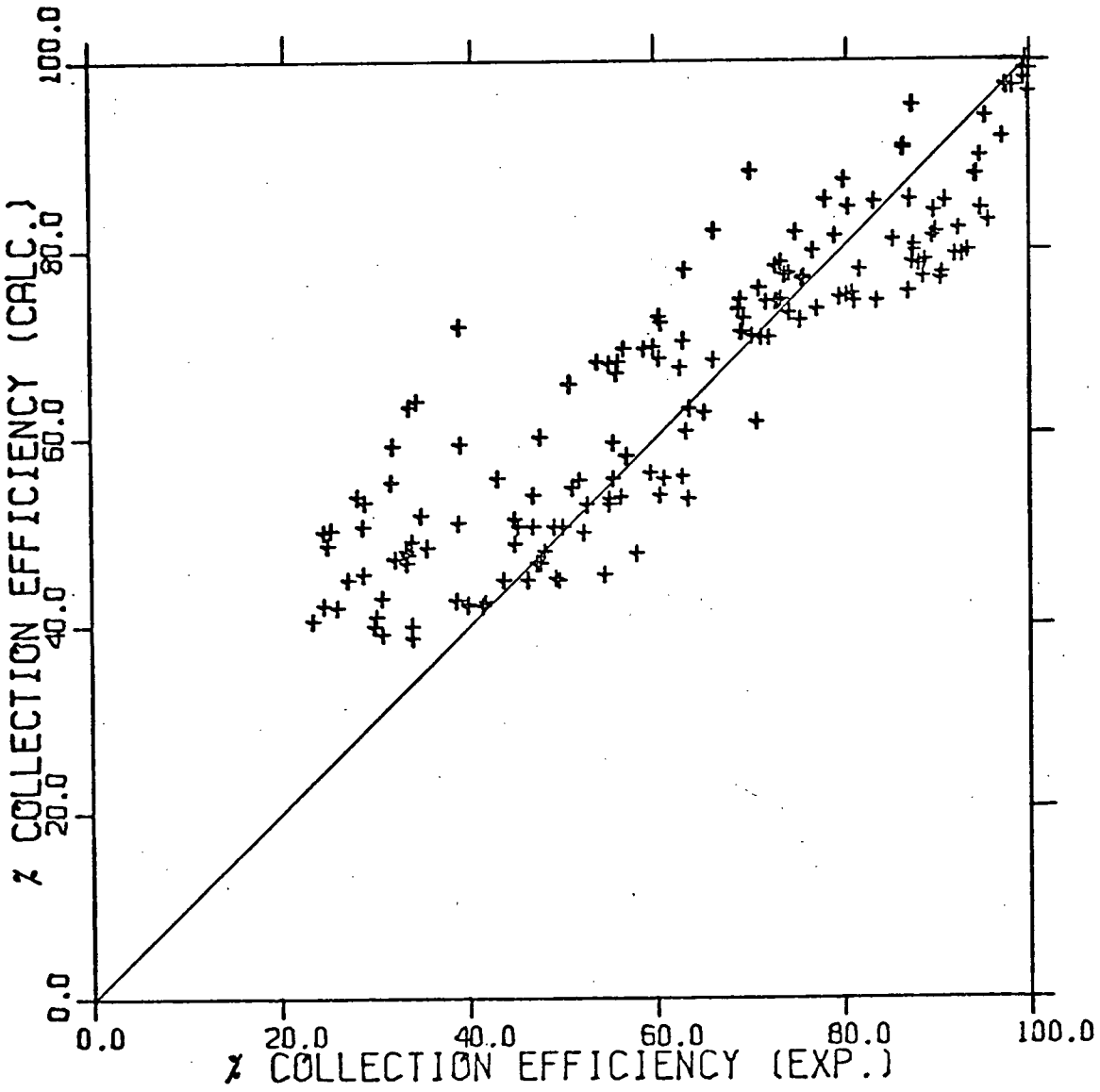

Fig. 7.10 Scatter Plot of Experimental and Calculated Collection Efficiencies (using Eqs. 3.6 and 7.5; aerosol diameters in the range 0.1 to 5.0 μm)

applicability. By comparison with other experimental data the equation is capable of predicting collection efficiencies for beds of spherical collectors up to 7000 μm in diameter. Unfortunately the equation is unable to determine an aerosol size which gives a minimum collection efficiency for a given gas velocity. Thus use of Eq. 7.3 should therefore be limited to gas velocities greater than about 5 cm/sec.

CHAPTER 8

CONCLUSIONS

i) Granular beds of particles 100 to 600 μm in diameter were found to be highly efficient aerosol collectors. For example, at least 95% of 0.1 μm and greater diameter aerosols were collected by a 2.27 cm deep bed of 126 μm diameter nickel shot, having a pressure drop across the bed of 2.5 cm of mercury.

ii) At superficial gas velocities below 10 cm/sec aerosol removal was found to be mainly due to diffusional deposition, and, to a lesser extent, gravitational settling.

iii) At superficial velocities greater than about 20 cm/sec, aerosol removal was mainly due to inertial impaction.

iv) For all experimental conditions tested, interception was found to be insignificant.

v) Aerosol collection was found to be unaffected by bed loading and to take place in an electrically neutral environment.

vi) Bounce-off probably occurred at superficial gas velocities greater than about 50 cm/sec causing the theoretical predictions to over-estimate collection efficiencies.

vii) The present experimental results agreed fairly well with the results of other studies although conclusions on collection mechanisms differed.

viii) An empirical equation (Eq. 7.3) was developed which was able to predict the single collector efficiency of a bed particle for the

experimental conditions chosen in this work.

ix) The theoretical expression (eq. 3.4) relating the single collector efficiency to the overall bed efficiency was confirmed by the results of this study.

x) The difference between the experimental and calculated (using Eqs. 7.3 and 3.4) bed collection efficiencies was within ten percentage points).

xi) The pressure drop through the bed was adequately described by an equation of the Ergun form (Eq. 3.15).

NOMENCLATURE

Symbol	Explanation and Typical Units
a,b,c	Constants used in empirical equations
D_a	Diffusivity coefficient of aerosols, cm^2/sec
d_a	Diameter of aerosol particle, cm or μm
d_c	Diameter of collector particle, cm or μm
D.O.P.	Dioctyl phthlate
E	Single collector efficiency of an isolated collector
EB	Single collector efficiency of a collector in a granular bed
EBT	Total collection efficiency of a granular bed
ED	Single collector efficiency due to diffusion
EDR	Single collector efficiency due to diffusion and interception
EDIR	Single collector efficiency due to diffusion, inertia and interception
EG	Single collector efficiency due to gravity
EI	Single collector efficiency due to inertia
EIR	Single collector efficiency due to inertia and interception
ER	Single collector efficiency due to interception
g	Gravitational acceleration, cm/sec^2
H	Bed depth, cm
ND	Dimensionless diffusion parameter $(Pe^{-2/3})$
ND	Dimensionless gravitational parameter (U_s/U)
NR	Dimensionless interceptional parameter (d_a/d_c)
P	Penetration, (1 - EBT)
ΔP	Pressure drop across the granular bed, mm Hg
Pe	Peclet number $(d_c U/D_a)$
R	Multiple correlation coefficient

Symbol	Explanation and Typical Units
Re	Reynolds number (ρ_F U d_c/μ)
St	Stokes number (d_a^2 U $\rho_F/9\,\mu\, d_c$)
U	Superficial gas velocity, cm/sec
U_s	Settling velocity of aerosol particle, cm/sec

Greek Symbols

$\alpha,\beta,\gamma,\sigma$	Constants used in empirical equations
$\alpha_0,\alpha_1,\alpha_2,\alpha_3,$ α_4,α_5	Constants used in empirical equations
ε	Bed voidage
μ	Viscosity of gas, gm/cm sec
ρ_a	Density of aerosol particle, gm/cm^3
ρ_F	Density of dispersion medium, gm/cm^3

REFERENCES

1. Paretsky, L. C., Theodore, L., Pfeffer, R., and Squires, A. M., J. Air Polln. Control Assoc., 21, 204 (1971).

2. Black, C. H., and Boubel, R. W., Ind. Eng. Chem. Proc. Des. S. Dev., 8, 573 (1969).

3. Squires, A. M., and Pfeffer, R., J. Air Polln. Control Assoc., 20, 523 (1970).

4. Kalen, B., and Zenz, F. A., Chem. Eng. Prog., 69(5), 67 (1973).

5. Engelbrecht, H. L., J. Air Polln. Control Assoc., 15(2), 43 (1965).

6. Egleson, G. C., Simons, H. P., Kane, L. J., and Sands, A. E., Ind. Eng. Chem., 46(6), 1157 (1954).

7. Meissner, H. P., and Mickley, M. S., Ind. Eng. Chem., 41, 1238 (1949).

8. Meisen, A., and Mathur, K. B., Inst. Chem. Engrs. Symp. Ser., 38(K3), (1974).

9. Dahneke, B., J. Colloid and Interface Sci., 37, 342 (1971).

10. Corn, M., J. Air Polln. Control Assoc., 11, 523 (1961).

11. Corn, M., and Silverman, L., Am. Ind. Hyg. Assoc. J., 22, 337 (1961).

12. Kraemer, H. F., and Johnstone, H. F., Ind. Eng. Chem., 47, 2426 (1955).

13. Langmuir, I., and Blodgett, K., U.S. Army Air Force Tech. Report 5418, (1946).

14. Gillespie, T., J. Colloid Sci., 10, 281 (1951).

15. Fuchs, N. A., "The Mechanics of Aerosols", Pergamon Press, Oxford (1964).

16. Davies, C. N., Ed. of "Aerosol Science", Academic Press, London (1966).

17. Dorman, R. G., "Dust Control and Air Cleaning", Pergamon Press, Oxford, (1974).

18. Strauss, W., "Industrial Gas Cleaning", Pergamon Press, Oxford (1966).

19. Silverman, L., Am. Ind. Hyg. Assoc. J., 25(6), 529 (1964).

20. Figueroa, A., Ph.D. Thesis, Univ. Cincinnati (1975).

21. Tardos, G. I., Abuaf, N., and Gutfinger, C., Paper from Dept. Mech. Eng. Technion, Israel Inst. of Tech., Haifa (1977).

22. Pich, J., From "Aerosol Science", Ed. C. N. Davis, (1966).

23. Doganoglu, Y., Ph.D. Thesis, McGill Univ. (Aug. 1975).

24. Knettig, P., and Beeckmans, J. M., Can. J. Chem. Eng., 52, 703 (1974).

25. McCarthy, D., Yankel, A. J., Patterson, R. G., and Jackson, M. L., Ind. Eng. Chem. Proc. Des. S. Dev., 15, 266 (1976).

26. Ramskill, E. A., and Anderson, W. L., J. Colloid Sci., 6, 416 (1951).

27. Thomas, J. W., and Yoder, R. E., A.M.A. Archives Ind. Health, 13, 545 (1956).

28. Freundlich, H., "Colloid and Capillary Chemistry", Methuen Press, London (1926).

29. Chen, C. Y., Chem. Rev., 55, 595 (1955).

30. La Mer, V. K., A.E.C. Rep. NYO-512 Tech. Info. Serv., (1951).

31. Paretsky, L. C., Ph.D. Thesis, The City Univ. of N.Y., (1972).

32. Gebhart, J., Roth, C., and Stahlhofen, W., J. Aerosol Sci., 4, 371 (1973).

33. Cleaver, J. W., and Yates, B., Chem. Eng. Sci., 31, 147 (1976).

34. Jordon, D. W., Brit. J. App. Phys., Suppl. No. 3, 5194 (1966).

35. Leers, R., Staub., 50, 402 (1957).

36. Walkenhorst, W., Staub., 32(6), 256 (1972).

37. Balasubramanian, M., Meisen, A., and Mathur, K. B., Can. J. Chem. Eng., (1976).

38. Mazumder, M. K., and Thomas, K. T., Filtration and Sepn., 25 (Jan/ Feb. 1967).

39. Katz., S. H., and Macrae, D. J., J. Phys. Colloid Chem., 52, 695 (1948).

40. Anderson, D. M., and Silverman, L., Proc. of 5th Air Cleaning Conference, A.E.C. 140 (1957).

41. Yoder, R. E., and Empsom, F. M., Am. Ind. Hyg. Assoc. J., 19, 107 (1958).

42. Scott, D. S., and Guthrie, D. A., Can. J. Chem. Eng., 37, 200 (1959).

43. Silverman, L., Proc. of U.S. Tech. Conf. on Air Polln., Ed. L. C. McCabe (1952).

44. Jackson, S., and Calvert, S., A. I. Ch. E. J., 12, 1075 (1966).

45. Calvert, S. P., "Air Pollution", Stern (Ed.) Vol. 3, Academic Press (1968).

46. Yankel, A., Jackson, M., and Patterson, R., Presented Air Polln. Control Assoc., (Nov. 1972).

47. First, M. W., and Hinds, W. C., J. Air Polln. Control Assoc., 26, 119 (1976).

48. Doganoglu, Y., Jog, V., Thambimuthu, K. V., and Clift, R., to be published (1978).

49. Azaniouch, M. K., Can. J. Chem. Eng., (in print 1978).

50. Fairs, G. L., and Godfrey, E., From "Dust in Industry", Soc. of Chem. Ind., London (1948).

51. Strauss, W., and Thring, M. W., J. Iron and Steel Inst. (London), 196 (1960).

52. Cook, C. C., Swany, G. R., and Colpitts, J. W., J. Air Polln. Control Assoc., 21, 479 (1971).

53. Rubin, Yu M., and Margolin, Y. A., Coke and Chem. (USSR), 3, 15 (1974).

54. Rush, D., Russel, J. C., and Iverson, R. E., J. Air Polln. Control Assoc., 23, 75 (1973).

55. Dumont, G., Goossens, W., Taeymans, A., and Balleux, W., Het. Ingesieusblad, 103 (1973).

56. Böhm, L., and Jordan, S., J. Aersol Sci., 7, 311 (1976).

57. Reese, R. G., Proc. (P. 76) of the Conf. Energy and Wood Product Industry, Forest Product Research Society, Atlanta, Georgia (1976).

58. Herne, H., "Aerodynamic Capture of Particles", Ed. by E. G. Richardson, Pergamon Press, Oxford (1960).

59. Landahl, H., and Hermann, K., J. Colloid Sci., 4, 103 (1949).

60. Behie, S. W., and Beeckmans, J. M., Can. J. Chem. Eng., 51, 430 (1973).

61. Friedlander, S. K., Ind. Eng. Chem., 50, 1161 (1958).

62. Natanson, G. L., Dokl. Akad. Nauk. SSSR, 112, 100 (1957).

63. Johnstone, H. F., and Roberts, M. H., Ind. Eng. Chem., 41, 2417 (1949).

64. Stairmand, C. J., Trans. Inst. Chem. Engrs. (London), 28, 130 (1950).

65. Boussinesque, J., "Theorie Analytique de Chaleur", Vol. II, 224, Paris (1903).

66. Tardos, G. I., Gutfinger, C., and Abuaf, N., A.I. Ch. E.J., 22(6), 1147 (1976).

67. Ranz, W. E., and Wong, J. B., Ind. Eng. Chem., 44(6), 1371 (1952).

68. Davies, C. N., Proc. Inst. Mech. Engrs., 1, 185 (1952).

69. Schmidt, E. W., Gieseke, J. A., Gelfand, P., Lugar, T. W., and Furlong, D. A., J. Air Polln. Control Assoc., 28(2), 143 (1978).

70. Rajagopalan, R., and Tien, C., A.I. Ch. E. J., 22(3), 523 (1976).

71. Tardos, G. I., Gutfinger, C., and Abuaf, N., Israel J. of Tech., 12, 184 (1974).

72. Le Clair, B. P., and Hamielec, A. E., Can. J. Chem. Eng., 49, 713 (1971).

73. Happel, J., A.I. Ch. E. J., 4, 197 (1958).

74. Kuwabara, S., J. Phys. Soc. Japan, 144, 527 (1959).

75. Davies, C. N., "Air Filtration", Academic Press, London (1973).

76. Spielman, L. A., and Fitzpatrick, J. A., J. Coll. Interface Sci., 42, 607 (1973).

77. Fitzpatrick, J. A., Ph.D. Thesis, Harvard Univ. (1972).

78. Neale, G. H., and Nader, W. K., A.I. Ch. E. J., 20(3), 531 (1974).

79. Tam, C. K. W., J. Fluid. Mech., 38, 537 (1969).

80. Ergun, S., Chem. Eng. Prog., 48, 89 (1952).

81. Wilson, E. J., and Geankoplis, C. J., Ind. Eng. Chem. Fund., 5, 9 (1966).

APPENDIX A

EXPERIMENTAL RESULTS FOR THE REMOVAL OF AEROSOL PARTICLES BY GRANULAR BEDS

For each set of conditions the aerosol removal by the granular bed is expressed as percentage penetration. The relationship between bed penetration (P) and bed collection efficiency (EBT) is:

$$P = 1 - EBT$$

or $$\%P = 100\ (1 - EBT)$$

All the results were obtained with the apparatus set up in the low velocity configuration unless otherwise stated. Tables A.1 to A.21 give the measured penetrations for each set of conditions. Tables A.22 to A.27 give the results of pressure drop measurements across beds of each collector for varying superficial gas velocity.

TABLE A.1 PENETRATIONS FOR NICKEL SHOT 598.1 UM DIAMETER.
(DOWNFLOW; BED DEPTH = 4.536 CM)

GAS VEL. CM/SEC	AEROSOL DIAMETER UM					
	0.109	0.500	0.600	0.804	1.011	2.020
5.24	82.50	66.90	61.30	49.30	39.60	11.88
8.30	83.70	70.10	65.60	52.30	42.60	14.09
11.16	85.10	72.70	67.00	56.70	46.00	15.50
16.97	83.70	72.30	69.80	60.70	51.20	13.50
22.37	86.00	75.80	70.40	60.70	53.20	7.88
27.08	84.40	75.80	70.50	61.80	52.50	1.95

TABLE A.2 PENETRATIONS FOR NICKEL SHOT 598.1 UM DIAMETER.
(UPFLOW AND DOWNFLOW; BED DEPTH = 4.536 CM)

GAS VEL. CM/SEC	AEROSOL DIAMETER UM					
	0.500		0.804		1.011	
	UP	DOWN	UP	DOWN	UP	DOWN
5.24	71.00	66.90	53.20	49.30	43.80	36.90
8.30	74.20	70.10	54.50	52.30	52.00	42.60
11.16	75.30	72.70	57.50	56.70	53.50	46.00
16.97	76.60	72.30	62.40	60.70	56.80	51.20
22.37	79.90	75.80	63.60	60.70	57.80	53.20
27.08	78.20	75.80	60.10	61.80	55.20	52.50
16.33*	76.40	71.80	60.90	58.90	-	50.89
22.57*	77.60	74.50	64.40	59.00	-	52.70
35.46*	73.60	69.70	54.90	54.10	-	47.77
50.75*	72.00	66.50	52.50	48.10	-	37.20
67.00*	-	66.60	-	48.60	-	34.12

* APPARATUS IN HIGH VELOCITY CONFIGURATION

TABLE A.3 PENETRATIONS FOR NICKEL SHOT 598.1 UM DIAMETER.
(DOWNFLOW; VARYING BED DEPTH;
AEROSOL DIAMETER = 0.5 UM)

GAS VEL. CM/SEC	BED DEPTH CM			
	4.536	9.071	13.607	18.142
5.24	66.90	44.60	30.20	20.50
8.30	70.10	46.30	32.20	23.00
11.16	72.70	50.80	36.50	26.50
16.97	72.30	54.40	40.60	31.00
22.37	75.80	56.90	45.30	35.00
27.08	75.80	60.50	47.50	37.50

TABLE A.4 PENETRATIONS FOR NICKEL SHOT 598.1 UM DIAMETER.
(DOWNFLOW; BED DEPTH = 2.268 CM)

GAS VEL. CM/SEC	AEROSOL DIAMETER UM			
	0.109	0.500	0.600	0.804
5.24	92.30	85.70	83.00	77.70
27.08	90.40	78.40	76.70	71.70

TABLE A.5 PENETRATIONS FOR NICKEL SHOT 511.0 UM DIAMETER.
(DOWNFLOW; BED DEPTH = 4.536 CM)

GAS VEL. CM/SEC	AEROSOL DIAMETER UM 0.109	0.500	0.600	0.804	1.011	2.020
5.24	75.7	60.00	45.40	36.80	29.50	6.802
8.30	78.50	65.30	52.70	41.00	37.50	8.614
11.16	80.50	69.00	57.30	45.40	40.00	10.909
16.97	83.00	71.30	61.60	50.30	44.10	8.387
22.37	83.60	75.00	66.60	55.20	45.00	1.526
27.08	83.60	73.10	67.20	55.50	43.50	0.096

TABLE A.6 PENETRATIONS FOR NICKEL SHOT 511.0 UM DIAMETER.
(UPFLOW AND DOWNFLOW; BED DEPTH = 4.536 CM)

GAS VEL. CM/SEC	AEROSOL DIAMETER UM 0.500		0.804		1.011	
	UP	DOWN	UP	DOWN	UP	DOWN
5.24	62.20	60.00	39.80	36.80	33.80	29.50
8.30	66.80	65.30	44.90	41.00	38.70	37.50
11.16	69.00	69.00	48.90	45.40	42.50	40.00
16.97	75.00	71.30	53.30	50.30	48.70	44.10
22.37	75.70	75.00	56.20	55.20	48.90	45.00
27.08	76.20	73.10	59.50	55.50	46.00	43.50
16.33*	73.80	72.30	54.00	51.30	-	45.45
22.57*	76.00	75.90	57.40	53.50	-	39.69
35.46*	73.00	68.40	56.00	53.60	-	35.24
50.75*	70.20	67.20	54.00	45.00	-	30.03
67.00*	-	65.00	45.00	49.60	-	27.46

* APPARATUS IN HIGH VELOCITY CONFIGURATION

TABLE A.7 PENETRATIONS FOR NICKEL SHOT 511.0 UM DIAMETER.
(DOWNFLOW; VARYING BED DEPTH;
AEROSOL DIAMETER = 0.5 UM)

GAS VEL. CM/SEC	BED DEPTH CM 2.268	4.536	9.071	13.607	18.142
5.24	75.20	60.00	37.20	25.00	18.30
8.30	78.20	65.30	43.00	30.00	24.30
11.16	82.20	69.00	46.50	32.60	27.30
16.97	82.70	71.30	51.20	37.50	31.50
22.37	85.20	75.00	55.70	44.00	37.00
27.08	87.40	73.10	59.10	45.00	38.70

TABLE A.8 PENETRATIONS FOR NICKEL SHOT 511.0 UM DIAMETER.
(DOWNFLOW; BED DEPTH = 2.268 CM)

GAS VEL. CM/SEC	AEROSOL DIAMETER UM 0.109	0.600	0.804
5.24	90.20	82.80	73.50
27.08	87.00	66.80	55.60

TABLE A.9 PENETRATIONS FOR NICKEL SHOT 363.9 UM DIAMETER.
(DOWNFLOW; BED DEPTH = 4.536 CM)

GAS VEL. CM/SEC	AEROSOL DIAMETER UM					
	0.109	0.500	0.600	0.804	1.011	2.020
5.24	40.50	29.10	21.90	14.80	12.50	0.561
8.30	48.20	33.30	26.70	19.20	19.90	0.736
11.16	51.20	36.90	31.10	24.70	22.90	1.129
16.97	57.60	38.10	37.30	29.00	26.80	0.055
22.37	62.20	43.00	39.90	31.00	26.40	0.0016
27.08	65.40	46.70	44.30	30.80	23.30	0.0003

TABLE A.10 PENETRATIONS FOR NICKEL SHOT 363.9 UM DIAMETER.
(UPFLOW AND DOWNFLOW; BED DEPTH = 4.536 CM)

GAS VEL. CM/SEC	AEROSOL DIAMETER UM				
	0.500		0.804		1.011
	UP	DOWN	UP	DOWN	DOWN
5.24	32.30	29.10	21.10	14.80	12.50
8.30	36.00	33.30	22.10	19.20	19.90
11.16	40.30	36.90	25.60	24.70	22.90
16.97	43.40	38.10	29.40	29.00	26.80
22.37	45.60	43.00	33.20	31.00	26.40
27.08	49.30	46.70	33.90	30.80	23.30
16.33*	42.50	40.00	31.00	28.10	27.30
22.57*	50.00	41.60	33.90	31.10	26.04
35.46*	46.70	44.60	32.00	29.20	19.63
50.75*	-	37.80	24.60	25.10	13.62
67.00*	-	40.70	-	20.00	12.60

* APPARATUS IN HIGH VELOCITY CONFIGURATION

TABLE A.11 PENETRATIONS FOR NICKEL SHOT 363.9 UM DIAMETER.
(DOWNFLOW; VARYING BED DEPTH;
AEROSOL DIAMETER = 0.5 UM)

GAS VEL. CM/SEC	BED DEPTH CM				
	2.268	4.536	9.071	13.607	18.142
5.24	54.40	29.10	10.00	4.20	3.40
8.30	58.00	33.30	12.40	5.00	3.90
11.16	61.00	36.90	14.00	6.00	4.90
16.97	63.70	38.10	16.50	8.20	6.40
22.37	66.00	43.00	20.00	11.40	9.30
27.08	66.40	46.70	24.40	14.90	12.00

TABLE A.12 PENETRATIONS FOR NICKEL SHOT 363.9 UM DIAMETER.
(DOWNFLOW; BED DEPTH = 2.268 CM)

GAS VEL. CM/SEC	AEROSOL DIAMETER UM		
	0.109	0.600	0.804
5.24	80.80	35.80	46.00
27.08	66.60	54.00	62.80

TABLE A.13 PENETRATIONS FOR NICKEL SHOT 216.1 UM DIAMETER.
(DOWNFLOW; BED DEPTH = 2.268 CM)

GAS VEL. CM/SEC	AEROSOL DIAMETER UM 0.109	0.500	0.600	0.804	1.011	2.020#
5.24	31.60	14.30	6.00	5.45	4.50	1.891
8.30	35.00	16.50	7.80	7.46	6.90	3.138
11.16	37.10	20.90	11.40	9.60	8.10	1.218
16.97	42.10	24.30	13.20	11.50	10.20	0.261
22.37	48.30	27.60	16.60	12.00	9.20	0.080
27.08	48.50	28.40	19.02	12.50	5.80	0.180

BED DEPTH = 0.567 CM

TABLE A.14 PENETRATIONS FOR NICKEL SHOT 216.1 UM DIAMETER.
(UPFLOW AND DOWNFLOW; BED DEPTH = 2.268 CM)

GAS VEL. CM/SEC	AEROSOL DIAMETER UM 0.500 UP	0.500 DOWN	0.804 UP	0.804 DOWN	1.011 DOWN
5.24	14.90	14.30	7.00	5.45	4.50
8.30	15.70	16.50	8.70	7.45	6.80
11.16	17.90	20.90	10.50	9.60	8.10
16.97	24.70	24.30	12.50	11.50	10.20
22.37	28.90	27.60	12.20	12.00	9.20
27.08	28.30	28.40	16.20	12.50	5.80
16.33*	25.00	24.30	12.00	9.70	10.51
22.57*	29.50	27.20	13.70	12.80	13.01
35.46*	28.00	25.90	12.30	10.30	2.98
50.75*	21.50	20.50	6.50	5.40	0.20
67.00*	-	18.30	-	4.80	0.01

* APPARATUS IN HIGH VELOCITY CONFIGURATION

TABLE A.15 PENETRATIONS FOR NICKEL SHOT 216.1 UM DIAMETER.
(DOWNFLOW; VARYING BED DEPTH;
AEROSOL DIAMETER = 0.5 UM)

GAS VEL. CM/SEC	BED DEPTH CM 0.567	1.134	2.268	4.536
5.24	58.70	38.30	14.30	7.40
8.30	64.00	41.00	16.50	9.40
11.16	68.00	45.40	20.90	11.80
16.97	70.80	49.20	24.30	16.80
22.37	73.80	53.00	27.60	20.50
27.08	74.80	56.00	31.30	22.00

TABLE A.16 PENETRATIONS FOR NICKEL SHOT 216.1 UM DIAMETER.
(DOWNFLOW; BED DEPTH = 1.134 CM)

GAS VEL. CM/SEC	AEROSOL DIAMETER UM 0.109	0.600	0.804
5.24	68.20	46.20	35.70
27.08	56.40	25.00	21.50

TABLE A.17 PENETRATIONS FOR NICKEL SHOT 126.0 UM DIAMETER.
(DOWNFLOW; BED DEPTH = 2.268 CM)

GAS VEL. CM/SEC	AEROSOL DIAMETER UM					
	0.109	0.500	0.600	0.804	1.011	2.020#
5.24	3.50	0.827	0.3536	0.2527	0.1015	1.2030
8.30	4.90	1.612	0.5110	0.4000	0.1721	1.1700
11.16	5.70	2.576	0.6350	0.5416	0.3370	1.4722
16.97	9.90	3.588	1.7390	1.5603	0.0982	1.4454
22.37	13.70	5.004	2.4230	2.1699	0.0196	1.3170
27.08	15.00	6.876	2.6850	2.3655	0.0024	1.1041

BED DEPTH = 0.283 CM

TABLE A.18 PENETRATIONS FOR NICKEL SHOT 126.1 UM DIAMETER.
(UPFLOW AND DOWNFLOW; BED DEPTH = 2.268 CM)

GAS VEL. CM/SEC	AEROSOL DIAMETER UM					
	0.500		0.600	0.804		1.011
	UP	DOWN	DOWN	UP	DOWN	DOWN
5.24	1.352	0.827	0.3536	2.1510	0.2527	0.1015
8.30	2.400	1.612	0.5110	1.9910	0.4000	0.1721
11.16	2.873	2.576	0.6350	1.4170	0.5416	0.3370
16.97	3.717	3.588	1.7390	1.3890	1.5603	0.0982
22.37	5.396	5.004	2.4230	1.5510	2.1699	0.0196
27.08	5.352	6.876	2.6850	1.6150	2.3655	0.0024
16.33*	-	-	2.5000	-	0.4244	0.1034
22.57*	-	-	2.8280	-	0.4260	0.0348
35.46*	-	-	1.3690	-	0.0765	0.0016
50.75*	-	-	0.3940	-	0.0100	0.0005
67.00*	-	-	0.2410	-	0.0032	0.0002

* APPARATUS IN HIGH VELOCITY CONFIGURATION

TABLE A.19 PENETRATIONS FOR NICKEL SHOT 126.1 UM DIAMETER.
(DOWNFLOW; VARYING BED DEPTH;
AEROSOL DIAMETER = 0.5 UM)

GAS VEL. CM/SEC	BED DEPTH CM		
	0.567	1.134	2.268
5.24	29.00	9.00	0.827
8.30	34.60	12.30	1.612
11.16	38.10	15.30	2.576
16.97	41.00	17.00	3.588
22.37	43.70	19.20	5.004
27.08	47.00	25.60	6.876

TABLE A.20 PENETRATIONS FOR NICKEL SHOT 126.1 UM DIAMETER.
(DOWNFLOW; BED DEPTH = 1.134 CM)

GAS VEL. CM/SEC	AEROSOL DIAMETER UM		
	0.109	0.600	0.804
5.24	38.60	17.80	15.50
27.08	20.90	5.50	5.80

TABLE A.21 PENETRATIONS FOR LEAD SHOT 1800 UM DIAMETER.
(DOWNFLOW; AEROSOL DIAMETER = 0.5 UM)

GAS VEL. CM/SEC	BED DEPTH CM 4.536	9.071	13.607	18.142
5.24	95.80	92.90	83.90	78.60
11.16	90.20	92.80	86.05	80.50
16.97	89.50	87.50	86.20	85.60
22.37	96.50	87.70	86.50	85.00
27.08	92.40	85.60	88.30	84.40

TABLE A.22 PRESSURE DROP (MM.HG) ACROSS BEDS OF NICKEL SHOT 598.1 UM DIAMETER.

GAS VEL. CM/SEC	BED DEPTH CM 4.536	9.071	13.607	18.141	DP/H MM.HG/CM
5.24	1.4	3.5	4.4	5.5	0.312
8.30	2.5	4.5	5.0	7.0	0.416
11.16	3.0	5.5	8.0	10.0	0.602
16.97	5.0	9.0	13.0	15.5	0.974
22.37	6.4	13.0	16.5	21.5	1.311
27.08	7.3	16.0	21.0	29.0	1.584
16.33	5.0	-	-	-	1.102
22.57	6.5	-	-	-	1.433
35.46	10.0	-	-	-	2.205
50.75	14.0	-	-	-	3.086
67.00	18.7	-	-	-	4.120

TABLE A.23 PRESSURE DROP (MM.HG) ACROSS BEDS OF NICKEL SHOT 511.0 UM DIAMETER.

GAS VEL. CM/SEC	BED DEPTH CM 4.536	9.071	13.607	18.141	DP/H MM.HG/CM
5.24	2.5	3.5	5.5	6.5	0.392
8.30	3.0	4.0	5.5	8.0	0.429
11.16	4.1	6.0	9.5	12.5	0.683
16.97	6.5	9.5	14.0	17.5	1.014
22.37	7.0	13.5	18.0	25.0	1.432
27.08	8.0	15.0	22.5	31.0	1.695
16.33	5.0	-	-	-	1.102
22.57	7.0	-	-	-	1.543
35.46	11.7	-	-	-	2.579
50.75	16.0	-	-	-	3.527
67.00	21.3	-	-	-	4.960

TABLE A.24 PRESSURE DROP (MM.HG) ACROSS BEDS OF NICKEL SHOT 363.9 UM DIAMETER.

GAS VEL. CM/SEC	BED DEPTH CM 4.536	9.071	13.607	18.141	DP/H MM.HG/CM
5.24	4.3	7.0	10.0	13.0	0.741
8.30	5.1	8.0	13.0	18.0	0.982
11.16	7.0	13.0	18.5	27.5	1.497
16.97	10.3	19.5	28.0	40.0	2.209
22.37	13.4	27.0	38.0	54.0	2.969
27.08	16.4	31.0	47.0	68.0	3.496
16.33	11.0	-	-	-	2.425
22.57	14.3	-	-	-	3.153
35.46	26.3	-	-	-	5.798
50.75	35.0	-	-	-	7.716
67.00	43.0	-	-	-	9.480

TABLE A.25 PRESSURE DROP (MM.HG) ACROSS BEDS OF NICKEL SHOT 216.1 UM DIAMETER.

GAS VEL. CM/SEC	BED DEPTH CM 1.134	2.268	4.536	6.804	DP/H MM.HG/CM
5.24	3.5	7.0	12.0	19.0	3.870
8.30	5.0	9.5	16.0	26.5	4.005
11.16	7.0	12.5	24.0	37.0	5.413
16.97	11.5	19.4	34.0	55.0	8.568
22.40	14.0	26.0	45.0	73.0	10.563
27.08	16.5	32.0	56.0	91.0	13.595
16.33	-	20.5	-	-	9.039
22.57	-	28.0	-	-	12.346
35.46	-	44.0	-	-	19.400
50.75	-	59.0	-	-	26.014
67.00	-	76.0	-	-	33.510

TABLE A.26 PRESSURE DROP (MM.HG) ACROSS BEDS OF NICKEL SHOT 126.0 UM DIAMETER.

GAS VEL. CM/SEC	BED DEPTH CM 0.567	1.134	2.268	4.536	DP/H MM.HG/CM
5.24	5.0	8.0	17.0	30.0	7.489
8.30	7.0	12.0	24.0	47.5	10.545
11.16	8.5	16.0	33.0	60.0	14.219
16.97	12.0	22.0	46.0	86.0	19.950
22.37	15.4	28.5	61.5	114.0	26.135
27.08	18.0	34.0	73.0	143.0	31.820

TABLE A.27 PRESSURE DROP (MM.HG) ACROSS BEDS OF LEAD SHOT 1800 UM DIAMETER.

GAS VEL. CM/SEC	BED DEPTH CM 4.536	9.071	13.607	18.141	DP/H MM.HG/CM
5.24	0.13	0.26	0.35	0.44	0.0268
11.16	0.26	0.49	0.76	0.96	0.0551
16.97	0.44	0.83	1.20	1.54	0.0905
22.37	0.66	1.23	1.81	2.32	0.1322
27.08	0.88	1.75	2.51	3.14	0.1860

APPENDIX B

CALCULATIONS OF EB AND DIMENSIONLESS GROUPS

For each set of experimental conditions the value of EB was calculated from the experimentally measured value of EBT using Eq. 3.6. The values of EB are listed with the corresponding dimensionless groups, viz., Re, St, NR, Pe, and NG.

Sample calculation of EB:

Consider the downflow filtration of 0.5 μm diameter aerosols by a granular bed of 598.1 μm diameter nickel shot.

Bed depth (H) = 4.536 cm

Voidage (ε) = 0.415

Superficial gas velocity = 5.24 cm/sec

Experimental bed collection efficiency (EBT) = 0.331

From Eq. 3.6 it follows:

$$EB = -\ln(1 - 0.0331)\ \frac{0.05981}{1.5}\ \left(\frac{0.415}{1 - 0.415}\right)\ \frac{1}{4.536}$$

$$= 2.5184 \times 10^{-3}$$

TABLE B.1 DIMENSIONLESS GROUPS AND SINGLE COLLECTOR EFFICIENCY CORRESPONDING TO TESTS ON BEDS OF NICKEL SHOT 598.1 UM DIAMETER.
(DOWNFLOW)

d_a UM	VEL. CM/SEC	RE	ST	NR	PE	NG	EB
0.109	5.24	2.176	0.674659E-05	0.182244E-03	0.522870E 05	0.719975E-05	0.119953E-02
0.109	8.30	3.447	0.106864E-04	0.182244E-03	0.828209E 05	0.454538E-05	0.110949E-02
0.109	11.16	4.635	0.143687E-04	0.182244E-03	0.111359E 06	0.338053E-05	0.100605E-02
0.109	16.97	7.048	0.218492E-04	0.182244E-03	0.169334E 06	0.222314E-05	0.110949E-02
0.109	22.37	9.291	0.288018E-04	0.182244E-03	0.223217E 06	0.168649E-05	0.940452E-03
0.109	27.08	11.248	0.348660E-04	0.182244E-03	0.270216E 06	0.139316E-05	0.105755E-02
0.500	5.24	2.176	0.141962E-03	0.835981E-03	0.489255E 06	0.151497E-03	0.251840E-02
0.500	8.30	3.447	0.224863E-03	0.835981E-03	0.774966E 06	0.956440E-04	0.232389E-02
0.500	11.16	4.635	0.302346E-03	0.835981E-03	0.104200E 07	0.711331E-04	0.206494E-02
0.500	16.97	7.048	0.459751E-03	0.835981E-03	0.158448E 07	0.467793E-04	0.193148E-02
0.500	22.37	9.291	0.606047E-03	0.835981E-03	0.208867E 07	0.354870E-04	0.171063E-02
0.500	27.08	11.248	0.733650E-03	0.835981E-03	0.252844E 07	0.293148E-04	0.161401E-02
0.500	16.33	6.783	0.442412E-03	0.835981E-03	0.152472E 07	0.486127E-04	0.206572E-02
0.500	22.57	9.374	0.611466E-03	0.835981E-03	0.210735E 07	0.351725E-04	0.183554E-02
0.500	35.46	14.728	0.960681E-03	0.835981E-03	0.331088E 07	0.223870E-04	0.225082E-02
0.500	50.75	21.079	0.137492E-02	0.835981E-03	0.473849E 07	0.156423E-04	0.254388E-02
0.500	67.00	27.828	0.181516E-02	0.835981E-03	0.625575E 07	0.118484E-04	0.253451E-02
0.600	5.24	2.176	0.204425E-03	0.100318E-02	0.613062E 06	0.218156E-03	0.305158E-02
0.600	8.30	3.447	0.323803E-03	0.100318E-02	0.971071E 06	0.137727E-03	0.262884E-02
0.600	11.16	4.635	0.435379E-03	0.100318E-02	0.130568E 07	0.102432E-03	0.249717E-02
0.600	16.97	7.048	0.662041E-03	0.100318E-02	0.198543E 07	0.673622E-04	0.224188E-02
0.600	22.37	9.291	0.872707E-03	0.100318E-02	0.261721E 07	0.511013E-04	0.218851E-02
0.600	27.08	11.248	0.105646E-02	0.100318E-02	0.316826E 07	0.422133E-04	0.217966E-02

TABLE B.1 (CONTINUED)

d_a UM	VEL. CM/SEC	RE	ST	NR	PE	NG	EB
0.804	5.24	2.176	0.367066E-03	0.134426E-02	0.869726E 06	0.391721E-03	0.441002E-02
0.804	8.30	3.447	0.581421E-03	0.134426E-02	0.137762E 07	0.247303E-03	0.404167E-02
0.804	11.16	4.635	0.781765E-03	0.134426E-02	0.185232E 07	0.183926E-03	0.353799E-02
0.804	16.97	7.048	0.118876E-02	0.134426E-02	0.281665E 07	0.120956E-03	0.311292E-02
0.804	22.37	9.291	0.156703E-02	0.134426E-02	0.371293E 07	0.917576E-04	0.311292E-02
0.804	27.08	11.248	0.189697E-02	0.134426E-02	0.449469E 07	0.757982E-04	0.300093E-02
0.804	16.33	6.783	0.114393E-02	0.134426E-02	0.271043E 07	0.125696E-03	0.330062E-02
0.804	22.57	9.374	0.158104E-02	0.134426E-02	0.374613E 07	0.909444E-04	0.329004E-02
0.804	35.46	14.728	0.248400E-02	0.134426E-02	0.588559E 07	0.578854E-04	0.383068E-02
0.804	50.75	21.079	0.355507E-02	0.134426E-02	0.842340E 07	0.404456E-04	0.456367E-02
0.804	67.00	27.828	0.469340E-02	0.134426E-02	0.111205E 08	0.306361E-04	0.449919E-02
1.011	5.24	2.176	0.580409E-03	0.169035E-02	0.113349E 07	0.619394E-03	0.621651E-02
1.011	8.30	3.447	0.919349E-03	0.169035E-02	0.179541E 07	0.391039E-03	0.532083E-02
1.011	11.16	4.635	0.123614E-02	0.169035E-02	0.241408E 07	0.290826E-03	0.484203E-02
1.011	16.97	7.048	0.187968E-02	0.169035E-02	0.367087E 07	0.191256E-03	0.417422E-02
1.011	22.37	9.291	0.247781E-02	0.169035E-02	0.483896E 07	0.145088E-03	0.393528E-02
1.011	27.08	11.248	0.299952E-02	0.169035E-02	0.585781E 07	0.119853E-03	0.367137E-02
1.011	16.33	6.783	0.180879E-02	0.169035E-02	0.353242E 07	0.198752E-03	0.421209E-02
1.011	22.57	9.374	0.249997E-02	0.169035E-02	0.488223E 07	0.143802E-03	0.399416E-02
1.011	35.46	14.728	0.392773E-02	0.169035E-02	0.767053E 07	0.915291E-04	0.460568E-02
1.011	50.75	21.079	0.562133E-02	0.169035E-02	0.109780E 08	0.639531E-04	0.616603E-02
1.011	67.00	27.828	0.742126E-02	0.169035E-02	0.144931E 08	0.484421E-04	0.670492E-02
2.020	5.24	2.176	0.226629E-02	0.337736E-02	0.243670E 07	0.241845E-02	0.132835E-01
2.020	8.30	3.447	0.358974E-02	0.337736E-02	0.385966E 07	0.152683E-02	0.122197E-01
2.020	11.16	4.635	0.482668E-02	0.337736E-02	0.518962E 07	0.113554E-02	0.116250E-01
2.020	16.97	7.048	0.733950E-02	0.337736E-02	0.789138E 07	0.746769E-03	0.124864E-01
2.020	22.37	9.291	0.967498E-02	0.337736E-02	0.104025E 08	0.566503E-03	0.158433E-01
2.020	27.08	11.248	0.117120E-01	0.337736E-02	0.125927E 08	0.467971E-03	0.245512E-01

TABLE B.2 DIMENSIONLESS GROUPS AND SINGLE COLLECTOR EFFICIENCY CORRESPONDING TO TESTS ON BEDS OF NICKEL SHOT 598.1 UM DIAMETER.
(UPFLOW)

d_a UM	VEL. CM/SEC	RE	ST	NR	PE	NG	EB
0.500	5.24	2.176	0.141962E-03	0.835981E-03	0.489255E 06	0.151497E-03	0.213559E-02
0.500	8.30	3.447	0.224863E-03	0.835981E-03	0.774966E 06	0.956440E-04	0.186070E-02
0.500	11.16	4.635	0.302346E-03	0.835981E-03	0.104200E 07	0.711331E-04	0.176894E-02
0.500	16.97	7.048	0.459751E-03	0.835981E-03	0.158448E 07	0.467793E-04	0.166221E-02
0.500	22.37	9.291	0.606047E-03	0.835981E-03	0.208867E 07	0.354870E-04	0.139921E-02
0.500	27.08	11.248	0.733650E-03	0.835981E-03	0.252844E 07	0.293148E-04	0.153331E-02
0.500	16.33	6.783	0.442412E-03	0.835981E-03	0.152472E 07	0.486127E-04	0.167851E-02
0.500	22.57	9.374	0.611466E-03	0.835981E-03	0.210735E 07	0.351725E-04	0.158133E-02
0.500	35.46	14.728	0.960681E-03	0.835981E-03	0.331088E 07	0.223870E-04	0.191133E-02
0.500	50.75	21.079	0.137492E-02	0.835981E-03	0.473849E 07	0.156423E-04	0.204838E-02
0.500	67.00	27.828	0.181516E-02	0.835981E-03	0.625575E 07	0.118484E-04	0.187753E-02
0.804	5.24	2.176	0.367066E-03	0.134426E-02	0.869726E 06	0.391721E-03	0.393528E-02
0.804	8.30	3.447	0.581421E-03	0.134426E-02	0.137762E 07	0.247303E-03	0.378475E-02
0.804	11.16	4.635	0.781765E-03	0.134426E-02	0.185232E 07	0.183926E-03	0.345062E-02
0.804	16.97	7.048	0.118876E-02	0.134426E-02	0.281665E 07	0.120956E-03	0.294068E-02
0.804	22.37	9.291	0.156703E-02	0.134426E-02	0.371293E 07	0.917576E-04	0.282191E-02
0.804	27.08	11.248	0.189697E-02	0.134426E-02	0.449469E 07	0.757982E-04	0.317486E-02
0.804	16.33	6.783	0.114393E-02	0.134426E-02	0.271043E 07	0.125696E-03	0.309241E-02
0.804	22.57	9.374	0.158104E-02	0.134426E-02	0.374613E 07	0.909444E-04	0.274396E-02
0.804	35.46	14.728	0.248400E-02	0.134426E-02	0.588559E 07	0.578854E-04	0.373915E-02
0.804	50.75	21.079	0.355507E-02	0.134426E-02	0.842340E 07	0.404456E-04	0.356002E-02
0.804	67.00	27.828	0.469340E-02	0.134426E-02	0.111205E 08	0.306361E-04	0.361545E-02
1.011	5.24	2.176	0.580409E-03	0.169035E-02	0.113349E 07	0.619394E-03	0.514760E-02
1.011	8.30	3.447	0.919349E-03	0.169035E-02	0.179541E 07	0.391039E-03	0.407755E-02
1.011	11.16	4.635	0.123614E-02	0.169035E-02	0.241408E 07	0.290826E-03	0.390022E-02
1.011	16.97	7.048	0.187968E-02	0.169035E-02	0.367087E 07	0.191256E-03	0.352700E-02
1.011	22.37	9.291	0.247781E-02	0.169035E-02	0.483896E 07	0.145088E-03	0.341818E-02
1.011	27.08	11.248	0.299952E-02	0.169035E-02	0.585781E 07	0.119853E-03	0.337517E-02

TABLE B.3 DIMENSIONLESS GROUPS AND SINGLE COLLECTOR EFFICIENCY CORRESPONDING TO TESTS ON BEDS OF NICKEL SHOT 511.0 UM DIAMETER.
(DOWNFLOW)

d_a UM	VEL. CM/SEC	RE	ST	NR	PE	NG	EB
0.109	5.24	1.859	0.772358E-05	0.213307E-03	0.446725E 05	0.704185E-05	0.148311E-02
0.109	8.30	2.945	0.122339E-04	0.213307E-03	0.707599E 05	0.444570E-05	0.128962E-02
0.109	11.16	3.960	0.164495E-04	0.213307E-03	0.951423E 05	0.330639E-05	0.115559E-02
0.109	16.97	6.022	0.250132E-04	0.213307E-03	0.144674E 06	0.217438E-05	0.992655E-03
0.109	22.37	7.938	0.329726E-04	0.213307E-03	0.190711E 06	0.164950E-05	0.954282E-03
0.109	27.08	9.610	0.399150E-04	0.213307E-03	0.230865E 06	0.136260E-05	0.954282E-03
0.500	5.24	1.859	0.162520E-03	0.978474E-03	0.418006E 06	0.148175E-03	0.260589E-02
0.500	8.30	2.945	0.257426E-03	0.978474E-03	0.662109E 06	0.935464E-04	0.221898E-02
0.500	11.16	3.960	0.346130E-03	0.978474E-03	0.890258E 06	0.695731E-04	0.200242E-02
0.500	16.97	6.022	0.526328E-03	0.978474E-03	0.135373E 07	0.457534E-04	0.177579E-02
0.500	22.37	7.938	0.693810E-03	0.978474E-03	0.178450E 07	0.347088E-04	0.151652E-02
0.500	27.08	9.610	0.839892E-03	0.978474E-03	0.216023E 07	0.286719E-04	0.149617E-02
0.500	16.33	5.795	0.506478E-03	0.978474E-03	0.130268E 07	0.475466E-04	0.172793E-02
0.500	22.57	8.009	0.700013E-03	0.978474E-03	0.180046E 07	0.344012E-04	0.146905E-02
0.500	35.46	12.583	0.109980E-02	0.978474E-03	0.282872E 07	0.218961E-04	0.202334E-02
0.500	50.75	18.009	0.157402E-02	0.978474E-03	0.404844E 07	0.152992E-04	0.211763E-02
0.500	67.00	23.776	0.207802E-02	0.978474E-03	0.534474E 07	0.115886E-04	0.229496E-02
0.600	5.24	1.859	0.234028E-03	0.117417E-02	0.523783E 06	0.213372E-03	0.420684E-02
0.600	8.30	2.945	0.370694E-03	0.117417E-02	0.829656E 06	0.134707E-03	0.341250E-02
0.600	11.16	3.960	0.498427E-03	0.117417E-02	0.111554E 07	0.100185E-03	0.296668E-02
0.600	16.97	6.022	0.757912E-03	0.117417E-02	0.169630E 07	0.658849E-04	0.258118E-02
0.600	22.37	7.938	0.999086E-03	0.117417E-02	0.223607E 07	0.499807E-04	0.216541E-02
0.600	27.08	9.610	0.120944E-02	0.117417E-02	0.270688E 07	0.412876E-04	0.211763E-02

TABLE B.3 (CONTINUED)

d_a UM	VEL. CM/SEC	RE	ST	NR	PE	NG	EB
0.804	5.24	1.859	0.420221E-03	0.157339E-02	0.743070E 06	0.383130E-03	0.532568E-02
0.804	8.30	2.945	0.665618E-03	0.157339E-02	0.117700E 07	0.241880E-03	0.474992E-02
0.804	11.16	3.960	0.894974E-03	0.157339E-02	0.158257E 07	0.179893E-03	0.420684E-02
0.804	16.97	6.022	0.136091E-02	0.157339E-02	0.240647E 07	0.118303E-03	0.366082E-02
0.804	22.37	7.938	0.179396E-02	0.157339E-02	0.317223E 07	0.897453E-04	0.316559E-02
0.804	27.08	9.610	0.217168E-02	0.157339E-02	0.384014E 07	0.741359E-04	0.313672E-02
0.804	16.33	5.795	0.130958E-02	0.157339E-02	0.231571E 07	0.122939E-03	0.355594E-02
0.804	22.57	8.009	0.181000E-02	0.157339E-02	0.320059E 07	0.889500E-04	0.333224E-02
0.804	35.46	12.583	0.284371E-02	0.157339E-02	0.502848E 07	0.566159E-04	0.332229E-02
0.804	50.75	18.009	0.406989E-02	0.157339E-02	0.719672E 07	0.395586E-04	0.425399E-02
0.804	67.00	23.776	0.537306E-02	0.157339E-02	0.950108E 07	0.299642E-04	0.373548E-02
1.011	5.24	1.859	0.664459E-03	0.197847E-02	0.968423E 06	0.605810E-03	0.650360E-02
1.011	8.30	2.945	0.105248E-02	0.197847E-02	0.153395E 07	0.382463E-03	0.522529E-02
1.011	11.16	3.960	0.141515E-02	0.197847E-02	0.206252E 07	0.284448E-03	0.488146E-02
1.011	16.97	6.022	0.215188E-02	0.197847E-02	0.313629E 07	0.187062E-03	0.436161E-02
1.011	22.37	7.938	0.283663E-02	0.197847E-02	0.413428E 07	0.141906E-03	0.425399E-02
1.011	27.08	9.610	0.343388E-02	0.197847E-02	0.500475E 07	0.117225E-03	0.443459E-02
1.011	16.33	5.795	0.207073E-02	0.197847E-02	0.301801E 07	0.194393E-03	0.420086E-02
1.011	22.57	8.009	0.286199E-02	0.197847E-02	0.417124E 07	0.140649E-03	0.492291E-02
1.011	35.46	12.583	0.449651E-02	0.197847E-02	0.655349E 07	0.895218E-04	0.555689E-02
1.011	50.75	18.009	0.643536E-02	0.197847E-02	0.937929E 07	0.625506E-04	0.640856E-02
1.011	67.00	23.776	0.849595E-02	0.197847E-02	0.123825E 08	0.473798E-04	0.688537E-02
2.020	5.24	1.859	0.265258E-02	0.395303E-02	0.208185E 07	0.241845E-02	0.143198E-01
2.020	8.30	2.945	0.420161E-02	0.395303E-02	0.329759E 07	0.152683E-02	0.130617E-01
2.020	11.16	3.960	0.564939E-02	0.395303E-02	0.443387E 07	0.113554E-02	0.118033E-01
2.020	16.97	6.022	0.859052E-02	0.395303E-02	0.674218E 07	0.746769E-03	0.132039E-01
2.020	22.37	7.938	0.113241E-01	0.395303E-02	0.888760E 07	0.566503E-03	0.222820E-01
2.020	27.08	9.610	0.137084E-01	0.395303E-02	0.107589E 08	0.467971E-03	0.370180E-01

TABLE B.4 DIMENSIONLESS GROUPS AND SINGLE COLLECTOR EFFICIENCY CORRESPONDING TO TESTS ON BEDS OF NICKEL SHOT 511.0 UM DIAMETER.
(UPFLOW)

d_a UM	VEL. CM/SEC	RE	ST	NR	PE	NG	EB
0.500	5.24	1.859	0.162520E-03	0.978474E-03	0.418006E 06	0.148175E-03	0.252954E-02
0.500	8.30	2.945	0.257426E-03	0.978474E-03	0.662109E 06	0.935464E-04	0.214944E-02
0.500	11.16	3.960	0.346130E-03	0.978474E-03	0.890258E 06	0.695731E-04	0.197681E-02
0.500	16.97	6.022	0.526328E-03	0.978474E-03	0.135373E 07	0.457534E-04	0.153260E-02
0.500	22.37	7.938	0.693810E-03	0.978474E-03	0.178450E 07	0.347088E-04	0.148311E-02
0.500	27.08	9.610	0.839892E-03	0.978474E-03	0.216023E 07	0.286719E-04	0.144804E-02
0.500	16.33	5.795	0.506478E-03	0.978474E-03	0.130268E 07	0.475466E-04	0.161853E-02
0.500	22.57	8.009	0.700013E-03	0.978474E-03	0.180046E 07	0.344012E-04	0.146204E-02
0.500	35.46	12.583	0.109980E-02	0.978474E-03	0.282872E 07	0.218961E-04	0.167660E-02
0.500	50.75	18.009	0.157402E-02	0.978474E-03	0.404844E 07	0.152992E-04	0.174268E-02
0.500	67.00	23.776	0.207802E-02	0.978474E-03	0.534474E 07	0.115886E-04	0.180213E-02
0.804	5.24	1.859	0.420221E-03	0.157339E-02	0.743070E 06	0.383130E-03	0.490817E-02
0.804	8.30	2.945	0.665618E-03	0.157339E-02	0.117700E 07	0.241880E-03	0.426584E-02
0.804	11.16	3.960	0.894974E-03	0.157339E-02	0.158257E 07	0.179893E-03	0.381120E-02
0.804	16.97	6.022	0.136091E-02	0.157339E-02	0.240647E 07	0.118303E-03	0.335219E-02
0.804	22.37	7.938	0.179396E-02	0.157339E-02	0.317223E 07	0.897453E-04	0.306994E-02
0.804	27.08	9.610	0.217168E-02	0.157339E-02	0.384014E 07	0.741359E-04	0.276596E-02
0.804	16.33	5.795	0.130958E-02	0.157339E-02	0.231571E 07	0.122939E-03	0.328268E-02
0.804	22.57	8.009	0.181000E-02	0.157339E-02	0.320059E 07	0.889500E-04	0.294812E-02
0.804	35.46	12.583	0.284371E-02	0.157339E-02	0.502848E 07	0.566159E-04	0.251244E-02
0.804	50.75	18.009	0.406989E-02	0.157339E-02	0.719672E 07	0.395586E-04	0.293886E-02
0.804	67.00	23.776	0.537306E-02	0.157339E-02	0.950108E 07	0.299642E-04	0.318493E-02
1.011	5.24	1.859	0.664459E-03	0.197847E-02	0.968423E 06	0.605810E-03	0.577870E-02
1.011	8.30	2.945	0.105248E-02	0.197847E-02	0.153395E 07	0.382463E-03	0.505750E-02
1.011	11.16	3.960	0.141515E-02	0.197847E-02	0.206252E 07	0.284448E-03	0.455850E-02
1.011	16.97	6.022	0.215188E-02	0.197847E-02	0.313629E 07	0.187062E-03	0.383304E-02
1.011	22.37	7.938	0.283663E-02	0.197847E-02	0.413428E 07	0.141906E-03	0.381120E-02
1.011	27.08	9.610	0.343388E-02	0.197847E-02	0.500475E 07	0.117225E-03	0.347351E-02

TABLE B.5 DIMENSIONLESS GROUPS AND SINGLE COLLECTOR EFFICIENCY CORRESPONDING TO TESTS ON BEDS OF NICKEL SHOT 363.9 UM DIAMETER.
(DOWNFLOW)

d_a UM	VEL. CM/SEC	RE	ST	NR	PE	NG	EB
0.109	5.24	1.324	0.108457E-04	0.299533E-03	0.318128E 05	0.704185E-05	0.342913E-02
0.109	8.30	2.097	0.171793E-04	0.299533E-03	0.503905E 05	0.444570E-05	0.276878E-02
0.109	11.16	2.820	0.230989E-04	0.299533E-03	0.677539E 05	0.330639E-05	0.253971E-02
0.109	16.97	4.288	0.351244E-04	0.299533E-03	0.103027E 06	0.217438E-05	0.209286E-02
0.109	22.37	5.653	0.463012E-04	0.299533E-03	0.135811E 06	0.164950E-05	0.180137E-02
0.109	27.08	6.843	0.560499E-04	0.299533E-03	0.164407E 06	0.136260E-05	0.161104E-02
0.500	5.24	1.324	0.228215E-03	0.137400E-02	0.297676E 06	0.148175E-03	0.455698E-02
0.500	8.30	2.097	0.361486E-03	0.137400E-02	0.471510E 06	0.935464E-04	0.408838E-02
0.500	11.16	2.820	0.486046E-03	0.137400E-02	0.633982E 06	0.695731E-04	0.375427E-02
0.500	16.97	4.288	0.739087E-03	0.137400E-02	0.964039E 06	0.457534E-04	0.350035E-02
0.500	22.37	5.653	0.974270E-03	0.137400E-02	0.127080E 07	0.347088E-04	0.313599E-02
0.500	27.08	6.843	0.117940E-02	0.137400E-02	0.153837E 07	0.286719E-04	0.289057E-02
0.500	16.33	4.127	0.711213E-03	0.137400E-02	0.927681E 06	0.475466E-04	0.347625E-02
0.500	22.57	5.704	0.982981E-03	0.137400E-02	0.128217E 07	0.344012E-04	0.332746E-02
0.500	35.46	8.961	0.154437E-02	0.137400E-02	0.201443E 07	0.218961E-04	0.306328E-02
0.500	50.75	12.825	0.221029E-02	0.137400E-02	0.288303E 07	0.152992E-04	0.369087E-02
0.500	67.00	16.931	0.291802E-02	0.137400E-02	0.380616E 07	0.115886E-04	0.341044E-02
0.600	5.24	1.324	0.328630E-03	0.164880E-02	0.373003E 06	0.213372E-03	0.576163E-02
0.600	8.30	2.097	0.520540E-03	0.164880E-02	0.590825E 06	0.134707E-03	0.500978E-02
0.600	11.16	2.820	0.699907E-03	0.164880E-02	0.794411E 06	0.100185E-03	0.443105E-02
0.600	16.97	4.288	0.106428E-02	0.164880E-02	0.120799E 07	0.658849E-04	0.374139E-02
0.600	22.37	5.653	0.140295E-02	0.164880E-02	0.159238E 07	0.499807E-04	0.347720E-02
0.600	27.08	6.843	0.169834E-02	0.164880E-02	0.192766E 07	0.412876E-04	0.308888E-02

TABLE B.5 (CONTINUED)

d_a UM	VEL. CM/SEC	RE	ST	NR	PE	NG	EB
0.804	5.24	1.324	0.590088E-03	0.220940E-02	0.529164E 06	0.383130E-03	0.724828E-02
0.804	8.30	2.097	0.934682E-03	0.220940E-02	0.838180E 06	0.241880E-03	0.626081E-02
0.804	11.16	2.820	0.125675E-02	0.220940E-02	0.112700E 07	0.179893E-03	0.530517E-02
0.804	16.97	4.288	0.191103E-02	0.220940E-02	0.171373E 07	0.118303E-03	0.469629E-02
0.804	22.37	5.653	0.251914E-02	0.220940E-02	0.225905E 07	0.897453E-04	0.444327E-02
0.804	27.08	6.843	0.304954E-02	0.220940E-02	0.273469E 07	0.741359E-04	0.446783E-02
0.804	16.33	4.127	0.183896E-02	0.220940E-02	0.164910E 07	0.122939E-03	0.481589E-02
0.804	22.57	5.704	0.254166E-02	0.220940E-02	0.227925E 07	0.889500E-04	0.443105E-02
0.804	35.46	8.961	0.399323E-02	0.220940E-02	0.358095E 07	0.566159E-04	0.467021E-02
0.804	50.75	12.825	0.571507E-02	0.220940E-02	0.512502E 07	0.395586E-04	0.524422E-02
0.804	67.00	16.931	0.754502E-02	0.220940E-02	0.676603E 07	0.299642E-04	0.610594E-02
1.011	5.24	1.324	0.933055E-03	0.277824E-02	0.689646E 06	0.605810E-03	0.788905E-02
1.011	8.30	2.097	0.147793E-02	0.277824E-02	0.109238E 07	0.382463E-03	0.612495E-02
1.011	11.16	2.820	0.198719E-02	0.277824E-02	0.146879E 07	0.284448E-03	0.559223E-02
1.011	16.97	4.288	0.302174E-02	0.277824E-02	0.223345E 07	0.187062E-03	0.499560E-02
1.011	22.37	5.653	0.398329E-02	0.277824E-02	0.294416E 07	0.141906E-03	0.505264E-02
1.011	27.08	6.843	0.482197E-02	0.277824E-02	0.356405E 07	0.117225E-03	0.552654E-02
1.011	16.33	4.127	0.290778E-02	0.277824E-02	0.214922E 07	0.194393E-03	0.492547E-02
1.011	22.57	5.704	0.401890E-02	0.277824E-02	0.297048E 07	0.140649E-03	0.510532E-02
1.011	35.46	8.961	0.631414E-02	0.277824E-02	0.466695E 07	0.895218E-04	0.617658E-02
1.011	50.75	12.825	0.903674E-02	0.277824E-02	0.667930E 07	0.625506E-04	0.756434E-02
1.011	67.00	16.931	0.119303E-01	0.277824E-02	0.881799E 07	0.473798E-04	0.785852E-02
2.020	5.24	1.324	0.372484E-02	0.555097E-02	0.148256E 07	0.241845E-02	0.196635E-01
2.020	8.30	2.097	0.590003E-02	0.555097E-02	0.234832E 07	0.152683E-02	0.186367E-01
2.020	11.16	2.820	0.793305E-02	0.555097E-02	0.315750E 07	0.113554E-02	0.170123E-01
2.020	16.97	4.288	0.120631E-01	0.555097E-02	0.480133E 07	0.746769E-03	0.284475E-01
2.020	22.37	5.653	0.159016E-01	0.555097E-02	0.632915E 07	0.566503E-03	0.418950E-01
2.020	27.08	6.843	0.192497E-01	0.555097E-02	0.766176E 07	0.467971E-03	0.485075E-01

TABLE B.6 DIMENSIONLESS GROUPS AND SINGLE COLLECTOR EFFICIENCY CORRESPONDING TO TESTS ON BEDS OF NICKEL SHOT 363.9 UM DIAMETER.
(UPFLOW)

d_a UM	VEL. CM/SEC	RE	ST	NR	PE	NG	EB
0.500	5.24	1.324	0.228215E-03	0.137400E-02	0.297676E 06	0.148175E-03	0.428742E-02
0.500	8.30	2.097	0.361486E-03	0.137400E-02	0.471510E 06	0.935464E-04	0.387597E-02
0.500	11.16	2.820	0.486046E-03	0.137400E-02	0.633982E 06	0.695731E-04	0.344791E-02
0.500	16.97	4.288	0.739087E-03	0.137400E-02	0.964039E 06	0.457534E-04	0.316675E-02
0.500	22.37	5.653	0.974270E-03	0.137400E-02	0.127080E 07	0.347088E-04	0.297915E-02
0.500	27.08	6.843	0.117940E-02	0.137400E-02	0.153837E 07	0.286719E-04	0.268317E-02
0.500	16.33	4.127	0.711213E-03	0.137400E-02	0.927681E 06	0.475466E-04	0.324625E-02
0.500	22.57	5.704	0.982981E-03	0.137400E-02	0.128217E 07	0.344012E-04	0.262968E-02
0.500	35.46	8.961	0.154437E-02	0.137400E-02	0.201443E 07	0.218961E-04	0.288872E-02
0.500	50.75	12.825	0.221029E-02	0.137400E-02	0.288303E 07	0.152992E-04	0.283228E-02
0.500	67.00	16.931	0.291802E-02	0.137400E-02	0.380616E 07	0.115886E-04	0.315802E-02
0.804	5.24	1.324	0.590088E-03	0.220940E-02	0.529164E 06	0.383130E-03	0.590281E-02
0.804	8.30	2.097	0.934682E-03	0.220940E-02	0.838180E 06	0.241880E-03	0.572714E-02
0.804	11.16	2.820	0.125675E-02	0.220940E-02	0.112700E 07	0.179893E-03	0.516939E-02
0.804	16.97	4.288	0.191103E-02	0.220940E-02	0.171373E 07	0.118303E-03	0.464431E-02
0.804	22.37	5.653	0.251914E-02	0.220940E-02	0.225905E 07	0.897453E-04	0.418315E-02
0.804	27.08	6.843	0.304954E-02	0.220940E-02	0.273469E 07	0.741359E-04	0.410400E-02
0.804	16.33	4.127	0.183896E-02	0.220940E-02	0.164910E 07	0.122939E-03	0.444327E-02
0.804	22.57	5.704	0.254166E-02	0.220940E-02	0.227925E 07	0.889500E-04	0.410400E-02
0.804	35.46	8.961	0.399323E-02	0.220940E-02	0.358095E 07	0.566159E-04	0.432282E-02
0.804	50.75	12.825	0.571507E-02	0.220940E-02	0.512502E 07	0.395586E-04	0.532056E-02
0.804	67.00	16.931	0.754502E-02	0.220940E-02	0.676603E 07	0.299642E-04	0.541424E-02

TABLE B.7 DIMENSIONLESS GROUPS AND SINGLE COLLECTOR EFFICIENCY CORRESPONDING TO TESTS ON BEDS OF NICKEL SHOT 216.0 UM DIAMETER.
(DOWNFLOW)

d_a UM	VEL. CM/SEC	RE	ST	NR	PE	NG	EB
0.109	5.24	0.786	0.182635E-04	0.504396E-03	0.188918E 05	0.704185E-05	0.519085E-02
0.109	8.30	1.246	0.289289E-04	0.504396E-03	0.299241E 05	0.444570E-05	0.473038E-02
0.109	11.16	1.675	0.388972E-04	0.504396E-03	0.402353E 05	0.330639E-05	0.446783E-02
0.109	16.97	2.547	0.591474E-04	0.504396E-03	0.611822E 05	0.217438E-05	0.389815E-02
0.109	22.37	3.357	0.779686E-04	0.504396E-03	0.806509E 05	0.164950E-05	0.327911E-02
0.109	27.08	4.064	0.943849E-04	0.504396E-03	0.976319E 05	0.136260E-05	0.326049E-02
0.500	5.24	0.786	0.384301E-03	0.231374E-02	0.176773E 06	0.148175E-03	0.900468E-02
0.500	8.30	1.246	0.608722E-03	0.231374E-02	0.280003E 06	0.935464E-04	0.806578E-02
0.500	11.16	1.675	0.818474E-03	0.231374E-02	0.376487E 06	0.695731E-04	0.704028E-02
0.500	16.97	2.547	0.124458E-02	0.231374E-02	0.572489E 06	0.457534E-04	0.633001E-02
0.500	22.37	3.357	0.164062E-02	0.231374E-02	0.754660E 06	0.347088E-04	0.566594E-02
0.500	27.08	4.064	0.198605E-02	0.231374E-02	0.913553E 06	0.286719E-04	0.523074E-02
0.500	16.33	2.451	0.119764E-02	0.231374E-02	0.550898E 06	0.475466E-04	0.637446E-02
0.500	22.57	3.387	0.165528E-02	0.231374E-02	0.761407E 06	0.344012E-04	0.586646E-02
0.500	35.46	5.321	0.260063E-02	0.231374E-02	0.119626E 07	0.218961E-04	0.608713E-02
0.500	50.75	7.616	0.372200E-02	0.231374E-02	0.171207E 07	0.152992E-04	0.714069E-02
0.500	67.00	10.055	0.491378E-02	0.231374E-02	0.226027E 07	0.115886E-04	0.765222E-02
0.600	5.24	0.786	0.553394E-03	0.277649E-02	0.221506E 06	0.213372E-03	0.126769E-01
0.600	8.30	1.246	0.876560E-03	0.277649E-02	0.350858E 06	0.134707E-03	0.114947E-01
0.600	11.16	1.675	0.117860E-02	0.277649E-02	0.471756E 06	0.100185E-03	0.978480E-02
0.600	16.97	2.547	0.179219E-02	0.277649E-02	0.717357E 06	0.658849E-04	0.912422E-02
0.600	22.37	3.357	0.236248E-02	0.277649E-02	0.945626E 06	0.499807E-04	0.809154E-02
0.600	27.08	4.064	0.285991E-02	0.277649E-02	0.114473E 07	0.412876E-04	0.747833E-02

TABLE B.7 (CONTINUED)

d_a UM	VEL. CM/SEC	RE	ST	NR	PE	NG	EB
0.804	5.24	0.786	0.993674E-03	0.372050E-02	0.314241E 06	0.383130E-03	0.131101E-01
0.804	8.30	1.246	0.157395E-02	0.372050E-02	0.497749E 06	0.241880E-03	0.116956E-01
0.804	11.16	1.675	0.211630E-02	0.372050E-02	0.669262E 06	0.179893E-03	0.105591E-01
0.804	16.97	2.547	0.321806E-02	0.372050E-02	0.101769E 07	0.118303E-03	0.974545E-02
0.804	22.37	3.357	0.424208E-02	0.372050E-02	0.134152E 07	0.897453E-04	0.955368E-02
0.804	27.08	4.064	0.513525E-02	0.372050E-02	0.162398E 07	0.741359E-04	0.936974E-02
0.804	16.33	2.451	0.309670E-02	0.372050E-02	0.979306E 06	0.122939E-03	0.105124E-01
0.804	22.57	3.387	0.428000E-02	0.372050E-02	0.135352E 07	0.889500E-04	0.926287E-02
0.804	35.46	5.321	0.672437E-02	0.372050E-02	0.212653E 07	0.566159E-04	0.102420E-01
0.804	50.75	7.616	0.962385E-02	0.372050E-02	0.304346E 07	0.395586E-04	0.131517E-01
0.804	67.00	10.055	0.127054E-01	0.372050E-02	0.401797E 07	0.299642E-04	0.136824E-01
1.011	5.24	0.786	0.157121E-02	0.467839E-02	0.409542E 06	0.605810E-03	0.139732E-01
1.011	8.30	1.246	0.248875E-02	0.467839E-02	0.648703E 06	0.382463E-03	0.121130E-01
1.011	11.16	1.675	0.334632E-02	0.467839E-02	0.872231E 06	0.284448E-03	0.113247E-01
1.011	16.97	2.547	0.508844E-02	0.467839E-02	0.132632E 07	0.187062E-03	0.102860E-01
1.011	22.37	3.357	0.670762E-02	0.467839E-02	0.174837E 07	0.141906E-03	0.107509E-01
1.011	27.08	4.064	0.811992E-02	0.467839E-02	0.211649E 07	0.117225E-03	0.128297E-01
1.011	16.33	2.451	0.489654E-02	0.467839E-02	0.127630E 07	0.194393E-03	0.101511E-01
1.011	22.57	3.387	0.676760E-02	0.467839E-02	0.176400E 07	0.140649E-03	0.919128E-02
1.011	35.46	5.321	0.106327E-01	0.467839E-02	0.277145E 07	0.895218E-04	0.158303E-01
1.011	50.75	7.616	0.152173E-01	0.467839E-02	0.396646E 07	0.625506E-04	0.279486E-01
1.011	67.00	10.055	0.200899E-01	0.467839E-02	0.523651E 07	0.473798E-04	0.424503E-01
2.020	5.24	0.786	0.627241E-02	0.934752E-02	0.880407E 06	0.241845E-02	0.715000E-01
2.020	8.30	1.246	0.993531E-02	0.934752E-02	0.139454E 07	0.152683E-02	0.624000E-01
2.020	11.16	1.675	0.133588E-01	0.934752E-02	0.187507E 07	0.113554E-02	0.794600E-01
2.020	16.97	2.547	0.203135E-01	0.934752E-02	0.285124E 07	0.746769E-03	0.107230E 00
2.020	22.37	3.357	0.267775E-01	0.934752E-02	0.375853E 07	0.566503E-03	0.128550E 00
2.020	27.08	4.064	0.324154E-01	0.934752E-02	0.454989E 07	0.467971E-03	0.113930E 00

TABLE B.8 DIMENSIONLESS GROUPS AND SINGLE COLLECTOR EFFICIENCY CORRESPONDING TO TESTS ON BEDS OF NICKEL SHOT 216.0 UM DIAMETER.
(UPFLOW)

d_a UM	VEL. CM/SEC	RE	ST	NR	PE	NG	EB
0.500	5.24	0.786	0.384301E-03	0.231374E-02	0.176773E 06	0.148175E-03	0.857836E-02
0.500	8.30	1.246	0.608722E-03	0.231374E-02	0.280003E 06	0.935464E-04	0.834270E-02
0.500	11.16	1.675	0.818474E-03	0.231374E-02	0.376487E 06	0.695731E-04	0.775180E-02
0.500	16.97	2.547	0.124458E-02	0.231374E-02	0.572489E 06	0.457534E-04	0.688436E-02
0.500	22.37	3.357	0.164062E-02	0.231374E-02	0.754660E 06	0.347088E-04	0.559329E-02
0.500	27.08	4.064	0.198605E-02	0.231374E-02	0.913553E 06	0.286719E-04	0.568783E-02
0.500	16.33	2.451	0.119764E-02	0.231374E-02	0.550898E 06	0.475466E-04	0.624649E-02
0.500	22.57	3.387	0.165528E-02	0.231374E-02	0.761407E 06	0.344012E-04	0.550070E-02
0.500	35.46	5.321	0.260063E-02	0.231374E-02	0.119626E 07	0.218961E-04	0.573584E-02
0.500	50.75	7.616	0.372200E-02	0.231374E-02	0.171207E 07	0.152992E-04	0.672124E-02
0.500	67.00	10.055	0.491378E-02	0.231374E-02	0.226027E 07	0.115886E-04	0.672124E-02
0.804	5.24	0.786	0.993674E-03	0.372050E-02	0.314241E 06	0.383130E-03	0.119823E-01
0.804	8.30	1.246	0.157395E-02	0.372050E-02	0.497749E 06	0.241880E-03	0.110027E-01
0.804	11.16	1.675	0.211630E-02	0.372050E-02	0.669262E 06	0.179893E-03	0.101554E-01
0.804	16.97	2.547	0.321806E-02	0.372050E-02	0.101769E 07	0.118303E-03	0.936974E-02
0.804	22.37	3.357	0.424208E-02	0.372050E-02	0.134152E 07	0.897453E-04	0.947920E-02
0.804	27.08	4.064	0.513525E-02	0.372050E-02	0.162398E 07	0.741359E-04	0.820144E-02
0.804	16.33	2.451	0.309670E-02	0.372050E-02	0.979306E 06	0.122939E-03	0.955368E-02
0.804	22.57	3.387	0.428000E-02	0.372050E-02	0.135352E 07	0.889500E-04	0.895670E-02
0.804	35.46	5.321	0.672437E-02	0.372050E-02	0.212653E 07	0.566159E-04	0.944242E-02
0.804	50.75	7.616	0.962385E-02	0.372050E-02	0.304346E 07	0.395586E-04	0.108499E-01
0.804	67.00	10.055	0.127054E-01	0.372050E-02	0.401797E 07	0.299642E-04	0.110027E-01

TABLE B.9 DIMENSIONLESS GROUPS AND SINGLE COLLECTOR EFFICIENCY CORRESPONDING TO TESTS ON BEDS OF NICKEL SHOT 126.1 UM DIAMETER.
(DOWNFLOW)

d_a UM	VEL. CM/SEC	RE	ST	NR	PE	NG	EB
0.109	5.24	0.458	0.313234E-04	0.865079E-03	0.110151E 05	0.704185E-05	0.880751E-02
0.109	8.30	0.726	0.496153E-04	0.865079E-03	0.174477E 05	0.444570E-05	0.792353E-02
0.109	11.16	0.976	0.667117E-04	0.865079E-03	0.234597E 05	0.330639E-05	0.752621E-02
0.109	16.97	1.485	0.101442E-03	0.865079E-03	0.356731E 05	0.217438E-05	0.607580E-02
0.109	22.37	1.957	0.133722E-03	0.865079E-03	0.470246E 05	0.164950E-05	0.522232E-02
0.109	27.08	2.369	0.161878E-03	0.865079E-03	0.569256E 05	0.136260E-05	0.498415E-02
0.500	5.24	0.458	0.659107E-03	0.396825E-02	0.103070E 06	0.148175E-03	0.127530E-01
0.500	8.30	0.726	0.104401E-02	0.396825E-02	0.163260E 06	0.935464E-04	0.110029E-01
0.500	11.16	0.976	0.140375E-02	0.396825E-02	0.219516E 06	0.695731E-04	0.987256E-02
0.500	16.97	1.485	0.213455E-02	0.396825E-02	0.333797E 06	0.457534E-04	0.914087E-02
0.500	22.37	1.957	0.281379E-02	0.396825E-02	0.440014E 06	0.347088E-04	0.841301E-02
0.500	27.08	2.369	0.340623E-02	0.396825E-02	0.532660E 06	0.286719E-04	0.737581E-02
0.600	5.24	0.458	0.949115E-03	0.476190E-02	0.129152E 06	0.213372E-03	0.148300E-01
0.600	8.30	0.726	0.150337E-02	0.476190E-02	0.204573E 06	0.134707E-03	0.138627E-01
0.600	11.16	0.976	0.202140E-02	0.476190E-02	0.275064E 06	0.100185E-03	0.132919E-01
0.600	16.97	1.485	0.307375E-02	0.476190E-02	0.418265E 06	0.658849E-04	0.106451E-01
0.600	22.37	1.957	0.405185E-02	0.476190E-02	0.551360E 06	0.499807E-04	0.977369E-02
0.600	27.08	2.369	0.490497E-02	0.476190E-02	0.667449E 06	0.412876E-04	0.950394E-02
0.600	16.33	1.429	0.295783E-02	0.476190E-02	0.402491E 06	0.684671E-04	0.969150E-02
0.600	22.57	1.975	0.408807E-02	0.476190E-02	0.556290E 06	0.495377E-04	0.936762E-02
0.600	35.46	3.103	0.642283E-02	0.476190E-02	0.873994E 06	0.315304E-04	0.112736E-01
0.600	50.75	4.441	0.919228E-02	0.476190E-02	0.125085E 07	0.220309E-04	0.145458E-01
0.600	67.00	5.862	0.121356E-01	0.476190E-02	0.165137E 07	0.166876E-04	0.158372E-01

TABLE B.9 (CONTINUED)

d_a UM	VEL. CM/SEC	RE	ST	NR	PE	NG	EB
0.804	5.24	0.458	0.170423E-02	0.638095E-02	0.183223E 06	0.383130E-03	0.157127E-01
0.804	8.30	0.726	0.269945E-02	0.638095E-02	0.290219E 06	0.241880E-03	0.145061E-01
0.804	11.16	0.976	0.362962E-02	0.638095E-02	0.390222E 06	0.179893E-03	0.137099E-01
0.804	16.97	1.485	0.551923E-02	0.638095E-02	0.593376E 06	0.118303E-03	0.109300E-01
0.804	22.37	1.957	0.727550E-02	0.638095E-02	0.782193E 06	0.897453E-04	0.100635E-01
0.804	27.08	2.369	0.880735E-02	0.638095E-02	0.946884E 06	0.741359E-04	0.983679E-02
0.804	16.33	1.429	0.531108E-02	0.638095E-02	0.570998E 06	0.122939E-03	0.143505E-01
0.804	22.57	1.975	0.734055E-02	0.638095E-02	0.789187E 06	0.889500E-04	0.143407E-01
0.804	35.46	3.103	0.115328E-01	0.638095E-02	0.123990E 07	0.566159E-04	0.188520E-01
0.804	50.75	4.441	0.165057E-01	0.638095E-02	0.177453E 07	0.395586E-04	0.241976E-01
0.804	67.00	5.862	0.217907E-01	0.638095E-02	0.234273E 07	0.299642E-04	0.271912E-01
1.011	5.24	0.458	0.269475E-02	0.802381E-02	0.238789E 06	0.605810E-03	0.181096E-01
1.011	8.30	0.726	0.426840E-02	0.802381E-02	0.378235E 06	0.382463E-03	0.167220E-01
1.011	11.16	0.976	0.573920E-02	0.802381E-02	0.508566E 06	0.284448E-03	0.149565E-01
1.011	16.97	1.485	0.872708E-02	0.802381E-02	0.773331E 06	0.187062E-03	0.181965E-01
1.011	22.37	1.957	0.115041E-01	0.802381E-02	0.101941E 07	0.141906E-03	0.224270E-01
1.011	27.08	2.369	0.139263E-01	0.802381E-02	0.123405E 07	0.117225E-03	0.280023E-01
1.011	16.33	1.429	0.839795E-02	0.802381E-02	0.744166E 06	0.194393E-03	0.180604E-01
1.011	22.57	1.975	0.116070E-01	0.802381E-02	0.102853E 07	0.140649E-03	0.209214E-01
1.011	35.46	3.103	0.182358E-01	0.802381E-02	0.161593E 07	0.895218E-04	0.289634E-01
1.011	50.75	4.441	0.260990E-01	0.802381E-02	0.231270E 07	0.625506E-04	0.319150E-01
1.011	67.00	5.862	0.344558E-01	0.802381E-02	0.305322E 07	0.473798E-04	0.341082E-01
2.020	5.24	0.458	0.107577E-01	0.160317E-01	0.513333E 06	0.241845E-02	0.929000E-01
2.020	8.30	0.726	0.170398E-01	0.160317E-01	0.813104E 06	0.152683E-02	0.935000E-01
2.020	11.16	0.976	0.229114E-01	0.160317E-01	0.109328E 07	0.113554E-02	0.886000E-01
2.020	16.97	1.485	0.348393E-01	0.160317E-01	0.166246E 07	0.746769E-03	0.890500E-01
2.020	22.37	1.957	0.459255E-01	0.160317E-01	0.219146E 07	0.566503E-03	0.910000E-01
2.020	27.08	2.369	0.555950E-01	0.160317E-01	0.265288E 07	0.467971E-03	0.947000E-01

TABLE B.10 DIMENSIONLESS GROUPS AND SINGLE COLLECTOR EFFICIENCY CORRESPONDING TO TEST ON BEDS OF NICKEL SHOT 126.1 UM DIAMETER.
(UPFLOW)

d_a UM	VEL. CM/SEC	RE	ST	NR	PE	NG	EB
0.500	5.24	0.458	0.659107E-03	0.396825E-02	0.103070E 06	0.148175E-03	0.113065E-01
0.500	8.30	0.726	0.104401E-02	0.396825E-02	0.163260E 06	0.935464E-04	0.979875E-02
0.500	11.16	0.976	0.140375E-02	0.396825E-02	0.219516E 06	0.695731E-04	0.932615E-02
0.500	16.97	1.485	0.213455E-02	0.396825E-02	0.333797E 06	0.457534E-04	0.864948E-02
0.500	22.37	1.957	0.281379E-02	0.396825E-02	0.440014E 06	0.347088E-04	0.767020E-02
0.500	27.08	2.369	0.340623E-02	0.396825E-02	0.532660E 06	0.286719E-04	0.769171E-02
0.804	5.24	0.458	0.170423E-02	0.638095E-02	0.183223E 06	0.383130E-03	0.100865E-01
0.804	8.30	0.726	0.269945E-02	0.638095E-02	0.290219E 06	0.241880E-03	0.102896E-01
0.804	11.16	0.976	0.362962E-02	0.638095E-02	0.390222E 06	0.179893E-03	0.111831E-01
0.804	16.97	1.485	0.551923E-02	0.638095E-02	0.593376E 06	0.118303E-03	0.112355E-01
0.804	22.37	1.957	0.727550E-02	0.638095E-02	0.782193E 06	0.897453E-04	0.109457E-01
0.804	27.08	2.369	0.880735E-02	0.638095E-02	0.946884E 06	0.741359E-04	0.108395E-01

APPENDIX C

REGRESSION ANALYSIS OF EQUATIONS SUGGESTED BY OTHER WORKERS

C.1 Introduction

Equations developed by other workers were tested by fitting them to the present experimental data to study their ability to predict the single collector efficiency (EB). Several other types of equations were also tried in an attempt to improve on the predictions of EB. This section gives the results of the regression analyses.

C.2 Empirical Equations Developed by Other Workers

$$EB = \alpha_0 + \alpha_1(E) \qquad [C.1]$$

where $E = EI + ER + ED + EG$

$EI = 2\ St^{1.13}$ (Paretsky[31])

$ER = 1.5\ NR^{2}$ (Friedlander[61])

$ED = 8\ Pe^{-1} + 2.3\ Pe^{-5/8}\ Re^{1/8}$ (Johnstone and Roberts[63])

$EG = NG$ (Ranz[67])

The equation for EI was chosen because other inertial type equations could not be applied to the experimental data. For example, the equation of Langmuir and Blodgett[13] (Eq. 2.2) predicts a minimum value of the Stokes number (0.83) below which no inertial collection takes place. It was evident this was not the case with the results of this work. Other equations such as that of Landahl and Hermann[59] (Eq. 2.5) gave excessively low collection efficiencies again bearing no relation to this data.

For the value of ED equations of the type $ED = \beta\ Pe^{-2/3}$ (Eq. 2.15) would have been satisfactory. However, the equation of Johnstone and Roberts was chosen as it possibly contains an interactive term which may be more realistic. Equations developed by Langmuir[13] (Eq. 2.11) and Natanson[62] (Eq. 2.16) were of little use as the limit of Re had to be less than 7.38 which was not the case in this work.

The interception term ER was chosen from Eq. 2.7 as most of the experiments were conducted in the creeping flow region. Again equations of Langmuir and Natanson suffered due to the limiting value of Re.

The other equations tested were:-

$$EB = \alpha_0 + \alpha_1\ St + \alpha_2\ NR\ St + \alpha_3\ NR\ St^2 \quad \text{(Davies}^{16}\text{)} \qquad [C.2]$$

$$EB = \alpha_0 + \alpha_1\ NR + \alpha_2\ St \quad \text{(Davies}^{16}\text{, Meisen}^{8}\text{, Paretsky}^{31}\text{)} \qquad [C.3]$$

$$EB = \alpha_0 + \alpha_1\ NG + \alpha_2\ St \quad \text{(Doganoglu}^{23}\text{)} \qquad [C.4]$$

$$EB = \alpha_0 + \alpha_1\ NG + \alpha_2\ Re\ St \quad \text{(Doganoglu}^{23}\text{)} \qquad [C.5]$$

$$EB = \alpha_0 + \alpha_1\ Sc^{-2/3}\ Re^{-\frac{1}{2}} + \alpha_2\ NR^2\ Re^{\frac{1}{2}} \quad \text{(Friedlander}^{61}\text{)} \qquad [C.6]$$

Tables C.1 to C.11 give the results of fitting the above equations to the data by multiple regression. The value of the α's are listed for conditions relating to constant aerosol or collector size, i.e., for each aerosol the variables are gas velocity and collector diameter and for each collector the variables are gas velocity and aerosol diameter. Also, the value of the α's were calculated for all the data. To compare the degree of fit of each equation the square of the multiple correlation coefficient (R) was calculated. This is defined as:-

$$R^2 = \frac{\sum_{k=1}^{n} (\hat{Y}k - \bar{Y})^2}{\sum_{k=1}^{n} (Yk - \bar{Y})^2}$$

where $\hat{Y}k$ = kth calculated value of Y

Yk = kth experimental value of Y

$\bar{Y}$ = mean of the experimental values of Y

Ideally, the closer R^2 is to unity the better the model. The actual value of R^2 measures the proportion of total variation about the mean accounted for by the regression. For example if $R^2 = 0.9$ then the model explains 90% of the total variation within the data.

TABLE C.1. RESULTS OF FITTING EQUATION C.1 TO THE EXPERIMENTAL DATA BY MULTIPLE REGRESSION

d_c μm	$\alpha_0 \times 10^3$	α_1	R^2
598.1	0.704	1.590	0.855
511.0	0.102	1.870	0.874
363.9	0.391	2.012	0.935
216.0	0.308	3.411	0.870
126.0	9.396	1.484	0.684
d_a μm			
0.109	2.467	1.985	0.498
0.500	2.364	0.509	0.397
0.600	2.470	0.289	0.353
0.804	3.990	1.157	0.748
1.011	4.667	0.623	0.755
2.020	10.270	0.967	0.711
All results	1.630	1.890	0.692

TABLE C.2. RESULTS OF FITTING EQUATION C.2 TO THE EXPERIMENTAL DATA BY MULTIPLE REGRESSION

d_c μm	$\alpha_0 \times 10^3$	α_1	$\alpha_2 \times 10^{-2}$	$\alpha_3 \times 10^{-4}$	R^2
598.1	2.46	-	5.126	-	0.867
511.1	2.66	-	3.430	1.5576	0.893
363.9	3.30	-	4.150	-	0.956
216.1	7.10	-	4.510	-	0.9101
126.1	12.60	-	1.247	-	0.744
d_a μm					
0.109	2.705	-	3.330	-	0.489
0.500	2.749	-	2.654	-	0.425
0.600	4.180	-	1.117	-	0.365
0.804	8.060	-	-	1.724	0.889
1.011	10.800	-	1.005	-	0.801
2.02	0.507	-	1.616	-	0.716
All results	7.055	-	1.700	-	0.513

TABLE C.3. RESULTS OF FITTING EQUATION C.3 TO THE EXPERIMENTAL DATA BY MULTIPLE REGRESSION

d_c μm	$\alpha_0 \times 10^{-4}$	α_1	α_2	R^2
598.1	-2.76	2.35	1.03	0.852
511.0	2.36	0.11	0.17	0.870
363.9	6.68	0.86	0.21	0.922
216.0	-78.62	4.41	2.87	0.903
126.1	-103.70	4.66	0.57	0.887
d_a μm				
0.109	-2.61	3.31	1.41	0.800
0.500	-2.83	2.69	0.22	0.780
0.600	-11.24	3.03	0.11	0.808
0.804	12.90	1.60	0.09	0.618
1.011	-19.60	1.05	1.16	0.701
2.020	6.92	1.67	0.63	0.828
All results	-0.08	1.817	0.66	0.854

TABLE C.4. RESULTS OF FITTING EQUATION C.4 TO THE EXPERIMENTAL DATA BY MULTIPLE REGRESSION

d_c μm	$\alpha_0 \times 10^{-3}$	α_1	α_2	R^2
598.1	1.11	3.76	1.48	0.947
511.0	0.89	2.97	0.19	0.895
363.9	1.26	3.76	0.22	0.884
216.0	-0.90	21.60	3.66	0.941
126.1	3.06	34.60	1.48	0.960
d_a μm				
0.109	0.62	12.44	2.35	0.774
0.500	1.31	7.85	0.69	0.960
0.600	1.13	9.61	0.65	0.922
0.804	2.70	8.73	0.39	0.899
1.011	2.15	17.80	1.44	0.785
2.020	6.47	19.15	0.89	0.848
All results	0.99	15.80	1.24	0.764

TABLE C.5. RESULTS OF FITTING EQUATION C.5 TO THE EXPERIMENTAL DATA BY MULTIPLE REGRESSION

d_c μm	$\alpha_0 \times 10^{3}$	α_1	$\alpha_2 \times 10^{-1}$	R^2
598.1	1.204	5.51	1.42	0.960
511.0	0.968	5.56	2.19	0.941
363.9	1.512	7.97	3.35	0.943
216.0	0.342	34.20	9.09	0.884
126.1	3.970	43.40	6.26	0.931
d_a μm				
0.109	1.590	1.93	4.46	0.511
0.500	1.810	8.12	0.25	0.878
0.600	1.730	9.72	0.25	0.796
0.804	3.130	9.08	0.24	0.874
1.011	4.390	20.77	1.52	0.837
2.020	10.560	17.17	1.38	0.682
All results	4.250	13.45	0.74	0.204

TABLE C.6. RESULTS OF FITTING EQUATION C.6 TO THE EXPERIMENTAL DATA BY MULTIPLE REGRESSION

d_c μm	$\alpha_0 \times 10^3$	α_1	$\alpha_2 \times 10^{-2}$	R^2
598.1	1.31	-	4.85	0.904
511.0	0.93	-	0.51	0.848
363.9	1.13	-	4.81	0.910
216.0	-4.17	9.92	7.37	0.953
126.1	4.99	-	2.74	0.882
d_a μm				
0.109	3.78	-	7.47	0.764
0.500	1.98	-	2.89	0.573
0.600	1.92	-	2.52	0.533
0.804	3.58	-	1.17	0.402
1.011	2.83	-	3.33	0.605
2.020	6.13	-	1.79	0.792
All results	0.80	20.53	2.32	0.837

In general it was possible to obtain relatively good predictions for equations fitted to the results relating to one collector or aerosol size. However, attempts to produce equations to fit all the data met with little success with R^2 values in the range of 0.5 to 0.7.

In many cases the value of the intercept α_0 was comparable to the single collector efficiency and therefore dominated the equations. This was obviously unrealistic and the regression analysis was repeated by forcing the equations through the origin. Furthermore, the total single collector efficiency, which by definition is made up of the individual efficiencies, should equal zero when all these individual efficiencies are zero. Thus setting $\alpha_0 = 0$ should probably result in a more precise model.

TABLE C.7. RESULTS OF FITTING EQUATION C.1 TO THE EXPERIMENTAL DATA BY MULTIPLE REGRESSION (INTERCEPT SET TO ZERO)

d_c μm	α_1	R^2
598.1	1.65	0.829
511.0	1.79	0.843
363.9	1.89	0.872
216.0	3.14	0.814
126.1	1.64	0.640
d_a μm		
0.109	1.17	0.706
0.500	2.75	0.490
0.600	2.2	0.090
0.804	1.64	0.187
1.011	1.37	0.661
2.020	1.97	0.865
All results	1.97	0.689

TABLE C.8. RESULTS OF FITTING EQUATION C.3 TO THE EXPERIMENTAL DATA BY MULTIPLE REGRESSION (INTERCEPT SET TO ZERO)

d_c μm	α_1	α_2	R^2
598.1	2.12	0.96	0.874
511.0	1.28	1.51	0.817
363.9	1.18	1.71	0.832
216.0	2.19	2.90	0.803
126.1	2.90	0.84	0.817
d_a μm			
0.109	7.75	-	0.869
0.500	2.57	-	0.884
0.600	2.62	-	0.810
0.804	2.29	0.06	0.810
1.011	1.70	0.72	0.903
2.020	1.35	1.84	0.828
All results	2.53	1.38	0.757

TABLE C.9. RESULTS OF FITTING EQUATION C.4 TO THE EXPERIMENTAL DATA BY MULTIPLE REGRESSION (INTERCEPT SET TO ZERO)

d_c μm	α_1	α_2	R^2
598.1	4.67	1.52	0.899
511.0	4.11	1.80	0.846
363.9	5.74	1.95	0.865
216.0	24.00	3.13	0.884
126.1	37.10	1.49	0.960
d_a μm			
0.109	48.00	4.10	0.476
0.500	39.70	2.26	0.518
0.600	37.90	1.82	0.533
0.804	22.50	1.39	0.757
1.011	13.90	1.42	0.846
2.020	2.90	2.17	0.846
All results	14.00	2.16	0.765

TABLE C. 10. RESULTS OF FITTING EQUATION C.5 TO THE EXPERIMENTAL DATA BY MULTIPLE REGRESSION (INTERCEPT SET TO ZERO)

d_c μm	α_1	α_2	R^2
598.1	7.2	0.11	0.781
511.0	9.7	0.15	0.723
363.9	11.4	0.22	0.689
216.0	40.3	0.58	0.740
126.1	49.5	0.50	0.865
d_a μm			
0.109	67.33	4.04	0.006
0.500	46.30	0.14	0.096
0.600	45.00	0.37	0.075
0.804	27.22	0.10	0.025
1.011	18.80	0.10	0.144
2.020	6.46	0.26	0.576
All results	23.20	0.31	0.434

TABLE C.11. RESULTS OF FITTING EQUATION C.6 TO THE EXPERIMENTAL DATA BY MULTIPLE REGRESSION (INTERCEPT SET TO ZERO)

d_c μm	α_1	$\alpha_2 \times 10^{-2}$	R^2
598.1	3.19	5.35	0.869
511.0	2.66	5.30	0.843
363.9	3.95	4.80	0.891
216.0	3.06	6.60	0.914
126.1	7.09	2.88	0.878
d_a μm			
0.109	3.06	32.30	0.865
0.500	20.40	2.38	0.895
0.600	32.20	1.85	0.870
0.804	38.70	1.80	0.857
1.011	36.30	2.17	0.899
2.020	42.20	5.62	0.783
All results	5.96	3.78	0.750

Once again equations could be fitted reasonably well to the data relating to one aerosol or collector size but the fit to all the data was still poor. Generally there was little improvement in forcing the equations (C.1 to C.6) through the origin except they are more realistic. Equations of this type are good for predicting EB for a given collector diameter but have limited ability for predicting EB over large collector and aerosol size ranges.

Comparisons of the coefficients from the equations of Doganoglu[23] with those from equivalent equations developed in this work are shown in Tables C.12 and C.13.

TABLE C.12. COMPARISON OF THE COEFFICIENTS OF EQUATION C.4 WITH THOSE FROM DOGANOGLU'S WORK

d_c μm	This work		Doganoglu	
	α_1	α_2	α_1	α_2
110	37.10	1.49	6.89	2.89
600	4.67	1.52	0.97	0.83
All	14.00	2.16	8.60	2.69

TABLE C.13. COMPARISON OF THE COEFFICIENTS OF EQUATION C.5 WITH THOSE FROM DOGANOGLU'S WORK

d_c μm	This work		Doganoglu	
	α_1	α_2	α_1	α_2
110	4.95	0.50	9.27	2.53
600	7.20	0.11	1.42	0.06
All	23.2	0.31	9.8	0.15

The coefficients agree in magnitude if not in actual value and demonstrate equations of this form can adequately predict EB for a given collector diameter.

C.3 Parameter Equations

Equations were formulated based on single dimensionless groups and were fitted by regression analysis to the experimental data. The equations were of the type:-

$$EB = \alpha_0 + \alpha_1 \, Re + \alpha_2 \, St + \alpha_3 \, ND + \alpha_4 \, NR + \alpha_5 \, NG \qquad [C.7]$$

and $$EB = \alpha_0 + \alpha_1 \, Re \, St + \alpha_2 \, ND + \alpha_3 \, NR + \alpha_4 \, NG \qquad [C.8]$$

Tables C.14 to C.17 give the results of fitting the above equations to the data by multiple regression.

TABLE C.14. RESULTS OF FITTING EQUATION C.7 TO THE EXPERIMENTAL DATA BY MULTIPLE REGRESSION

d_c μm	$\alpha_0 \times 10^3$	α_1	α_2	α_3	α_4	α_5	R^2
598.1	1.11	-	1.48	-	-	3.76	0.946
511.0	14.10	-	2.09	-	-	-	0.869
363.9	1.92	-	2.32	-	-	-	0.916
216.0	-0.89	-	3.66	-	-	21.60	0.943
126.1	3.06	-	1.48	-	-	34.60	0.966
d_a μm							
0.109	1.07	-	0.66	0.52	2.34	2.56	0.964
0.500	0.27	-	0.49	-	0.96	7.44	0.941
0.600	2.70	-	0.39	-	-	8.73	0.903
0.804	2.15	-	1.42	-	-	17.7	0.785
1.011	0.69	-	0.63	-	1.67	-	0.824
2.011	-1.95	-	1.02	27.06	0.85	6.44	0.899
All results	-6.08	-	1.30	9.39	2.62	10.31	0.810

TABLE C.15. RESULTS OF FITTING EQUATION C.8 TO THE EXPERIMENTAL DATA BY MULTIPLE REGRESSION

d_c μm	$\alpha_0 \times 10^3$	α_1	α_2	α_3	α_4	R
598.1	1.20	0.14	-	-	5.51	0.958
511.0	0.97	0.22	-	-	5.55	0.941
363.9	1.51	0.33	-	-	7.97	0.943
216.0	0.34	0.91	-	-	34.20	0.884
126.0	-	-	-	-	-	-
d_a μm						
0.109	0.38	0.020	-	1.53	5.35	0.960
0.500	-0.39	0.015	-	1.95	5.53	0.935
0.600	2.30	0.020	-	0.54	7.44	0.903
0.804	0.08	0.117	-	2.22	-	0.794
1.011	-1.76	0.098	-	2.47	-	0.819
2.020	-2.06	0.053	9.82	2.61	-	0.810
All results	-8.77	0.091	9.55	4.91	7.43	0.767

These equations had the same problem as the previous equations that the values of α_0 were too large. Therefore, the regression analysis was repeated forcing the equations through the origin, i.e., α_0 was set to zero.

Little improvement was obtained from equations of this form and generally the regression program produced equations similar to those already tested, i.e., equation (C.7) resulted in an equation similar to equation (C.4).

TABLE C.16. RESULTS OF FITTING EQUATION C.7 TO THE EXPERIMENTAL DATA BY MULTIPLE REGRESSION (INTERCEPT SET TO ZERO)

d_c μm	α_1	α_2	α_3	α_4	α_5	R^2
598.1	-	1.26	2.60	0.755	3.45	0.927
511.0	-	2.08	4.15	-	-	0.789
363.9	-	2.22	5.70	-	-	0.821
216.0	-	3.14	-	-	24.5	0.891
126.1	-	1.49	5.56	-	36.4	0.968
d_a μm						
0.109	-	-	4.57	-	-	0.762
0.500	-	1.31	25.06	-	-	0.905
0.600	-	1.17	37.25	-	-	0.893
0.804	-	1.08	47.50	-	-	0.908
1.011	-	1.22	50.40	-	-	0.916
2.020	-	2.09	104.00	-	-	0.846
All results	-	2.34	-	-	15.3	0.740

TABLE C.17. RESULTS OF FITTING EQUATION C.8 TO THE EXPERIMENTAL DATA BY MULTIPLE REGRESSION (INTERCEPT SET TO ZERO)

d_c μm	$\alpha_1 \times 10^2$	α_2	α_3	α_4	R^2
598.0	6.70	1.35	1.76	3.62	0.865
511.0	11.32	1.49	1.31	4.53	0.757
363.9	15.90	2.50	1.51	6.23	0.723
216.0	46.5	2.25	1.71	30.60	0.750
126.1	33.0	2.56	1.43	35.00	0.904
d_a μm					
0.109	-	4.57	-	-	0.762
0.500	1.78	11.57	1.71	-	0.949
0.600	2.40	42.66	-	-	0.792
0.804	3.81	-	2.10	5.39	0.828
1.011	4.91	-	2.43	-	0.828
2.020	15.90	-	3.08	-	0.757
All results	4.89	-	3.90	5.8	0.689

C.4 Polynomial Equations

It was attempted to develop an equation which avoided the problem of combining the dimensionless numbers which was equivalent to combining the collection efficiencies of the individual capture mechanism. The variables were therefore reduced to their simplest form, namely the superficial gas velocity (U), collector diameter (d_c) and aerosol diameter (d_a).

Several combinations of these variables were tried, the best results being obtained by a term of the form:

$$C = \left(\frac{d_a}{d_c}\right) U^n$$

where n was a variable chosen to obtain the best fit.

The equation tested was of the form

$$EB = \alpha_0 + \alpha_1 C + \alpha_2 C^2 + \alpha_3 C^3 + \alpha_4 C^4 \qquad [C.9]$$

Table C.18 gives some of the results of fitting this equation to all

the data using multiple regression.

As there was no improvement with this approach, further work with equations of this type were discontinued. Also the equation bore little relation to the data as it could not predict a minimum value for the collection efficiency with increasing gas velocity.

TABLE C.18. RESULTS OF FITTING EQUATION C.9 TO ALL THE EXPERIMENTAL DATA BY MULTIPLE REGRESSION

n	$\alpha_0 \times 10^4$	α_1	$\alpha_2 \times 10^{-2}$	$\alpha_3 \times 10^{-3}$	α_4	R^2
0.05	4.47	-	25.72	-	-	0.712
0.20	5.21	0.89	-	4.79	-	0.803
0.30	4.79	-	7.11	-	-	0.756
0.50	47.90	-	0.17	-	-	0.717

APPENDIX D

DEVELOPMENT OF THE BEST EMPIRICAL EQUATION

D.1 Introduction

This section shows the steps taken to obtain the best empirical equation which could predict the single collector efficiency from the basic variables (d_a, d_c, and U). The equations were tested by fitting them to the experimental data using regression analysis.

Having established the best empirical equation, its predictions for EB were converted into the overall bed efficiency EBT using Eq. 3.4. These calculated values for EBT were then compared with the experimentally measured values. Also the best empirical equation was used to predict the experimental results of other workers.

D.2 Development of the Best Equation for Predicting EB

An equation of the following form was selected.

$$EB = \alpha_0 + \alpha_1 NR + \alpha_2 NR\ U + \alpha_3 NR\ U^{-2/3} + \alpha_4 NR\ U^{-1} \qquad [D.1]$$

where $NR = d_a/d_c$

This equation is based on:

Inertia being proportional to U

Diffusion being proportional to $U^{-2/3}$

Gravity being proportional to U^{-1}

and Interception being independent of U.

TABLE D.1. RESULTS OF FITTING EQUATION D.1 TO THE EXPERIMENTAL DATA BY MULTIPLE REGRESSION

d_c μm	$\alpha_0 \times 10^3$	α_1	$\alpha_2 \times 10^2$	$\alpha_3 \times 10^{-2}$	α_4	R^2
598.1	-1.70	4.53	-	-	-	0.803
511.0	-2.78	4.87	-	-	-	0.672
363.9	-4.30	5.16	-	-	-	0.656
216.0	-1.97	10.41	-	-	-	0.740
126.1	-1.52	5.48	-	0.37	-	0.810
d_a μm						
0.109	-0.294	-	-	-	-	0.884
0.500	-0.017	-	-	3.49	-	0.949
0.600	0.336	-	3.95	1.02	-	0.922
0.804	0.192	-	3.95	1.02	-	0.912
1.011	-0.590	0.88	5.23	0.78	-	0.846
2.020	-1.610	6.69	6.53	0.73	-	0.689
All results	-5.30	5.58	-	-	-	0.706

As can be seen, the values of α_0 dominate the equation where the average value of EB was about 2.0 to 8.0 $\times 10^{-3}$ and thus these results are unrealistic. Therefore trials were made forcing the equation through the origin, i.e., using

$$EB = \alpha_1 NR + \alpha_2 NR\ U + \alpha_3 NR\ U^{-2/3} + \alpha_4 NR\ U^{-1} \qquad [D.2]$$

Trials were carried out just with data for constant aerosol size as the fit appeared better than for constant collector size (see Table D.2).

TABLE D.2. RESULTS OF FITTING EQUATION D.2 TO THE EXPERIMENTAL DATA BY MULTIPLE REGRESSION

d_a μm	α_1	$\alpha_2 \times 10^2$	$\alpha_3 \times 10^{-2}$	$\alpha_4 \times 10^{-2}$	R^2
0.109	-	-	3.730	-	0.880
0.500	-	4.20	1.006	-	0.953
0.600	-	4.11	1.062	-	0.908
0.804	-	5.47	0.788	-	0.897
1.011	0.593	7.11	-	1.19	0.922
2.020	6.54	-	-	-	0.689
All results	-	4.92	0.912	-	0.757

It was noticed that for aerosols up to 1.0 μm there was a tendency for the value of α_3 to decrease with increasing aerosol diameter (d_a). From a plot of versus d_a on log paper it was found that α_3 is roughly proportional to $(d_a)^{-2/3}$. Therefore the equation was modified to

$$EB = \alpha_1 NR + \alpha_2 NR\ U + \alpha_3 NR\ (d_a\ U)^{-2/3} + \alpha_4 NR\ U^{-1} \qquad [D.3]$$

TABLE D.3. RESULTS OF FITTING EQUATION D.3 TO THE EXPERIMENTAL DATA BY MULTIPLE REGRESSION

d_a μm	α_2	$\alpha_2 \times 10^2$	$\alpha_3 \times 10^2$	α_4	R^2
0.109	-	-	1.79	-	0.876
0.500	-	4.77	1.35	-	0.951
0.600	-	4.79	1.66	-	0.908
0.804	-	6.09	1.45	-	0.897
1.011	-	7.82	1.56	-	0.826
2.011	-	29.20	1.57	-	0.828

This change forced the value of α_3 to be nearly constant for all aerosol diameters at $\sim$ 0.0156. It was also noticed that there was an approximate linear relationship between α_2 and d_a with the exception of 2 μm aerosol. Therefore the inertia term was modified from NR U to NR (d_a U).

The equation needed a gravitational term to explain the effects of

upflow and downflow. Thus d_a/U and d_a^2/U were tried in the last term. The best results were obtained with a value of d_a^2/U for the gravitational term. The modified equation was now of the form

$$EB = \alpha_1 NR + \alpha_2 NR (d_a U) + \alpha_3 NR (d_a U)^{-2/3} + \alpha_4 d_a/U \qquad [D.4]$$

TABLE D.4. RESULTS OF FITTING EQUATION D.4 TO THE EXPERIMENTAL DATA BY MULTIPLE REGRESSION

d_a μm	α_1	$\alpha_2 \times 10^{-2}$	$\alpha_3 \times 10^{2}$	$\alpha_4 \times 10^{-5}$	R^2
0.109	-	-	1.79	-	0.876
0.500	-	9.49	1.48	6.7	0.929
0.600	-	8.11	1.58	7.4	0.910
0.804	-	7.79	1.17	4.9	0.914
1.011	-	8.40	1.21	6.3	0.850
2.020	-	14.45	1.57	-	0.850

After eliminating several experimental results (e.g., those at high velocities, i.e., 67 cm/sec, which are probably affected by bounce-off and the inaccurate results of the collection of 2.02 μm diameter aerosols on 210 and 126 μm diameter collectors), the equation was then fitted to the remaining results. In all cases, as noted previously, the interception constant α_1 was always set to zero and thus it can be assumed that interception plays no part in the collection.

TABLE D.5. RESULTS OF FITTING EQUATION D.4 TO ALL THE EXPERIMENTAL DATA BY MULTIPLE REGRESSION (α_1 SET TO ZERO)

	$\alpha_2 \times 10^{-2}$	$\alpha_3 \times 10^{2}$	$\alpha_4 \times 10^{-5}$	R^2
All results	12.41	0.916	32.59	0.784
All results less results for gas velocity of 67 cm/sec	7.58	1.359	5.84	0.93
All results less results for gas velocity of 67 cm/sec and 2.02 μm aerosols on 216 and 120 μm collectors	6.79	1.406	4.87	0.933

Using these regression results, further improvements were made by optimization and the final form of the equation was:

$$EB = 660 \frac{d_a}{d_c} (d_a U) + 0.0148 \frac{d_a}{d_c} (d_a U)^{-2/3} + 400{,}000 \frac{d_a^2}{U} \qquad [D.5]$$

where the multiple correlation coefficient (R) was 0.972.

Using this final form of the equation, comparisons were made with the predictions of EB by this equation and the experimental data of this work.

D.3 Comparison of Predicted and Experimental Bed Penetrations using Equation D.5

The comparison of predicted and experimental bed penetrations are summarized in Tables D.6 to D.25.

Aerosol removal is given in all of the tables as percent penetration where the relationship between penetration (P) and bed collection efficiency (EBT) is:

$$P = 1 - EBT$$

D.4 Comparison of Predicted Bed Penetrations Using Equation D.5 and the Experimental Results of Other Studies

The comparison of predicted bed penetrations and the experimental results of other studies are summarized in Tables D.26 to D.29.

D.5 Regression Trials of the Modified Form of Equation D.5

In order to make Eq. D.5 dimensionless it was modified as follows:

$$EB = \alpha_1 St + \alpha_2 NR^{4/3} Pe^{-2/3} + \alpha_3 NG \qquad [D.6]$$

The results of the regression analysis are given in Table D.30.

TABLE D.6 COMPARRISON BETWEEN PREDICTED AND EXPERIMENTAL PENETRATIONS FOR NICKEL SHOT 598.1 UM DIAMETER. (AEROSOL DIAMETER = 0.5 UM; BED DEPTH = 4.536 CM)

GAS VEL. CM/SEC	DOWNFLOW		UPFLOW	
	EXP.	CALC.	EXP.	CALC.
5.24	66.90	58.40	71.00	62.10
8.30	70.10	66.30	74.20	68.90
11.16	72.70	70.10	75.30	72.20
16.97	72.30	73.80	76.60	75.20
22.37	75.80	75.00	79.90	76.10
27.08	75.00	75.30	78.20	76.16
16.33	71.80	73.60	76.40	75.00
22.57	74.50	75.00	77.60	76.10
34.46	69.50	74.60	73.60	75.30
50.75	66.50	72.10	72.00	72.50
67.00	66.60	68.50	-	68.80

TABLE D.7 COMPARRISON BETWEEN PREDICTED AND EXPERIMENTAL PENETRATIONS FOR NICKEL SHOT 598.1 UM DIAMETER. (AEROSOL DIAMETER = 0.804 UM; BED DEPTH = 4.536 CM)

GAS VEL. CM/SEC	DOWNFLOW		UPFLOW	
	EXP.	CALC.	EXP.	CALC.
5.24	49.30	49.40	53.20	57.90
8.30	52.30	57.10	54.50	63.10
11.16	56.70	60.40	57.50	65.10
16.97	60.70	62.30	62.40	65.50
22.37	60.70	61.70	63.60	64.10
27.08	61.80	60.30	60.10	62.20
16.33	58.80	62.30	60.90	65.60
22.57	59.00	61.70	64.40	64.00
35.46	54.10	56.90	54.90	58.20
50.75	48.10	49.80	52.90	50.60
67.00	48.60	42.60	-	43.10

TABLE D.8 COMPARRISON BETWEEN PREDICTED AND EXPERIMENTAL PENETRATIONS FOR NICKEL SHOT 598.1 UM DIAMETER. (AEROSOL DIAMETER = 1.011 UM; BED DEPTH = 4.536 CM)

GAS VEL. CM/SEC	DOWNFLOW		UPFLOW	
	EXP.	CALC.	EXP.	CALC.
5.24	36.90	43.60	43.80	56.00
8.30	42.60	50.90	52.00	59.60
11.16	46.00	53.50	53.50	60.20
16.97	51.00	54.00	56.80	58.30
22.37	53.00	52.00	57.80	55.10
27.08	52.50	49.50	55.20	51.90
16.33	50.80	54.10	-	-
22.57	52.70	51.80	-	-
35.46	47.80	44.40	-	-
50.75	37.20	35.40	-	-
67.00	34.10	27.30	-	-

TABLE D.9 COMPARRISON BETWEEN PREDICTED AND EXPERIMENTAL PENETRATIONS FOR NICKEL SHOT 598.1 UM DIAMETER. (ADDITIONAL DOWNFLOW COMPARRISONS; BED DEPTH =4.536 CM)

GAS VEL. CM/SEC	AEROSOL DIAMETER UM					
	0.109		0.600		2.020	
	EXP.	CALC.	EXP.	CALC.	EXP.	CALC.
5.24	82.50	74.50	61.30	55.30	11.90	19.40
8.30	83.70	80.40	65.60	63.30	14.10	23.10
11.16	85.10	83.60	67.00	66.90	15.50	22.70
16.97	83.70	87.10	69.80	70.20	13.50	18.30
22.37	86.00	89.00	70.40	70.90	7.90	13.80
27.08	84.40	90.20	70.50	70.60	1.95	10.50

TABLE D.10 COMPARRISON BETWEEN PREDICTED AND EXPERIMENTAL PENETRATIONS FOR NICKEL SHOT 511.0 UM DIAMETER. (AEROSOL DIAMETER = 0.5 UM; BED DEPTH = 4.536 CM)

GAS VEL. CM/SEC	DOWNFLOW		UPFLOW	
	EXP.	CALC.	EXP.	CALC.
5.24	60.00	48.20	62.20	51.70
8.30	65.30	57.10	66.80	59.80
11.16	69.00	61.70	69.00	67.60
16.97	71.30	66.10	75.00	67.60
22.37	75.00	67.50	75.70	68.70
27.08	73.10	67.80	76.20	68.80
16.33	72.30	65.80	73.80	67.30
22.57	75.90	67.60	76.00	68.70
35.46	68.40	67.10	73.00	67.80
50.75	67.20	63.90	72.10	64.30
67.00	65.00	59.60	-	59.90

TABLE D.11 COMPARISSON BETWEEN PREDICTED AND EXPERIMENTAL PENETRATIONS FOR NICKEL SHOT 511.0 UM DIAMETER. (AEROSOL DIAMETER = 0.804 UM; BED DEPTH = 4.536 CM)

GAS VEL. CM/SEC	DOWNFLOW		UPFLOW	
	EXP.	CALC.	EXP.	CALC.
5.24	36.80	38.60	39.80	46.50
8.30	41.00	46.90	44.90	52.70
11.16	45.40	50.50	48.90	55.10
16.97	50.30	52.60	53.30	55.70
22.37	55.20	51.80	56.20	54.10
27.08	55.50	50.10	59.50	52.00
16.33	51.30	52.60	54.00	55.80
22.57	53.50	51.80	57.50	54.00
35.46	53.60	46.30	56.00	47.60
50.75	45.00	38.60	54.00	39.30
67.00	49.60	31.10	45.00	31.60

TABLE D.12 COMPARRISON BETWEEN PREDICTED AND EXPERIMENTAL PENETRATIONS FOR NICKEL SHOT 511.0 UM DIAMETER. (AEROSOL DIAMETER = 1.011 UM; BED DEPTH = 4.536 CM)

GAS VEL. CM/SEC	DOWNFLOW		UPFLOW	
	EXP.	CALC.	EXP.	CALC.
5.24	29.50	32.80	33.80	44.10
8.30	37.50	40.30	38.70	48.40
11.16	40.00	43.00	42.50	49.30
16.97	44.10	43.30	48.70	47.40
22.37	45.10	41.00	48.90	44.60
27.08	43.50	38.30	46.00	40.50
16.33	45.40	43.50	-	-
22.57	39.70	40.90	-	-
35.46	35.20	33.00	-	-
50.75	30.00	24.10	-	-
67.00	27.50	17.00	-	-

TABLE D.13 COMPARRISON BETWEEN PREDICTED AND EXPERIMENTAL PENETRATIONS FOR NICKEL SHOT 511.0 UM DIAMETER. (ADDITIONAL DOWNFLOW COMPARRISONS; BED DEPTH = 4.536 CM)

GAS VEL. CM/SEC	AEROSOL DIAMETER UM					
	0.109		0.600		2.020	
	EXP.	CALC.	EXP.	CALC.	EXP.	CALC.
5.24	75.70	66.85	45.40	44.90	6.80	11.70
8.30	78.50	74.30	52.70	53.70	8.60	14.30
11.16	80.50	78.20	57.30	58.00	10.90	13.70
16.97	83.00	82.90	61.60	61.80	8.40	10.10
22.37	83.60	85.30	66.60	62.50	1.50	6.80
27.08	83.60	86.80	67.20	62.20	0.096	4.70

TABLE D.14 COMPARRISON BETWEEN PREDICTED AND EXPERIMENTAL PENETRATIONS FOR NICKEL SHOT 363.9 UM DIAMETER. (AEROSOL DIAMETER = 0.5 UM; BED DEPTH = 4.536 CM)

GAS VEL. CM/SEC	DOWNFLOW EXP.	DOWNFLOW CALC.	UPFLOW EXP.	UPFLOW CALC.
5.24	29.10	24.20	32.30	26.70
8.30	33.30	33.60	36.00	35.70
11.16	36.90	38.90	40.30	40.80
16.97	38.10	44.50	43.40	45.90
22.37	43.00	46.40	45.60	47.50
27.08	46.60	46.60	49.30	47.60
16.33	40.00	44.10	42.50	45.50
22.57	41.60	46.40	50.00	47.50
35.46	44.60	45.60	46.70	46.30
50.75	37.80	41.40	-	41.80
67.00	40.80	36.10	-	36.30

TABLE D.15 COMPARRISON BETWEEN PREDICTED AND EXPERIMENTAL PENETRATIONS FOR NICKEL SHOT 363.9 UM DIAMETER. (AEROSOL DIAMETER = 0.804 UM; BED DEPTH = 4.536 CM)

GAS VEL. CM/SEC	DOWNFLOW EXP.	DOWNFLOW CALC.	UPFLOW EXP.	UPFLOW CALC.
5.24	14.80	16.20	21.00	21.10
8.30	19.20	23.20	22.10	27.40
11.16	24.70	26.70	25.60	30.10
16.97	29.00	28.70	29.40	31.00
22.37	31.00	27.70	33.20	29.40
27.08	30.80	26.00	33.90	27.30
16.33	28.10	28.60	31.00	31.10
22.57	31.10	27.60	33.90	29.30
35.46	29.20	22.10	32.00	22.90
50.75	25.10	15.40	24.60	15.80
67.00	20.00	10.00	-	10.20

TABLE D.16 COMPARRISON BETWEEN PREDICTED AND EXPERIMENTAL PENETRATIONS FOR NICKEL SHOT 363.9 UM DIAMETER. (AEROSOL DIAMETER = 1.011 UM; BED DEPTH = 4.536 CM)

GAS VEL. CM/SEC	DOWNFLOW	
	EXP.	CALC.
5.24	12.50	12.10
8.30	19.90	17.50
11.16	22.90	19.70
16.97	26.80	19.70
22.37	26.40	17.60
27.08	23.30	15.30
16.33	27.30	19.80
22.57	26.00	17.50
35.46	19.60	11.40
50.75	13.60	6.14
67.00	12.60	3.04

TABLE D.17 COMPARRISON BETWEEN PREDICTED AND EXPERIMENTAL PENETRATIONS FOR NICKEL SHOT 363.9 UM DIAMETER. (ADDITIONAL DOWNFLOW COMPARRISONS; BED DEPTH = 4.536 CM)

GAS VEL. CM/SEC	AEROSOL DIAMETER UM					
	0.109		0.600		2.020	
	EXP.	CALC.	EXP.	CALC.	EXP.	CALC.
5.24	40.50	45.20	21.90	21.20	0.56	2.03
8.30	48.20	55.70	26.70	29.90	0.74	2.67
11.16	51.20	61.70	31.10	34.60	1.13	2.34
16.97	57.60	69.10	37.30	39.00	0.06	1.20
22.37	62.20	73.20	39.90	39.90	0.02	0.54
27.08	65.40	75.70	44.30	39.40	0.003	0.25

TABLE D.18 COMPARRISON BETWEEN PREDICTED AND EXPERIMENTAL PENETRATIONS FOR NICKEL SHOT 216.1 UM DIAMETER. (AEROSOL DIAMETER = 0.5 UM; BED DEPTH = 2.268 CM)

GAS VEL. CM/SEC	DOWNFLOW		UPFLOW	
	EXP.	CALC.	EXP.	CALC.
5.24	14.30	13.70	14.90	14.96
8.30	16.50	21.70	15.70	22.70
11.16	20.90	26.50	17.90	27.70
16.97	24.50	32.00	24.70	32.80
22.37	27.60	33.70	28.90	34.50
27.08	28.40	34.10	28.30	34.80
16.33	24.30	31.60	25.00	32.50
22.57	27.20	33.90	29.50	34.60
35.46	25.90	33.00	28.00	33.40
50.75	20.50	28.70	21.50	29.00
67.00	18.30	23.60	-	23.70

TABLE D.19 COMPARRISON BETWEEN PREDICTED AND EXPERIMENTAL PENETRATIONS FOR NICKEL SHOT 216.1 UM DIAMETER. (AEROSOL DIAMETER = 0.804 UM; BED DEPTH = 2.268 CM)

GAS VEL. CM/SEC	DOWNFLOW		UPFLOW	
	EXP.	CALC.	EXP.	CALC.
5.24	5.50	8.16	7.00	10.10
8.30	7.50	13.20	8.70	15.20
11.16	9.60	15.90	10.50	17.60
16.97	11.50	17.40	12.50	18.60
22.37	12.70	16.40	12.20	17.30
27.08	12.50	14.90	16.20	15.60
16.33	9.70	17.40	12.00	18.70
22.57	12.80	16.40	13.70	17.30
35.46	10.30	11.70	12.30	12.30
50.75	5.40	7.10	6.50	7.20
67.00	4.80	3.90	-	3.90

TABLE D.20 COMPARRISON BETWEEN PREDICTED AND EXPERIMENTAL PENETRATIONS FOR NICKEL SHOT 216.1 UM DIAMETER. (AEROSOL DIAMETER = 1.011 UM; BED DEPTH = 2.268 CM)

GAS VEL. CM/SEC	DOWNFLOW	
	EXP.	CALC.
5.24	4.50	5.60
8.30	6.80	9.10
11.16	8.10	10.60
16.97	10.20	10.40
22.37	9.20	8.76
27.08	5.80	7.16
16.33	10.50	10.50
22.37	13.01	8.70
35.46	2.98	4.70
50.75	0.20	1.90
67.00	0.008	0.71

TABLE D.21 COMPARRISON BETWEEN PREDICTED AND EXPERIMENTAL PENETRATIONS FOR NICKEL SHOT 216.1 UM DIAMETER. (ADDITIONAL DOWNFLOW COMPARRISONS; BED DEPTH = 2.268 CM)

GAS VEL. CM/SEC	AEROSOL DIAMETER UM					
	0.109		0.600		2.020	
	EXP.	CALC.	EXP.	CALC.	EXP.	CALC.
5.24	31.60	32.50	6.00	11.60	0.00	0.64
8.30	35.00	43.60	7.80	18.50	0.00	0.79
11.16	37.10	51.40	11.40	22.70	0.00	0.61
16.97	42.10	59.40	13.20	26.70	0.00	0.22
22.37	48.30	59.20	16.60	27.40	0.00	0.07
27.08	48.50	64.20	19.02	26.90	0.00	0.02

TABLE D.22 COMPARRISON BETWEEN PREDICTED AND EXPERIMENTAL PENETRATIONS FOR NICKEL SHOT 126.0 UM DIAMETER. (AEROSOL DIAMETER = 0.5 UM; BED DEPTH = 2.268 CM)

GAS VEL. CM/SEC	DOWNFLOW EXP.	DOWNFLOW CALC.	UPFLOW EXP.	UPFLOW CALC.
5.24	0.35	0.19	1.35	0.36
8.30	0.51	0.74	2.40	1.26
11.16	0.64	1.32	2.87	2.23
16.97	1.74	2.10	3.72	3.72
22.37	2.42	2.27	5.39	4.30
27.08	2.69	2.14	5.35	4.40
16.33	2.50	2.05	-	-
22.57	2.83	2.27	-	-
35.46	1.37	1.65	-	-
50.75	0.39	0.81	-	-
67.00	0.24	0.32	-	-

TABLE D.23 COMPARRISON BETWEEN PREDICTED AND EXPERIMENTAL PENETRATIONS FOR NICKEL SHOT 126.0 UM DIAMETER. (AEROSOL DIAMETER = 0.804 UM; BED DEPTH = 2.268 CM)

GAS VEL. CM/SEC	DOWNFLOW EXP.	DOWNFLOW CALC.	UPFLOW EXP.	UPFLOW CALC.
5.24	0.250	0.072	2.150	0.105
8.30	0.400	0.280	1.990	0.360
11.16	0.540	0.470	1.420	0.570
16.97	1.560	0.610	1.390	0.680
22.37	2.170	0.510	1.550	0.560
27.08	2.360	0.380	1.615	0.410
16.33	0.420	0.610	-	-
22.57	0.430	0.510	-	-
35.46	0.076	0.190	-	-
50.75	0.010	0.042	-	-
67.00	0.003	0.007	-	-

TABLE D.24 COMPARRISON BETWEEN PREDICTED AND EXPERIMENTAL PENETRATIONS FOR NICKEL SHOT 126.0 UM DIAMETER. (AEROSOL DIAMETER = 1.011 UM; BED DEPTH = 2.268 CM)

GAS VEL. CM/SEC	DOWNFLOW	
	EXP.	CALC.
5.24	0.100	0.027
8.30	0.170	0.100
11.16	0.337	0.148
16.97	0.098	0.136
22.37	0.019	0.081
27.08	0.002	0.044
16.33	0.103	0.142
22.57	0.035	0.079
35.46	0.0016	0.0125
50.75	0.0005	0.0009
67.00	0.00023	0.00005

TABLE D.25 COMPARRISON BETWEEN PREDICTED AND EXPERIMENTAL PENETRATIONS FOR NICKEL SHOT 126.0 UM DIAMETER. (ADDITIONAL DOWNFLOW COMPARRISONS; BED DEPTH = 2.268 CM)

GAS VEL. CM/SEC	AEROSOL DIAMETER UM					
	0.109		0.500		2.020	
	EXP.	CALC.	EXP.	CALC.	EXP.	CALC.
5.24	3.50	3.68	0.35	0.19	0.0	0.027
8.30	4.90	8.70	0.51	0.73	0.0	0.100
11.16	5.70	13.30	0.64	1.30	0.0	0.150
16.97	9.90	21.40	1.74	2.10	0.0	0.130
22.37	13.70	27.20	2.40	2.27	0.0	0.081
27.08	15.00	31.30	2.69	2.14	0.0	0.040

TABLE D.26 COMPARRISON BETWEEN PREDICTED AND EXPERIMENTAL PENETRATIONS FOR LEAD SHOT 1800 UM DIAMETER.
(DOWNFLOW; AEROSOL DIAMETER =0.5 UM;
BED DEPTH = 4.536 CM)

GAS VEL. CM/SEC	EXP.	CALC.
5.24	93.76	93.47
11.16	94.36	95.89
16.97	95.00	96.53
22.37	96.29	96.75
27.08	96.07	96.80

TABLE D.27 COMPARRISON BETWEEN PREDICTED PENETRATIONS AND THE RESULTS OF A.FIGUEROA.
(COLLECTOR DIAMETER = 7000 UM;
BED DEPTH = 2 CM)

GAS VEL. CM/SEC	AEROSOL DIAMETER UM 0.500		1.099		2.020	
	EXP.	CALC.	EXP.	CALC.	EXP.	CALC.
3.10	80.3	78.5	81.2	67.1	64.4	47.9
4.11	81.9	81.8	82.4	71.6	66.9	53.8
5.14	84.0	84.0	84.6	74.6	68.9	57.4
6.17	83.8	85.5	86.4	76.5	73.9	59.5
7.20	87.1	86.7	84.6	77.8	70.1	60.8
8.20	87.2	87.6	88.6	78.8	76.0	61.5
9.30	85.9	88.3	85.0	79.4	68.8	61.7
10.30	90.0	88.8	88.8	80.0	74.0	61.6
11.30	87.2	89.3	86.4	80.2	69.7	61.3
12.30	89.0	89.7	89.7	80.3	71.3	60.9
13.40	90.1	90.0	88.5	80.4	67.6	60.3
14.40	87.5	90.3	86.0	80.4	67.8	59.6
15.40	88.7	90.5	87.2	80.3	64.9	58.8
16.50	88.4	90.7	86.1	80.2	57.7	58.0
17.50	89.8	90.8	87.8	80.0	56.7	57.1
18.50	90.2	90.9	88.6	79.8	51.6	56.2

TABLE D.28 COMPARRISON BETWEEN PREDICTED SINGLE COLLECTOR EFFICIENCY AND THE RESULTS OF Y.DOGANOGLU. (COLLECTOR DIAMETER = 596.0 UM; LIQUID D.O.P. AEROSOL)

GAS VEL. CM/SEC	AEROSOL DIAMETER UM			
	1.35		1.75	
	EXP.	CALC.	EXP.	CALC.
2.86	0.124E-2	0.935E-2	0.515E-2	0.120E-1
3.83	0.720E-3	0.779E-2	0.417E-2	0.101E-1
6.04	-	-	0.297E-2	0.814E-2
12.37	0.100E-3	0.536E-2	0.332E-2	0.762E-2
19.51	0.600E-4	0.593E-2	0.240E-2	0.893E-2
31.46	0.285E-2	0.765E-2	0.632E-2	0.121E-1
43.80	0.811E-2	0.975E-2	0.151E-1	0.158E-1

TABLE D.29 COMPARRISON BETWEEN PREDICTED SINGLE COLLECTOR EFFICIENCY AND THE RESULTS OF Y.DOGANOGLU. (COLLECTOR DIAMETER = 108.5 CM; LIQUID D.O.P. AEROSOL)

GAS VEL. CM/SEC	AEROSOL DIAMETER UM			
	1.35		1.75	
	EXP.	CALC.	EXP.	CALC
0.98	0.328E-1	0.784E-1	0.489E-1	0.906E-1
2.02	0.355E-1	0.489E-1	0.577E-1	0.568E-1
2.69	0.343E-1	0.413E-1	0.501E-1	0.483E-1
3.83	0.371E-1	0.342E-1	0.354E-1	0.408E-1
3.83	0.369E-1	0.342E-1	0.385E-1	0.408E-1
4.92	0.253E-1	0.306E-1	0.412E-1	0.374E-1
6.04	0.259E-1	0.285E-1	-	-
8.70	0.302E-1	0.265E-1	0.415E-1	0.349E-1
10.53	0.278E-1	0.264E-1	0.441E-1	0.360E-1
12.37	0.367E-1	0.268E-1	0.442E-1	0.374E-1
13.20	0.572E-1	0.271E-1	0.737E-1	0.382E-1
19.50	0.838E-1	0.320E-1	0.927E-1	0.562E-1

TABLE D.30. RESULTS OF FITTING EQUATION D.6 TO THE EXPERIMENTAL DATA BY MULTIPLE REGRESSION

d_c μm	α_1	$\alpha_2 \times 10^{-5}$	$\alpha_3 \times 10^{-1}$	R^2
598.7	1.29	1.76	0.26	0.91
511.0	1.52	1.11	0.27	0.87
363.9	1.64	0.71	0.43	0.84
216.0	2.87	-	2.68	0.93
126.1	1.36	1.43	3.39	0.89
d_a μm				
0.109	18.90	1.46	24.40	0.92
0.500	1.46	1.36	2.23	0.88
0.600	1.18	1.38	2.24	0.86
0.804	1.11	1.29	1.51	0.89
1.011	1.19	1.31	0.85	0.86
2.020	-	-	-	-
All results	1.76	1.48	1.15	0.89

The value of α_3 in all cases is too large and therefore Eq. D.6 does not fit the upflow data. Thus the value for α_3 (i.e., the gravity term constant) was fixed at 1.25 derived from Eq. D.5.

Table D.31 gives the results of the regression trials based on constant aerosol diameter.

TABLE D.31. RESULTS OF FITTING EQUATION D.6 TO THE EXPERIMENTAL DATA BY MULTIPLE REGRESSION (α_3 SET AT 1.25)

d_a μm	α_1	$\alpha_2 \times 10^{-5}$	R^2
0.109	20.79	1.57	0.82
0.500	1.58	1.48	0.86
0.600	1.14	1.55	0.88
0.804	1.12	1.45	0.89
1.011	1.20	1.42	0.94
2.020	1.55	1.89	0.72
All results less results of 2.02 μm aerosol*	1.16	1.47	0.91

*the results of 2.02 μm diameter aerosol were ignored owing to their possible innacuracies

By further optimization the final form of the equation was derived.

$$EB = 1.0\ St + 150{,}000\ NR^{4/3}\ Pe^{-2/3} + 1.25\ NG \qquad [D.7]$$

D.6 Regression Trials with the Equation of Schmidt[69]

The term for interception (NR) was ignored as interception plays no role in the present work. The equation used was of the form:

$$EB = \alpha_1\ St + \alpha_2\ (8\ Pe^{-1} + 2.3\ Pe^{-5/8}\ Re^{1/8}) + \alpha_3\ NG \qquad [D.8]$$

Again the value of α_3 was fixed at 1.25 and the regression trials carried out only for constant aerosol sizes.

TABLE D.32. RESULTS OF FITTING EQUATION D.8 TO THE EXPERIMENTAL DATA BY MULTIPLE REGRESSION

d_a μm	α_1	α_2	R^2
0.109	15.48	0.95	0.81
0.500	1.04	5.98	0.82
0.600	1.07	8.73	0.83
0.804	0.94	11.03	0.86
1.011	1.24	11.40	0.84
2.020	1.41	28.40	0.50
All results less the results of 2.02 μm aerosol	1.19	8.06	0.82

By further optimization the final form of the equation was derived.

$$EB = 0.8\ St + 8.0\ (8\ Pe^{-1} + 2.3\ Pe^{-5/8}\ Re^{-1/8}) + 1.25\ NG \quad [D.9]$$